THE UNIVERSITY OF CHICAGO

USE OF NANOMATERIALS FOR TRANSIENT TRANSFORMATION OF PLANTS

A DISSERTATION SUBMITTED TO

THE FACULTY OF THE DIVISION OF THE PHYSICAL SCIENCES

AND

THE FACULTY OF THE DIVISION OF THE BIOLOGICAL SCIENCES

AND THE PRITZKER SCHOOL OF MEDICINE

IN CANDIDACY FOR THE DEGREE OF

DOCTOR OF PHILOSOPHY

GRADUATE PROGRAM IN BIOPHYSICAL SCIENCES

BY

JESSICA MORGAN

CHICAGO, ILLINOIS

AUGUST 2023

TABLE OF CONTENTS

ACKNOWLEDGMENTS

My science journey began 16 years ago, when I was in the 7th grade. I was among a handful of students selected to take part in a class called "HOWL: Helping Others While Learning," taught by Mr. Warren Phillips. The purpose of this class was to perform service-based learning, where the students would take part in community service and also learning challenging curriculum at the same time. During this class, we were challenged to come up a future technology that could exist 20 years in the future. In preparation for this project, we were given a basic lesson about nanotechnology and I was fascinated. Thank you, Mr. Phillips, for sparking my interest in all things small and introducing me to the wonderful world of science. I still think back to your science classes and the different teaching strategies you employed in your lessons. Thank you for your unyielding support and invaluable mentorship. I wouldn't be where I am today if it wasn't for you. You're the best!

I have been fortunate to work closely with numerous mentors throughout high school and college, all of whom I am extremely grateful for. Thank you, Mrs. Stephen, for mentoring all four of my high school science fair projects, for answering my endless questions, and preparing me to tackle research as soon as I got to college. I am grateful for my college research advisors, Dr. Nathan Derr, Dr. Robert Merritt (aka Bio Bob), and Dr. Robert Newton (aka Geo Bob). Thank you for the opportunity to engage in research at the start of my college career. Thank you for training me how to become an independent researcher and for helping me to maintain my curiosity of science.

Five years ago, I had the crazy idea of combining two disperse fields into one project. To my graduate mentors, Dr. Jean Greenberg and Dr. Bozhi Tian, thank you so much for taking a leap of faith for supporting a project that was completely different than the rest. Thank you both

for your research mentorship and guidance. I am also grateful for my committee: Dr. David Kovar and Dr. Jiwoong Park. Thank you for taking the time to review this mammoth of a dissertation and for your insightful feedback. I am thankful for my collaborators at Oak Ridge National Laboratory: Dr. Scott Retterer, Dale Hensley, Dr. Jennifer Morrell-Falvey, Dr. Bernadeta Srijanto, and Kevin Lester. Thank you for all your insightful feedback and invaluable help in producing small nanomaterials. I am grateful for my collaborators at East Tennessee State University: Dr. Robert Standaert and all of the Master's students we have worked with: Bernard Abakah, Martin Tindi, Issaka Obuaba, Thomas Ntim, and Edward Offei. Thank you to all of the undergraduate students I have worked with over the years: Hannah Subramaniam, Adonis Coleman, Pierce Hoenigman, Marti Gendel, Allison Rosas, and Savannah Peralta. Thank you for all your hard work and enthusiasm!

I also want to express my sincere gratitude to the members of the Greenberg lab and Tian lab. Thank you for always being willing to talk shop, grab coffee, and celebrate the accomplishments of one and other. You made the time fly by! I want to give a special shout-out to my colleague and mentor Dr. Joanna Jelenska. I honestly do not think I would have survived grad school without you. Every time I had a question about a paper, procedure, or some weird, unexpected experimental result you were always available to chat. Thank you for all of your support!

I want to give a big shoutout to Dr. Michele Wittels and Dr. Julie Feder, the true hearts and souls of the BPHYs program. Thank you for always having an open door. Thank you for all the coffee chats and thank you for your unyielding support and help for starting new programs for the graduate program. I can't thank Dr. Adam Hammond enough for his support, advice, and insight on how to become a good mentor and leader.

Thank you to the Running Crew for meeting at early dawn, at dusk, midnight, and other absurd times for the most thrilling adventures. Everything from the brunch runs to supporting each other in ultramarathons and just trying to survive the day by day; you all are amazing. And I can't thank you enough for helping me get to this point.

To my Chicago community (in no particular order), Travis Bee, Andres Moya Rodriguez, Vishnu Nair, Rossy Natalie, Amanda Smith, Kelsey Stilson, Melvin Bonilla, Anna Petrosky, Anna Wisniewski, Stephanie Baumgart, Jean Salac, John Zang, Dimitrios Tanoglidis, Rodrigo Valdes Ortiz, Irene Farrah, Rafael Cruz Gil, Konstantinos Ameranis, Ignancio Cevallos Aleman, Theint Aung, Ethan Roeder, Alexis Thomas, Christopher Watkins, Keven Dooley, Ryan Dohn, Christina Roman, Christina Filippika, Kate Berger, Ben Rawe, Thomas Hameister, and Michaela Belcher, you have all played a key role in the success of my endeavors. I know that a lot of you no longer live in Chicago and have moved elsewhere, but you made my grad school experience memorable. Thank you for all the adventures and free food hunts.

I am so grateful friends in East Tennessee: Enzo Dinglasan and Boomer Russell. Thank you for always finding time to hang out with me on my countless trips to work at Oak Ridge National Laboratory. You made me feel at home!

I want to say thank you to my Massachusetts friends, fellow Smithies, and friends near and far who listened to my tales of Chicago and the current escapades in the lab: Missy Jaworsli, Colgan Powell, Isa, Bridget Guiney, Madison O'Connor, Tara Cappellucci, Erin Cappellucci, Jessica Magri, Tay Maynard, Leslie Carol, and Christian Montes. I promise I will come and visit more now that I have graduated.

I would like to thank my fiancé Georgios Zacharegkas for his unyielding support and persistent smiles when everything seemed dark and grey. Thank you for your patience, for all

your emotional support, for serving as a sounding board, and for the little family that we built with Janeway Iridessa Morgan Zacharegkas. I wouldn't have survived this journey if not for you. I look forward to our future as Dr. & Dr.!

Words cannot express much I appreciate the undevoted support of my family. Although my sisters, Jeanette, Carolyn, and Lauren, don't quite grasp the topics of this vast research, they always lent a listening ear and provided words of encouragement. Thank you so much for all of the sacrifices you made when I was growing up. Thank you for all of your support from the late nights preparing for science fair to the early morning phone calls as I stress talked about lab. You have always been my #1 fan! Thank you Grammy, Alan, Uncle Joel, Aunty Lynne, Uncle Don, and Aunty Crystal for all of your support. You all never doubted that I would get to this point. Thanks for believing in me when I didn't know if I could believe in myself.

Lastly, I would like to thank my funding sources: the Bioimaging Science Program, U.S. Department of Energy, Office of Science, Biological and Environmental Research, DE-SC001914 and the United States Department of Agriculture: National Institute of Food and Agriculture: Agriculture and Food Research Initiative Predoctoral Fellowship 2021-67034-35167.

LIST OF FIGURES

ABBREVIATIONS

- AALP: Arabidopsis aleurain-like protein
- CNF: carbon nanofibers
- CNMS: Center for Nanophase Materials Sciences
- CNT: carbon nanotube
- DC c-PECVD : direct current catalyst plasma enhanced chemical vapor deposition
- EDS: energy dispersive spectroscopy
- ICP-OES: inductively coupled plasma-optical emission spectroscopy
- IPA: isopropanol
- MWCNT: multiwalled carbon nanotube
- MS: Mursashige and Skoog
- MSNs: mesoporous silicon nanoparticles
- NP: nanoparticles
- PECVD: plasma enhanced chemical vapor deposition
- PEI: poly-ethylenimine
- PEG: polyethylene glycol
- PDMS: polydimethylsiloxane
- PMMA: polymethyl methacrylate
- Ri: root inducing
- SEM: scanning electron microscopy
- SiC whiskers: Silicon Carbide Whiskers
- SiNPs: silicon nanoparticles
- SiNW: silicon nanowire
- SWCNT: single walled carbon nanotube
- T-DNA: transfer DNA
- Ti: tumor inducing
- VACNF: vertically aligned carbon nanofibers
- VLS: vapor-liquid-solid

ABSTRACT

Plant transformation (both transient and stable) has yet to become widely achievable in all plant tissues and species. Traditional methods, including particle bombardment, protoplast transformation, and Agrobacteria- mediated transformation, are slow and not applicable to every plant species. The use of nanomaterials as a means for DNA delivery is a burgeoning field, still in its infancy. This thesis describes the use of carbon- and silicon-based nanomaterials as a means for delivery of DNA and dye in plants. Specifically, it highlights the work completed to use vertically aligned carbon nanofibers to transiently transform various plant species and organs as well as documenting the process utilized to transfer fibers from a rigid substrate to a flexible substrate and how fibers in flexible films can also be used for cargo delivery in plants. Additionally, in this thesis, I investigated the decomposition of silicon nanowires to crystalline silicon. This helps to inform what would happen to the silicon nanowires were they to be used as a nanovehicle in plant roots.

CHAPTER 1: INTRODUCTION

1.1 Transient Transformation in Plants

The ability to create transgenic plants has radically changed agriculture. There are two different forms of plant transformations, the first involving the integration of foreign DNA into a plant genome (stable transformation) and the second involves the introduction of DNA into plant cells without the incorporation of transgenes into the genome (transient transformation) (Alteper et al., 2016).

With the ability to stably transform plants we have been able to produce crops that are more resistant to insects, pathogens, and survive in extreme climates (Kumar et al., 2020b; Ahmad et al., 2012). There are two crucial steps of stable transformation in plants: 1. Delivery of foreign DNA (transgenes) to the nucleus of competent cells. 2. The recovery of fertile plants from that transformed cell (Jones and Sparks, 2009). Transient transformations are faster than stable transformations, in that the method is faster and they provide faster results. They also provide the opportunity to study gene functionality, protein localization, and subcellular process through the delivery of different molecular probes (Levy et al., 2018). Here, I will focus on applications to transient transformation. Three of the main methods employed for transient transformation and the delivery of genome-editing reagents into cells are *Agrobacterium*-mediated transformation, particle bombardment, and transformation of protoplasts using electroporation or polyethylene glycol (PEG).

Agrobacterium is the bacterium responsible for producing fleshy outgrowths, resembling tumors, on the crown roots of different trees. These tumor-like structures are known as crown galls. *Agrobacterium tumefaciens and Agrobacterium rhizogenes* have large tumor-inducing (Ti) or root inducing (Ri) plasmids. During infection, a specific portion of the plasmid (T-DNA) is

transferred between the bacterium to the host plant cells and inserted into the genome via a bacterial type IV secretion system (Hansen et al., 1994). The tumor-inducing T-DNA contains genes responsible for causing the proliferation of plant cells to form the gall. Additionally, the T-DNA encodes for genes responsible for producing necessary metabolites (octopine and nopaline) necessary for the survival of the inciting bacteria. Many dicots and gymnosperms are susceptible to *A. tumefaciens*, while monocots are not (Hansen et al., 1994). *A. rhizogenes* contain root-inducing plasmids to induce abnormal root production in host plants (Hwang et al., 2017). Pathogenic Ti-plasmids were not "out-of-the-box" ready for scientists to use for transformations. Ti-plasmids are large (>200kb) (Rogers et al., 1986) and generally have a low copy number, which makes them difficult to clone and isolate (Hwang et al., 2017). They do not replicate easily in *E. coli* (a preferred host for genetic manipulation in biology) (Lee and Galvin, 2008). Additionally, the WT Ti plasmids encode oncogenes that cause the bacterium to be pathogenic. The oncogene expression is the catalyst for the development of the crown gall or hairy root structures (Britton et al., 2008). To overcome these challenges, scientists first needed to remove the oncogenes. Secondly, they needed to determine the minimal characteristics necessary to achieve DNA transfer. In 1983, Hoekma et al. (1983) and de Framond et al. (1983) made the conclusion that the *vir* and T-DNA regions of the Ti-plasmid could be separated into two different plasmids, referred to as a binary vector system. If the two vectors were within the same cell, then proteins encoded by the *vir* genes could function to export the T-DNA into the host plant. T-DNA is encoded in the T-Binary vector, outside of the T-DNA region is the origin of replication (that has the ability to function in both *E. coli* and *A. tumefaciens*), cloning sites for the gene of interest, a bacterial selectable marker, a plant selectable marker, components for gene

expression, restriction endonuclease sites, and/or component for monitoring recombinant protein in transformed plant (Lee and Galvin, 2008; Hwang et al., 2017).

In terms of traditional transient transformation methods, *Agrobacterium*-mediated transformation using the binary vector system is one of the more commonly methods used. It is advantageous in that it requires minimal equipment and facilities to perform the technique, the technique itself is arguably easy to set-up and use, and it requires minimal DNA rearrangements in the plasmid (Hwang et al., 2017). However, there are several monocot crops and species that are recalcitrant to *A. tumefaciens*-mediated transformation. Additionally, for this method, high cell densities of *Agrobacteria* are required to perform transient transformation, which could be harmful plants (Karami, 2008; Li et al., 2009). The amount of *Agrobacteria* delivered will affect the signal of the delivered reporter/gene. The signal of the reporter will increase up until the optimal concentration of *Agrobacterium* delivered and then decrease after that optimal cell density (Li et al., 2009).

A second commonly used method for transient transformation in plants is particle bombardment, also known as biolistic transformation or biolistics. This method uses force to get DNA into plants. In 1987, Sanford and colleagues published their method for using a particle gun for delivering small particles into plants (i.e. tobacco, corn, and rice). They proclaimed that it was “a universal mechanism for transporting substances into any living cell.” Initially it was constructed to accelerate small tungsten particles 1-4 um in diameter at velocities of 1000-2000 ft/sec. They found with these speeds the particles would be able to penetrate cell walls (Sanford et al., 1987). Also in 1987, Klein and colleagues used a similar approach to transiently transform onion epidermal cells. In 1988, they achieved stable transformation using particle bombardment.

To do this, they had to isolate cells, blast those cells with particles coated with DNA, and wait for the cells to recover.

The original gene gun, described by Sanford et al. (1987), consisted of a macro-carrier filled with millions of tungsten nanoparticles coated with DNA. The macro-carrier would be placed in front of a 0.22 caliber barrel. When the gun powder was fired, the nanoparticles containing biomolecules were accelerated toward a stopping disk with a small hole. Only the tungsten particles could pass through this. Before firing the particle gun, they would align the desired tissue for delivery under the particle gun (Sanford et al., 1987). Modern day gene guns no longer rely on gunpowder charges; they use electrostatic, pneumatic, or compressed (high-pressure) gas propulsion forces (Ozyigit and Kurtoglu, 2020; Christou, 1992; Zhang et al., 2014). The benefits of this technique include: the ability to transform plant species recalcitrant to *Agrobacterium*-mediated transformation, the ability to transform diverse tissue and cell types, and the ability to transform plants with multiple plasmids to simultaneously conduct transformation of multiple genes using only one selectable marker (Ozyigit and Kurtoglu, 2020).

Because of the nonspecific localization of genetic cargo delivery, it can be used to mediate transformation of nuclear, plastid, and mitochondrial genomes (Cunningham et al., 2018). Some of the drawbacks of this method include the necessity of expensive equipment and supplies, it has a low throughput, and it requires more DNA than *Agrobacterium*-mediated delivery (Ozyigit and Kurtoglu, 2020; Cunnginham et al., 2018). Furthermore, there can be resulting damage to the target tissue from the particle bombardment and low penetration depth of the particles (Cunnginham et al., 2018).

Protoplasts are plant cells without their cell walls, often referred to as “naked cells.” Normally, there is not much space between cell walls and the plasma membrane of plant cells as

this membrane is involved in cell wall synthesis (Davey et al., 2005). When placed in hypertonic solutions, plant cell plasma membranes contract from the cell walls. Removal of the cell wall results in the production of spherical structures that are sensitive to changes in osmolarity (Davey et al., 2005). Protoplasts from plants were first isolated in 1960 by Cocking (Cocking, 1960). He reasoned that if bacterial and fungal protoplasts could be isolated using enzymes to digest the cell wall, then they could do something similar with plants. In this early work, Cocking placed the root tips of tomato seedlings in a phosphate buffer (pH 6.0) supplemented with 0.6 M sucrose, which acted as the osmotic stabilizer. He used cellulase to break down the cell wall. Cocking found two types of protoplasts, those with vacuoles and those without (Cocking, 1960). Before the enzymatic break down of cell walls, plant cells were first plasmolyzed by mannitol (reviewed by Yue et al., 2021).

The modern-day method for protoplast isolation is based on Cocking's enzymatic method. The plants are first plasmolyzed and then cell walls are digested enzymatically. The most used sources of protoplasts are leaf mesophyll (Sheen, 2001; Yue et al., 2021). To use leaves for protoplast isolation, the leaves are first cut into stripes. Then, in accordance with the *Nature* protocol from Dr. Jen Sheen's group, the strips are placed immediately in the enzyme cocktail that will eventually help to digest cell walls. To aid in the uptake of the enzymatic solution, the leaf strips are placed in a desiccator for vacuum infiltration (Yoo et al., 2007). There are some cases in which the epidermis on the abaxial side of a plant leaf is peeled off prior to forming leaf stripes (tobacco (Takebe et al., 1968), cereals: barely, wheat, and oat (Okuno and Furusawa, 1977), and Arabidopsis (Riazunnisa et al., 2007)). This has the benefit of allowing enzymes to enter the inter-mesophyll space and enhance cell wall digestion. A newer version of this protocol was developed by Wu et al. (2009) called the Tape-Arabidopsis Sandwich. This

method uses regular office tape to expose mesophyll cells on the abaxial side of a leaf. It is thought that this method is less physically damaging to a plant and can make protoplast isolation more convenient (Yu et al., 2021). There are some discrepancies as to which tape works best for the Tape-Arabidopsis Sandwich method, different tapes yield different peels (Riley, 2022, personal communication).

There are two commonly used methods to transiently transform protoplasts; PEG and electroporation (Sheen, 2001). With PEG transformation, protoplasts are placed in a solution of PEG supplemented with the plasmid of choice that the cells will be transformed with. The contents are mixed together by slow inversion of tubes and stored in the dark. After a certain period of time (variable between protoplast types and plasmids used for transformation), the protoplasts are ready for visualization/experimentation. PEG with the addition of calcium and magnesium at an alkaline pH can be used to promote binding of exogenous DNA to protoplasts; DNA is then taken in through endocytosis (Zerbini et al., 2014). For the electroporation method, protoplasts are first placed in a mixture of the plasmid of choice. This solution of foreign DNA and protoplasts is exposed to brief pulses of a continuous current with high voltage. These short pulses cause temporary pores to form in the protoplast cell membrane and allow plasmids to enter into the cells (Zerbini et al., 2014).

Protoplast transient transformation is advantageous in that it is versatile and that transformed protoplasts can be used for investigating plant genomics, transcriptomics, metabolomics, and epigenetic analyses (Xu et al., 2022). Additionally, protoplast transformation does not require any expensive equipment or sterile conditions and it can be performed in any laboratory (Xu et al., 2022). Some of the drawbacks for using protoplasts for transient transformation include the fact that they are artificial systems, protoplast cultures can be hard to

maintain (i.e. hard to get them to survive longer than a day), and protoplasts cannot be isolated from every plant species (Xu et al., 2022).

All three of the classic methods for plant transient transformation have benefits and limitations. They all affect plant physiology by inducing stress responses within plant tissues. Currently, nanomaterials are being developed for the delivery of biomolecules into plants because of their applicability to several different plant species and for their ability to increase transformation efficiency in planta (Kumar et al., 2020). Nanomaterials can be delivered into plants through passive delivery, a needless syringe, or with the air of ultrasound, a magnetic field, or a gene gun (Jat et al., 2020).

1.2 Plant Nanotechnology

What is nanotechnology?

Nanotechnology is a broad term encompassing many fields of technology. When first learning about this burgeoning field, we are taught what is means for something to be nano-sized. There is the concept there are 1,000,000,000 nanometers in a meter. To understand the nanoscale, consider that a hair strand is 80,000 -100,000 nanometers wide, and a sheet of paper is ~100,000 nm thick (National Nanotechnology Initiative, n.d.). Things on the nanoscale cannot be seen with the naked eye. Within this study, I used materials that were 1,000 times smaller than the thickness of a sheet of paper (on the order of hundreds of nanometers).

Nanotechnology was first termed by Dr. Norio Taniguchi in his paper “On the Basic Concept of Nanotechnology” in 1974. Taniguchi claimed that “Nano-technology mainly consists of the processing of separation, consolidation and deformation of materials by one atom or one molecule” (1974). While this was the first-time nanotechnology was termed, the origin behind

the idea of producing nanosized products employing atoms as the building blocks was introduced by Dr. Reymen in 1959 at the American Physics Society meeting in his lecture “There is a lot of space down there” (Tolochko, 2009). Since then, many different applications for nanotechnology have been developed, including the ability to create novel materials and products, and providing new tools to study biological phenomena (Kumar et al., 2023).

Application of Nanotechnology for Plants

The application of nanotechnology to plant systems/agronomy has been termed phytonanotechnology (Wang et al., 2016; Li and Yan, 2020). Phytonanotechnology allows for target-specific delivery of nanomaterials to plants. Such applications of nanomaterials could enhance existing functions within plants or create new functions in plants via delivery of DNA or genetic editing materials and help to increase resistance to pathogens through the deliver anti-pesticides/fungal-cides (Li and Yan, 2020; An et al., 2022). Nanomaterials can also be used to deliver fertilizers to plants (An et al., 2022).

Nanomaterials have tunable properties that can be altered to the requirements of different plants and tissues, including their size, shape, charge, and surface chemistry (Squire et al., 2023). The following nanomaterials have been used for delivery of genes/RNA/editing tools into plant cells: native or functionalized carbon nanotubes (Demirer et al., 2018; Liu et al., 2009), mesoporous silica nanoparticles (Torney et al., 2007; Chang et al., 2013), gold nanoparticles and nanoparticles made of other materials coated with gold, polymeric nanoparticles (Zhang et al., 2019b), DNA nanostructures (Zhang et al., 2019), layered double hydroxide clay nanosheets (Mitter et al., 2017), magnetic nanoparticles (used for pollen magnetofection) (Zhao et al., 2017), silicon carbide whiskers (Asad et al., 2011) and peptides as carriers for nucleic acids (Zheng et

al., 2017; Watanabe et al., 2021). There are several challenges associated with using nanomaterials. Nanoparticles have to be delivered to plant cells, which is most often achieved by diffusion in cell walls and endocytosis/diffusion through plasma membrane or by use of electric/magnetic field, and then cargo has to be released inside plant cells. Some of these methods and materials induce wounding or cytotoxicity and plant regeneration is difficult and time consuming for many crop species.

The following sections highlight work done in which silicon- and carbon-based nanomaterials were used as nanovehicles for delivery in plants.

1.3 Silicon Nanomaterials

Silicon is the second most abundant element in soils and considered to be the most common metalloid on earth (Epstein 1994; Rastogi et al., 2019). In soil, silicon is mainly in the form of silicic acid H_4SiO_4. In this form, silicon is readily absorbed by plants. Silicon content in plants has been reported to vary from 0.1 to 10%. Such variability in silicon content is thought to depend on mechanisms of silicon uptake and transport. Some plants have genetically encoded silicon transporters, others depend on lateral roots for silicon uptake, some may rely on passive diffusion for silicon transport, while others reject silicon uptake (Liang et al., 2007; Mitani and Ma 2005). Not all plants can take up silicon, it is considered to be a quasi-essential element for plants (Liang et al., 2007). While silicon is not essential for all plants for survival, plants still benefit from it. Silicon has been reported to help stimulate plant growth and help plants overcome both abiotic and biotic stressors (Souri et al., 2021). It can also help to strengthen the cell wall in some plants (Guerriero et al., 2016). In various plant biology papers, silica and silicon are used as interchangeable terms. This is not correct because they have different

chemical compositions. Silicon is a chemical element and silica is a chemical compound composed of silicon and oxygen. When reading the literature, make sure to confirm which compound the authors are referring to in their text. In summary, the benefits of bulk silicon in soil are well established. The advantages of Si nanomaterials over this bulk material are less explored (Rastogi et al., 2019).

Silicon carbide (SiC) whiskers are an example of a widely used silicon-based nanomaterial. They are produced through the thermal reduction of silica in a reducing atmosphere. Kaeppler and colleagues were the first to use SiC whiskers/fibers for DNA delivery in plant cells. They argued that it would be cheaper and less time-intensive to prepare than particle bombardment, more applicable to plant species recalcitrant to *Agrobacterium*-mediated transformation, and it would be fast (1990). SiC whiskers have high tensile strength, a high elastic modulus, and good shock and degradation resistance. SiC whiskers have a negatively charged surface. According to Asad and Arshad (2011) the whiskers function similarly to needles and facilitate DNA delivery by cell perforation and abrasion during mixing, which is the most important step of SiC whisker-mediated delivery. While effective, this method has only been effective in plant tissue culture and plant cells (Ramkumar et al., 2020).

Another widely used silicon-based nanomaterial is Si nanoparticles (SiNPs). There are two main types of SiNPs: solid and mesoporous (Hussain et al., 2013). Previous research using non-porous SiNPs focused on the uptake and phytotoxicity of these materials in rice and Arabidopsis (Hussain et al., 2013). Slombger and Schoenfisch (2012) noted that SiNPs accumulate in Arabidopsis roots, but that that silica scaffolds are not phytotoxic up to 1000 ppm despite uptake of vast amount of SiNPs in *A. thaliana.* Mesoporous Si nanoparticles (MSNs) are favorable in that they possess unique structural features, including their tunable pore size, large surface areas,

and well-defined surface properties to accommodate cargo of various sizes, shapes, and functionalities (Hussain et al., 2013). They were first used in 2007 for DNA delivery in plants via particle bombardment in intact plant tissue and in protoplasts (Torney et al., 2007). Hussain and colleagues (2013) expanded the use of MSNs to intact plant systems without the use of particle bombardment. To this end, they looked at the uptake of MSNs through the germination of wheat seeds in MS media supplemented with MSNs. Plants were grown in a hydroponic system and MSNs were uptaken through the roots. Additionally, they used vacuum infiltration in leaves and roots of Arabidopsis seedlings to deliver MSNs. They found that there was no phytotoxicity with the MSNs (Hussain et al., 2013).

Silicon nanowires, a type of semiconductor nanowire produced through vapor-liquid-solid mechanism, are of interest for plant delivery. They have unique properties that differ from bulk silicon materials. They have a high-aspect ratio, one-dimensional structure, and they are rigid enough to be mechanically manipulated (Kim et al., 2007). Additionally, they have been used for bioelectric modulation through photoelectrochemical or photothermal stimuli (Rotenberg, et al., 2020). Vertically aligned silicon nanowires attached to a rigid substrate have successfully been interfaced with mammalian cells (Kim et al., 2007) and have been shown to be a universal platform for delivering biomolecules into mammalian cells (Shalek et al., 2010). Freestanding silicon nanowires, those detached from their rigid substrate, have been shown to be internalized into several mammalian cell lines via endogenous phagocytosis pathway and are biocompatible (Zimmerman et al., 2016). Once inside a cell, it is possible that they are moved to different locations via motor proteins (Tian, personal communication, 2017). To the knowledge of the author, there have been no applications of silicon nanowires to plants. In chapter 2 the application of silicon nanowires to plants is explored.

1.4 Carbon Nanomaterials

Since 2004, graphene has been considered the "wonder material" of materials chemistry. It consists of a honeycomb lattice of a single layer of carbon atoms. It is one of the thinnest materials at 0.345 nm and one of the strongest materials (200 times stronger than steel). Graphene is also elastic and lightweight. Physicists Andre Geim and Konstantin Novoselov were awarded the Physics Nobel Prize in 2010 for their discovery. They isolated a monolayer of graphene from graphite using scotch tape (Puiu, 2023). Graphene is not the only carbon-based "wonder material." Carbon nanotubes and fullerenes are also considered to be "wonder-materials" for their wide-ranging, unique features and applicability to numerous fields (Zaytseva and Neumann 2016). Within the realm of plant biotechnology/plant nanotechnology there has been a large focus on using carbon-based nanomaterials for delivery in plants, mainly single-walled and multiwalled carbon nanotubes. They have been widely used for agricultural purposes because of their impacts on plant growth regulation, ability to cross plant cell walls, nano-transport, and potential use as biosensors (Safdar et al., 2022).

Fullerenes have cage-like structures made up of twelve 5-member carbon and unspecified number of 6-member carbon rings (Husen and Siddiqi 2014). They were first discovered by H.W. Kroto and colleagues in 1985 and later won the Nobel prize for chemistry in 1996. The most-well studied fullerene is C60, it is a symmetric spherical molecule comprised of 60 carbon atoms (Zaytseva and Neumann 2016). Fullerenes and fullerene-derivatives have been widely used to deliver drugs and to perform gene delivery in medicine and in cosmetics (Zaytseva and Neumann 2016; Kazemzadeh and Mozafari, 2019). At this point in time, fullerenes have not been used as a delivery system in plants. In 2010, Liu and colleagues investigated the effects of water-soluble fullerene (fullerene malonic acif derivative) on plants. For their experiments,

plants were grown in ½ MS plates supplemented with the water-soluble fullerene for 5 days. From these experiments, they noticed that the fullerenes had an inhibitory effect on plant growth, especially in the seedling roots. In addition to these growth assays, they performed fluorescence imaging on transgenic plants and observed cellular phytotoxic effects including microtubule disorganization and abnormal cell division in the root (Liu et al., 2010). In another study on bittermelons, it was found that exposure to fullerenes increased biomass yield and water content in the fruit (Kole et al., 2013).

One of the most used carbon-based nanomaterials in plant biology/agriculture is carbon nanotubes. They have a crystal structure that is close to that of graphite (both have sp^2 bonded carbon atoms). Different geometries of carbon nanotubes can impact their properties and applications to plants (Verma et al., 2019; Lahiani, et al., 2016). Single walled carbon nanotubes (SWCNTSs) are classified as one-dimensional nanomaters because of their large surface area. Multiwalled carbon nanotubes (MWCNTs), consist of multiple graphite shells with a lateral spacing of 0.34 nm between the shells. They are comprised of many graphite shells surrounding a hollow core. MWCNTs were discovered first, and SWCNTs were synthesized shortly thereafter (Rudakiya et al., 2019). MWCNTs and SWCNTs have the potential to be used as nanovehicles for delivery in plants. In 2009, SWCNTs were first used for gene delivery in plants (Liu et al., 2009). In this study, the authors used confocal microscopy to visualize SWCNTs labeled with FITC or ssDNA in *Nicotiana tabacum* cells (Liu et al., 2009). Demirer and colleagues demonstrated that functionalized SWCNTs could be used to deliver plasmid DNA into intact plants without transgene integration (Demirer et al., 2009; Demirer et al., 2009b). In preliminary experiments, Demirer reported that poly-ethylenimine (PEI) functionalized SWCNTs were 700 times more efficient than plasmid DNA absorbed on pristine MWCNTs for

delivery in plants; for this reason, all of their experiments/papers report using PEI functionalized SWCNTs (Demirer, 2020). To apply SWCNTs to intact plant systems, a needless syringe is filled with the CNTs and pressure infiltration is applied for delivery (Gonzalez-Grandio et al., 2021). Additionally, Gonzalez-Grandio and colleagues (2021) found that biocompatibility of SWCNTs in plants is determined by their surface chemistry. The SWCNTs have also been used for delivering nucleic acids to chloroplasts (Kwak et al., 2019). CNTs are efficient systems for delivery in plants as they are able to traverse the cell wall. Wong et al. described this phenomenon as the lipid exchange envelope penetration (2016). In this model, the ability of carbon nanotubes and other NPs to penetrate cell walls and membranes is controlled by the size of the nanomaterial and its surface charge (Wong et al., 2016).

While carbon-based nanomaterials present several benefits and opportunities, there are mixed results pertaining to the effect of these materials on plants, ranging from beneficial to acute toxicity (Verma et al., 2019). The effects of carbon-based nanomaterials are varied and depend on several factors including specific features of the nanomaterial (i.e. geometry and porosity), type of plant and the part of the plant exposed to the nanomaterial, concentration of the nanomaterial being used and application method/delivery method of the nanomaterial (Verma et al., 2019). In section VI, I discuss the application of vertically aligned carbon nanofibers (VACNF) arrays to plants as well as detailing details of how these fibers are microfabricated.

1.5 Which is the better material to use: carbon or silicon?

There have been no direct comparisons conducted between carbon-based nanomaterials and silicon-based nanomaterials in plants. However, there have been toxicology studies performed in sea urchins (Pikula et al., 2020), microalgae (Pikula et al., 2018; Pikkula et al., 2020b), and

marine bivalves (Pikula et al., 2020c). The results varied, and no conclusion can be drawn about which material is more cytotoxic (Pikula et al., 2020; Pikula et al., 2018; Pikula et al., 2020b; Pikula et al., 2020c). Conversely, there are studies in which silica- and carbon-based nanomaterials are used together for seed priming in *Brassica juncea* (Dhingra et al., 2022). Dhingra and colleagues (2022) found that this method increased silique length and the number of seeds per silique. Additionally, silica and carbon nanotubes have been combined to create a composite material (Saleh, 2015; Saleh, 2016). Elemental mapping showed a uniform distribution of silica NPs across CNTs (Saleh, 2015). These composite materials have the potential to be used for delivery in plants. In this dissertation, I explore the applications of both carbon- and silicon-based nanomaterials in plants.

1.6 Vertically Aligned Carbon Nanofibers (VACNF)

Based on existing issues with carbon nanotubes, we decided to focus on attention on vertically aligned carbon nanofiber (VACNF) arrays. These carbon nanofibers have successfully been used to deliver proteins, dextrans and dyes to plant leaves without causing a wound response (Davern et al., 2016). Unlike CNTs, carbon nanofibers are solid. Additionally, they resemble insect mouthpieces (stylets) with taper, diameter, and length (Davern et al., 2016; Guerrieri and Digilio, 2008). Aphids, insect pest to agriculture and forest crops, use their long, flexible stylets to penetrate intercellular boundaries of plants to feed off phloem sap (Guerrieri and Digilio, 2008). VACNFs usually have tip diameters <200 nm, based diameters of at least 500 nm, and a controllable height ranging from a few microns to >40 microns (Melechko et al., 2005). Because of these similarities it was thought that VACNF would be applicable to many

plant species, in addition to the poplar and Arabidopsis plants that they were applied to in the work of Davern and colleagues (2016).

The VACNFs described in this body of work are grown using a direct current catalytic plasma-enhanced chemical-vapor deposition (dc C-PECVD) machine with a Ni catalyst. The position, diameter, and the length of Ni catalyst were controlled using a combination of electron beam lithography, metal evaporation, and lift-off processes as described by Melechko et al. (2005; 2009). Fibers grown in this matter have been also applied to mammalian cells for gene delivery, for RNA interference and gene silencing, and to serve as a 3-D electrical interface for neurons (McKnight et al., 2004; Mann et al., 2008; McKnight et al., 2003; Nguyen et al., 2007). To use VACNFs with mammalian cells the following approach has been used. First, the fibers are coated with DNA (either wet DNA or the DNA is spot dried on a VACNF chip) (McKnight et al., 2004). Then, the VACNF chips are applied to cells by either centrifuging suspensions of cells onto the chips or by pressing the chips into groups of cells (McKnight et al., 2004). This transfer mechanism is the result of the simultaneous direct penetration into cells and delivery of DNA (McKnight et al., 2004). Prior to delivery to cells, it is possible to surface functionalize the fibers such that the DNA would be tethered to the fibers (Mann et al., 2007; Fletcher et al, 2006).

VACNF arrays were also applied to plants by Davern and colleagues (2016). They used the fibers to deliver 1-2 microliters of LYCH dye (1 mM), 500-kDa-FITC dextran (0.1 mg/ml), and pumpkin proteins OG-CmPP16-1 and 135I-CmPP16-1 (13 μM) (Davern et al., 2016). To use the VACNF chips to deliver the dyes and proteins, a 1-2 μl droplet of the dye or protein was placed on the adaxial side of the leaf. A VACNF chip would then be placed on top of the droplet such that the fibers would meet the tissue. Next, a pair of tweezers was used to gently tap the VACNF chip into the leaf. After the desired delivery period, the chip was removed from the plant surface

(Davern et al., 2016). Davern and colleagues (2016) found that VACNF-mediated delivery in the Poplar leaves was minimally invasive and did not elicit a wound response in the plant tissue.

As widely used as VACNF arrays are, the way they achieve delivery, especially in plants, has yet to be elucidated. In their paper, Davern et al. (2016) put forward three hypotheses for how the fibers were able to achieve delivery in plants. Hypothesis #1: After impalement of the fibers, the plasma membrane would tightly close-up around them. Molecules would be delivered during impalement and/or from desorption from the surface of the embedded fibers. Hypothesis #2: After tapping, the plasma membrane may not close completely around the fibers. This would leave channels/pore open around the fibers through which molecules could diffuse into cells. Hypothesis #3: During impalement, tissue wounding could occur, creating an opening through which molecules could enter. The damaged cell may or may not recover (Davern et al., 2016). Based on the results of their study, Davern et al. (2016) thought that the first two hypotheses/scenarios best explained what they observed. However, they could not determine whether delivery via impalement of VACNFs occurred from desorption of the fibers or from molecules essentially leaking into the plant (Davern et al., 2016). The results from Morgan et al., (2022, See Chapter 3) supports the notion that both scenarios could be taking place.

1.7 OBJECTIVES OF THIS THESIS

The objective of this study was to develop nanomaterials that could be utilized for transient transformation as well as to describe advancements in the use of vertically aligned carbon nanofibers for plant delivery.

1.8 WORKS CITED

Ahmad, P., Ashraf, M., Younis, M., Hu, X., Kumar, A., Akram, N. A., & Al-Qurainy, F. (2012). Role of transgenic plants in agriculture and biopharming. *Biotechnology Advances*, *30*(3), 524-540.

Altpeter, F., Springer, N. M., Bartley, L. E., Blechl, A. E., Brutnell, T. P., Citovsky, V., ... & Stewart, C. N. (2016). Advancing crop transformation in the era of genome editing. The *Plant Cell*, *28*(7), 1510-1520.

An, C., Sun, C., Li, N., Huang, B., Jiang, J., Shen, Y., ... & Wang, Y. (2022). Nanomaterials and nanotechnology for the delivery of agrochemicals: strategies towards sustainable agriculture. *Journal of Nanobiotechnology*, *20*(1), 1-19.

Asad, S. & Arshad, M. in Properties and Applications of Silicon Carbide (ed. Gerhardt, R.) Ch. 15 (InTech, London, 2011).

Britton, M. T., Escobar, M. A., & Dandekar, A. M. (2008). The oncogenes of *Agrobacterium tumefaciens* and *Agrobacterium rhizogenes*. *Agrobacterium: from biology to biotechnology*, 523-563.

Chang, F. P., Kuang, L. Y., Huang, C. A., Jane, W. N., Hung, Y., Yue-ie, C. H., & Mou, C. Y. (2013). A simple plant gene delivery system using mesoporous silica nanoparticles as carriers. *Journal of Materials Chemistry B*, *1*(39), 5279-5287.

Christou, P. (1992). Genetic transformation of crop plants using microprojectile bombardment. *The Plant Journal*, *2*(3), 275-281.

Cocking, E. C. (1960). A method for the isolation of plant protoplasts and vacuoles. *Nature*, *187*, 962-963.

Cunningham, F. J., Goh, N. S., Demirer, G. S., Matos, J. L., & Landry, M. P. (2018).

Nanoparticle-mediated delivery towards advancing plant genetic engineering. *Trends in Biotechnology*, *36*(9), 882-897.

Davern, S. M., McKnight, T. E., Standaert, R. F., Morrell-Falvey, J. L., Shpak, E. D., Kalluri, U. C., ... & Mirzadeh, S. (2016). Carbon nanofiber arrays: a novel tool for microdelivery of biomolecules to plants. *PLoS One*, *11*(4), e0153621.

Davey, M. R., Anthony, P., Power, J. B., & Lowe, K. C. (2005). Plant protoplasts: status and biotechnological perspectives. *Biotechnology Advances*, *23*(2), 131-171.

Demirer, G. S., Chang, R., Zhang, H., Chio, L., & Landry, M. P. (2018). Nanoparticle-guided biomolecule delivery for transgene expression and gene silencing in mature plants. *Biophysical Journal*, *114*(3), 217a.

Demirer, G. S., Zhang, H., Matos, J. L., Goh, N. S., Cunningham, F. J., Sung, Y., ... & Landry, M. P. (2019). High aspect ratio nanomaterials enable delivery of functional genetic material without DNA integration in mature plants. *Nature Nanotechnology*, *14*(5), 456-464.

Demirer, G. S., Zhang, H., Goh, N. S., González-Grandío, E., & Landry, M. P. (**2019) b.** Carbon nanotube–mediated DNA delivery without transgene integration in intact plants. *Nature Protocols*, *14*(10), 2954-2971.

Demirer, G. S. (2020). *Developing Nanomaterial Platforms for Gene Delivery and Transgene-Free Plant Genetic Engineering*. University of California, Berkeley.

Dhingra, P., Sharma, S., Singh, K. H., Kushwaha, H. S., Barupal, J. K., Haq, S., ... & Kachhwaha, S. (2022). Seed priming with carbon nanotubes and silicon dioxide nanoparticles influence agronomic traits of Indian mustard (Brassica juncea) in field experiments. *Journal of King Saud University-Science*, *34*(4), 102067.

Epstein, E. (1994). The anomaly of silicon in plant biology. *Proceedings of the National Academy of Sciences*, *91*(1), 11-17.

Fletcher, B. L., McKnight, T. E., Melechko, A. V., Simpson, M. L., & Doktycz, M. J. (2006). Biochemical functionalization of vertically aligned carbon nanofibres. *Nanotechnology*, *17*(8), 2032.

González-Grandío, E., Demirer, G. S., Jackson, C. T., Yang, D., Ebert, S., Molawi, K., ... & Landry, M. P. (2021). Carbon nanotube biocompatibility in plants is determined by their surface chemistry. *Journal of Nanobiotechnology*, *19*(1), 1-15.

Guerrieri, E., & Digilio, M. C. (2008). Aphid-plant interactions: a review. *Journal of Plant Interactions*, *3*(4), 223-232.

Guerriero, G., Hausman, J. F., & Legay, S. (2016). Silicon and the plant extracellular matrix. *Frontiers in Plant Science*, *7*, 463.

Hansen, G., Das, A., & Chilton, M. D. (1994). Constitutive expression of the virulence genes improves the efficiency of plant transformation by Agrobacterium. *Proceedings of the National Academy of Sciences*, *91*(16), 7603-7607.

He, P., Shan, L., & Sheen, J. (2007). The use of protoplasts to study innate immune responses. *Plant-Pathogen Interactions: Methods and Protocols*, 1-9.

Husen, A., & Siddiqi, K. S. (2014). Carbon and fullerene nanomaterials in plant system. *Journal of Nanobiotechnology*, *12*(1), 1-10.

Hussain, H. I., Yi, Z., Rookes, J. E., Kong, L. X., & Cahill, D. M. (2013). Mesoporous silica nanoparticles as a biomolecule delivery vehicle in plants. *Journal of Nanoparticle Research*, *15*, 1-15.

Hwang, H. H., Yu, M., & Lai, E. M. (2017). Agrobacterium-mediated plant transformation: biology and applications. *The Arabidopsis Book, 15*.

Jat, S. K., Bhattacharya, J., & Sharma, M. K. (2020). Nanomaterial based gene delivery: a promising method for plant genome engineering. *Journal of Materials Chemistry B, 8*(19), 4165-4175.

Jones, H. D., & Sparks, C. A. (2009). Stable transformation of plants. *Plant Genomics: Methods and Protocols*, 111-130.

Kaeppler, H. F., Gu, W., Somers, D. A., Rines, H. W., & Cockburn, A. F. (1990). Silicon carbide fiber-mediated DNA delivery into plant cells. *Plant Cell Reports, 9*, 415-418.

Karami, O. (2008). Factors affecting Agrobacterium-mediated transformation of plants. *Transgenic Plant J, 2*(2), 127-137.

Kazemzadeh, H., & Mozafari, M. (2019). Fullerene-based delivery systems. *Drug Discovery Today, 24*(3), 898-905.

Klein, T. M., Wolf, E. D., Wu, R., & Sanford, J. C. (1987). High-velocity microprojectiles for delivering nucleic acids into living cells. *Nature, 327*(6117), 70-73.

Klein, T. M., Harper, E. C., Svab, Z., Sanford, J. C., Fromm, M. E., & Maliga, P. (1988). Stable genetic transformation of intact Nicotiana cells by the particle bombardment process. *Proceedings of the National Academy of Sciences, 85*(22), 8502-8505.

Kole, C., Kole, P., Randunu, K. M., Choudhary, P., Podila, R., Ke, P. C., ... & Marcus, R. K. (2013). Nanobiotechnology can boost crop production and quality: first evidence from increased plant biomass, fruit yield and phytomedicine content in bitter melon (Momordica charantia). *BMC Biotechnology, 13*(1), 1-10.

Kumar, S., Nehra, M., Dilbaghi, N., Marrazza, G., Tuteja, S. K., & Kim, K. H. (2020).

Nanovehicles for plant modifications towards pest-and disease-resistance traits. *Trends in Plant Science*, *25*(2), 198-212.

Kumar, K., Gambhir, G., Dass, A., Tripathi, A. K., Singh, A., Jha, A. K., ... & Rakshit, S. (2020b). Genetically modified crops: current status and future prospects. *Planta*, *251*, 1-27.

Kumar, R., Kumar, M., & Luthra, G. (2023). Fundamental approaches and applications of nanotechnology: A mini review. *Materials Today: Proceedings*.

Kwak, S. Y., Lew, T. T. S., Sweeney, C. J., Koman, V. B., Wong, M. H., Bohmert-Tatarev, K., ... & Strano, M. S. (2019). Chloroplast-selective gene delivery and expression in planta using chitosan-complexed single-walled carbon nanotube carriers. *Nature Nanotechnology*, *14*(5), 447-455.

Lahiani, M. H., Dervishi, E., Ivanov, I., Chen, J., & Khodakovskaya, M. (2016). Comparative study of plant responses to carbon-based nanomaterials with different morphologies. *Nanotechnology*, *27*(26), 265102.

Lee, L. Y., & Gelvin, S. B. (2008). T-DNA binary vectors and systems. *Plant Physiology*, *146*(2), 325-332.

Li, J. F., Park, E., von Arnim, A. G., & Nebenführ, A. (2009). The FAST technique: a simplified *Agrobacterium*-based transformation method for transient gene expression analysis in seedlings of Arabidopsis and other plant species. *Plant Methods*, *5*, 1-15.

Li, C., & Yan, B. (2020). Opportunities and challenges of phyto-nanotechnology. *Environmental Science: Nano*, *7*(10), 2863-2874.

Liang, Y., Sun, W., Zhu, Y. G., & Christie, P. (2007). Mechanisms of silicon-mediated

alleviation of abiotic stresses in higher plants: a review. *Environmental Pollution*, *147*(2), 422-428.

Liu, Q., Chen, B., Wang, Q., Shi, X., Xiao, Z., Lin, J., & Fang, X. (2009). Carbon nanotubes as molecular transporters for walled plant cells. *Nano Letters*, *9*(3), 1007-1010.

Liu, Q., Zhao, Y., Wan, Y., Zheng, J., Zhang, X., Wang, C., ... & Lin, J. (2010). Study of the inhibitory effect of water-soluble fullerenes on plant growth at the cellular level. *ACS Nano*, *4*(10), 5743-5748.

Mann, D. G., McKnight, T. E., Melechko, A. V., Simpson, M. L., & Sayler, G. S. (2007). Quantitative analysis of EDC-condensed DNA on vertically aligned carbon nanofiber gene delivery arrays. *Biotechnology and Bioengineering*, *97*(4), 680-688.

Mann, D. G., McKnight, T. E., McPherson, J. T., Hoyt, P. R., Melechko, A. V., Simpson, M. L., & Sayler, G. S. (2008). Inducible RNA interference-mediated gene silencing using nanostructured gene delivery arrays. *Acs Nano*, *2*(1), 69-76.

McKnight, T. E., Melechko, A. V., Griffin, G. D., Guillorn, M. A., Merkulov, V. I., Serna, F., ... & Simpson, M. L. (2003). Intracellular integration of synthetic nanostructures with viable cells for controlled biochemical manipulation. *Nanotechnology*, *14*(5), 551

McKnight, T. E., Melechko, A. V., Hensley, D. K., Mann, D. G., Griffin, G. D., & Simpson, M. L. (2004). Tracking gene expression after DNA delivery using spatially indexed nanofiber arrays. *Nano Letters*, *4*(7), 1213-1219.

Melechko, A. V., Merkulov, V. I., McKnight, T. E., Guillorn, M. A., Klein, K. L., Lowndes, D. H., & Simpson, M. L. (2005). Vertically aligned carbon nanofibers and related structures: Controlled synthesis and directed assembly. *Journal of Applied Physics*, *97*(4), 3.

Melechko, A. V., Desikan, R., McKnight, T. E., Klein, K. L., & Rack, P. D. (2009). Synthesis of

vertically aligned carbon nanofibres for interfacing with live systems. *Journal of Physics D: Applied Physics*, *42*(19), 193001.

Mitani, N., & Ma, J. F. (2005). Uptake system of silicon in different plant species. *Journal of Experimental Botany*, *56*(414), 1255-1261.

Mitter, N., Worrall, E. A., Robinson, K. E., Li, P., Jain, R. G., Taochy, C., ... & Xu, Z. P. (2017). Clay nanosheets for topical delivery of RNAi for sustained protection against plant viruses. *Nature Plants*, *3*(2), 1-10.

Morgan, J. M., Jelenska, J., Hensley, D., Retterer, S. T., Morrell-Falvey, J. L., Standaert, R. F., & Greenberg, J. T. (2022). *An efficient and broadly applicable method for transient transformation of plants using vertically aligned carbon nanofiber arrays.*

Nguyen-Vu, T. B., Chen, H., Cassell, A. M., Andrews, R. J., Meyyappan, M., & Li, J. (2007). Vertically aligned carbon nanofiber architecture as a multifunctional 3-D neural electrical interface. *IEEE Transactions on Biomedical Engineering*, *54*(6), 1121-1128.

Okuno, T., & Furusawa, I. (1977). A simple method for the isolation of intact mesophyll protoplasts from cereal plants. *Plant and Cell Physiology*, *18*(6), 1357-1362.

Ozyigit, I. I., & Yucebilgili Kurtoglu, K. (2020). Particle bombardment technology and its applications in plants. *Molecular Biology Reports*, *47*, 9831-9847.

Pikula, K. S., Zakharenko, A. M., Chaika, V. V., Vedyagin, A. A., Orlova, T. Y., Mishakov, I. V., ... & Golokhvast, K. S. (2018). Effects of carbon and silicon nanotubes and carbon nanofibers on marine microalgae Heterosigma akashiwo. *Environmental Research, 166*, 473-480.

Pikula, K., Zakharenko, A., Chaika, V., Em, I., Nikitina, A., Avtomonov, E., ... & Golokhvast,

K. (2020). Toxicity of carbon, silicon, and metal-based nanoparticles to sea urchin strongylocentrotus intermedius. *Nanomaterials*, *10*(9), 1825.

Pikula, K., Chaika, V., Zakharenko, A., Markina, Z., Vedyagin, A., Kuznetsov, V., ... & Golokhvast, K. (2020b). Comparison of the level and mechanisms of toxicity of carbon nanotubes, carbon nanofibers, and silicon nanotubes in bioassay with four marine microalgae. *Nanomaterials*, *10*(3), 485.

Pikula, K., Chaika, V., Zakharenko, A., Savelyeva, A., Kirsanova, I., Anisimova, A., & Golokhvast, K. (2020c). Toxicity of carbon, silicon, and metal-based nanoparticles to the hemocytes of three marine bivalves. *Animals*, *10*(5), 827.

Puiu, T. (2019, March 27). *The 'wonder material': How graphene is set to change the world*. Lindau Nobel Laureate Meetings. Retrieved April 13, 2023, from https://www.lindau-nobel.org/blog-the-wonder-material-graphene/

Ramkumar, T. R., Lenka, S. K., Arya, S. S., & Bansal, K. C. (2020). A short history and perspectives on plant genetic transformation. *Biolistic DNA Delivery in Plants: Methods and Protocols*, 39-68.

Rastogi, A., Tripathi, D. K., Yadav, S., Chauhan, D. K., Živčák, M., Ghorbanpour, M., ... & Brestic, M. (2019). Application of silicon nanoparticles in agriculture. *3 Biotech*, *9*, 1-11.

Riazunnisa, K., Padmavathi, L., Scheibe, R., & Raghavendra, A. S. (2007). Preparation of Arabidopsis mesophyll protoplasts with high rates of photosynthesis. *Physiologia Plantarum*, *129*(4), 879-886.

Rogers, S. G., Horsch, R. B., & Fraley, R. T. (1986). Gene transfer in plants: production of

transformed plants using Ti plasmid vectors. In *Methods in Enzymology* (Vol. 118, pp. 627-640). Academic Press.

Rudakiya, D., Patel, Y., Chhaya, U., & Gupte, A. (2019). Carbon nanotubes in agriculture: production, potential, and prospects. *Nanotechnology for Agriculture: Advances for Sustainable Agriculture*, 121-130.

Saleh, T. A. (2015). Isotherm, kinetic, and thermodynamic studies on Hg (II) adsorption from aqueous solution by silica-multiwall carbon nanotubes. *Environmental Science and Pollution Research*, *22*, 16721-16731.

Saleh, T. A. (2016). Nanocomposite of carbon nanotubes/silica nanoparticles and their use for adsorption of Pb (II): from surface properties to sorption mechanism. *Desalination and Water Treatment*, *57*(23), 10730-10744.

Safdar, M., Kim, W., Park, S., Gwon, Y., Kim, Y. O., & Kim, J. (2022). Engineering plants with carbon nanotubes: a sustainable agriculture approach. *Journal of Nanobiotechnology*, *20*(1), 1-30.

Sanford, J. C., Klein, T. M., Wolf, E. D., & Allen, N. (1987). Delivery of substances into cells and tissues using a particle bombardment process. *Particulate Science and Technology*, *5*(1), 27-37.

Sheen, J. (2001). Signal transduction in maize and Arabidopsis mesophyll protoplasts. *Plant Physiology*, *127*(4), 1466-1475

Size of the nanoscale. National Nanotechnology Initiative. (n.d.). Retrieved April 13, 2023, from https://www.nano.gov/nanotech-101/what/nano-size

Squire, H. J., Tomatz, S., Voke, E., González-Grandío, E., & Landry, M. (2023). The emerging

role of nanotechnology in plant genetic engineering. *Nature Reviews Bioengineering*, 1-15.

Slomberg, D. L., & Schoenfisch, M. H. (2012). Silica nanoparticle phytotoxicity to Arabidopsis thaliana. *Environmental Science & Technology*, *46*(18), 10247-10254.

Souri, Z., Khanna, K., Karimi, N., & Ahmad, P. (2021). Silicon and plants: current knowledge and future prospects. *Journal of Plant Growth Regulation*, *40*, 906-925.

Takebe, I., Otsuki, Y., & Aoki, S. (1968). Isolation of tobacco mesophyll cells in intact and active state. *Plant and Cell Physiology*, *9*(1), 115-124.

Taniguchi, N. (1974). On the basic concept of nanotechnology. *Proceeding of the ICPE*.

Tolochko, N. K. (2009). History of nanotechnology. *Encyclopedia of Life Support Systems (EOLSS)*.

Torney, F., Trewyn, B. G., Lin, V. S. Y., & Wang, K. (2007). Mesoporous silica nanoparticles deliver DNA and chemicals into plants. *Nature Nanotechnology*, *2*(5), 295-300.

Verma, S. K., Das, A. K., Gantait, S., Kumar, V., & Gurel, E. (2019). Applications of carbon nanomaterials in the plant system: A perspective view on the pros and cons. *Science of the Total Environment*, *667*, 485-499.

Wang, P., Lombi, E., Zhao, F. J., & Kopittke, P. M. (2016). Nanotechnology: a new opportunity in plant sciences. *Trends in Plant Science*, *21*(8), 699-712.

Watanabe, K., Odahara, M., Miyamoto, T., & Numata, K. (2021). Fusion peptide-based biomacromolecule delivery system for plant cells. *ACS Biomaterials Science & Engineering*, *7*(6), 2246-2254.

Will, T., & van Bel, A. J. (2006). Physical and chemical interactions between aphids and plants. *Journal of Experimental Botany*, *57*(4), 729-737.

Wong, M. H., Misra, R. P., Giraldo, J. P., Kwak, S. Y., Son, Y., Landry, M. P., ... & Strano, M. S. (2016). Lipid exchange envelope penetration (LEEP) of nanoparticles for plant engineering: a universal localization mechanism. *Nano Letters*, *16*(2), 1161-1172.

Wu, F. H., Shen, S. C., Lee, L. Y., Lee, S. H., Chan, M. T., & Lin, C. S. (2009). Tape-Arabidopsis Sandwich-a simpler Arabidopsis protoplast isolation method. *Plant Methods*, *5*, 1-10.

Xu, Y., Li, R., Luo, H., Wang, Z., Li, M. W., Lam, H. M., & Huang, C. (2022). Protoplasts: small cells with big roles in plant biology. *Trends in Plant Science*, *27*(8).

Yoo, S. D., Cho, Y. H., & Sheen, J. (2007). Arabidopsis mesophyll protoplasts: a versatile cell system for transient gene expression analysis. *Nature Protocols*, *2*(7), 1565-1572.

Yue, J. J., Yuan, J. L., Wu, F. H., Yuan, Y. H., Cheng, Q. W., Hsu, C. T., & Lin, C. S. (2021). Protoplasts: From isolation to CRISPR/Cas genome editing application. *Frontiers in Genome Editing*, *3*, 717017.

Zaytseva, O., & Neumann, G. (2016). Carbon nanomaterials: production, impact on plant development, agricultural and environmental applications. *Chemical and Biological Technologies in Agriculture*, *3*(1), 1-26.

Zerbini, F. M., da Silva, F. N., Patricia, G., Urquiza, C., & Basso, M. F. (2014). Transgenic plants. *Biotechnology and Plant Breeding: Applications and Approaches for Developing Improved Cultivars*, *1*, 179-199.

Zhang, D., Das, D. B., & Rielly, C. D. (2014). Potential of microneedle-assisted micro-particle delivery by gene guns: a review. *Drug Delivery*, *21*(8), 571-587.

Zhang, H., Demirer, G. S., Zhang, H., Ye, T., Goh, N. S., Aditham, A. J., ... & Landry, M. P.

(2019). DNA nanostructures coordinate gene silencing in mature plants. *Proceedings of the National Academy of Sciences*, *116*(15), 7543-7548.

Zhang, Z., Wan, T., Chen, Y., Chen, Y., Sun, H., Cao, T., ... & Huang, J. (2019b). Cationic polymer-mediated CRISPR/Cas9 plasmid delivery for genome editing. *Macromolecular Rapid Communications*, *40*(5), 1800068.

Zhao, X., Meng, Z., Wang, Y., Chen, W., Sun, C., Cui, B., ... & Luo, D. (2017). Pollen magnetofection for genetic modification with magnetic nanoparticles as gene carriers. *Nature Plants*, *3*(12), 956-964.

Zheng, N., Song, Z., Liu, Y., Yin, L., Cheng, J. (2017). Gene delivery into isolated *Arabidopsis thaliana* protoplasts and intact leaves using cationic, α-helical polypeptide. *Frontiers in Chemical Science Engineering*, *11*, 521–528.

CHAPTER 2

Crystalline Silicon Transport and Processing in Plants

PREFACE:

This chapter includes a summary of the collaborative work of myself and Dr. Vishnu Nair completed under the supervision of Dr. Jean Greenberg and Dr. Bozhi Tian. The goal of this work was to test the utility of silicon nanowires for delivery in plants. Within the study we present preliminary evidence of the degradation of crystalline silicon to polysilicic acid. My contributions to the work are as follows: I collaborated with Dr. Vishnu Nair to perform all the experiments and wrote the document in its current form. I prepared all of the samples for electron microscopy, confocal microscopy, ICP-MES, and for the molybidic acid assay. I aided with the data analysis. Dr. Nair wrote a document about these experiments. I revised and edited the document in collaboration with Dr. Nair, Dr. Greenberg, and Dr. Tian.

ABSTRACT

Nanotechnology plays an important role in reforming agriculture and food production processes. Nanomaterials are being used for delivery of nutrients, to make genetically modified organisms, and to deliver pesticides. There is a lack of knowledge about the plant physiological response to nanocarrier uptake and delivery. The focus of this work is to investigate the biocompatibility of silicon nanowires with Arabidopsis seedlings and to understand how silicon nanowires degrade after they are taken up into Arabidopsis roots. Using electron microscopy, we tracked the changes in silicon nanowire geometry and morphology throughout the root. Silicon content of Arabidopsis seedlings grown with or without silicon nanowires was determined using inductively coupled plasma-optical emission spectroscopy and molybdic acid assays. With our

findings we postulate that the degradation of the crystalline silicon nanowires is a result of pH changes in the environment of the Arabidopsis root.

INTRODUCTION

Nanomaterials have been utilized for the delivery of pesticides, materials for stable and transient transformations of plants, and much needed nutrients (Banerjee et al, 2019). They have the advantages of timed-release, precise targeting, and the ability to overcome biological barriers, such as the cell wall.

Within the realm of plant biotechnology/plant nanotechnology there has been a large focus on using carbon-based nanomaterials for delivery in plants, i.e. single walled and multiwalled carbon nanotubes. Carbon-based nanomaterials have attracted more attention than other nanomaterials in part due to their physiochemical properties: small size, high surface area, and mechanical and thermal strength (Fincheria et al., 2021). Additionally, they have been used for agricultural purposes because of their impacts on plant growth regulation, ability to cross plant cell walls, nano-transport, and potential use as biosensors (Safdar et al., 2022). While carbon-based nanomaterials present several benefits and opportunities, there are mixed results pertaining to the effect of these materials on plants, ranging from beneficial to acute toxicity (Verma et al., 2019). The effects of carbon-based nanomaterials are varied and depend on several factors including specific features of the nanomaterial (i.e. geometry and porosity), type of plant and the part of the plant exposed to the nanomaterial, concentration of the nanomaterial being used and application method/delivery method of the nanomaterial (Verma et al., 2019).

Silicon-based nanomaterials have also been widely used in plants for delivery. Si has a beneficial role in plants, for example it can stimulate plant growth and help plants to overcome

biotic stressors (Souri et al., 2021). Si has been known to alleviate metal toxicity and osmotic stresses, regulate nutrient uptake, improve nutrient deficiency and imbalance in plants, and increase resistance to both biotic and abiotic stresses in plants (Souri et al., 2021).

One example of a silicon-based nanomaterial used with plants is silicon carbide whiskers. SiC whiskers are of interest due to their favorable characteristics (high tensile strength, high elastic modulus, and good shock resistance) (Asad and Arshad, 2008). There are different postulations about how SiC whiskers have been used for DNA delivery in plants. Kaeppler and colleagues thought SiC whiskers penetrate through the cell walls of maize plants (Asad and Arshad, 2008). Additionally, it is thought that the whiskers function similarly to needles and facilitate DNA delivery by cell perforation and abrasion during mixing, which is the most important step of SiC whisker mediated delivery (Ramkumar et al., 2020).

Another commonly used silica-based nanomaterial is mesoporous silica nanoparticles (MSN). MSNs are favorable in that they possess unique structural features, including their tunable pore size, large surface areas, and well-defined surface properties to accommodate cargo of various sizes, shapes, and functionalities (Hussain et al., 2013). They were first used in 2007 for DNA delivery to plants via particle bombardment in intact plant tissue and in protoplasts (Torney et al., 2007). Hussain and colleagues (2013) expanded the use of MSNs to intact plant systems without the use of particle bombardment. They grew wheat seeds in MS media supplemented with MSNs using a hydroponic system and found uptake of MSNs by roots. Hussian and colleagues (2013) also used vacuum infiltration in leaves and roots of Arabidopsis seedlings. They found that seed germination was not impacted by the presence of MSNs and that there was no phytotoxicity. Additionally, the MSNs were found to settle within the cells or cell walls when taken-up through the root (Hussain et al., 2013). Slombger and Schoenfisch noted

that silicon nanoparticles (SiNPs) accumulate in Arabidopsis roots, but that that silica scaffolds are not phytotoxic up to 1000 ppm despite uptake of vast amount of SiNPs in *A. thaliana* (2012).

Silicon nanowires, a type of semiconductor nanowire produced through vapor-liquid-solid mechanism, are of interest for plant delivery. They have unique properties that differ from bulk silicon materials. They have a high-aspect ratio, a one-dimensional structure, and rigid enough to be mechanically manipulated (Kim et al., 2007). Additionally, they have been used for bioelectric modulation through photoelectrochemical or photothermal stimuli (Rotenberg, et al., 2020). Vertically aligned silicon nanowires attached to a rigid substrate have successfully been interfaced with mammalian cells (Kim et al., 2007) and have been shown to be a universal platform for delivering biomolecules into mammalian cells (Shalek et al., 2010). Freestanding silicon nanowires, those detached from their rigid substrate, have been shown to be internalized into several mammalian cell lines via endogenous phagocytosis pathway and are not toxic to cells (Zimmerman et al., 2016). Although other 1D nanomaterials like carbon nanotubes have been utilized in delivery research in plants, they are not biodegradable, which raises concerns about potential harm to plants. On the other hand, Si nanowires are biodegradable. The modification of Si nanowires by an organism has not yet been investigated, and plants could serve as an excellent model system to explore this area.

One of the biggest hurdles to overcome when designing a nanocarrier for delivery in plants is the uptake and transport of the nanocarrier. Uptake and transport throughout a plant is limited by size exclusion limits and pore diameters of various plant tissues. Regardless of the heuristics used to navigate the choice of nanocarriers for plants, there is limited knowledge about plant physiological response to nanocarrier uptake and delivery (Cunningham et al., 2018).

This chapter discusses the potential application of free-standing silicon nanowires (SiNWs) for delivery in plants. I describe the approach of using SiNWs to produce macro-sized fibers and then transition to investigating the uptake of SiNWs in plants. We discuss how these materials are eventually broken down from crystalline silicon to silicate particles and incorporated into plant cell walls.

METHODS

Plants

Seeds for *Arabidopsis thaliana* (Columbia-0 accession) seedlings were sterilized (70% ethanol for 5 min, 50% chlorine laundry bleach supplemented with 0.5% Tween-20 for 10 min, and washed 4x with dH_2O) (Morgan et al., 2022) and vernalized in the dark at 4°C for 4 d in either liquid or agar ½ MS media (Murashige and Skoog) supplemented with or without SiNWs. Plants were grown in long day conditions (16 h light, 8 h dark) at ~20°C. 10 plants were grown on each agar plate. Round plates were used for this and contained 50 mLs of ½ MS solution, 0.07% agar and supplemented with sucrose (10 g per 1 L). For the hydroponic set-up, a 24-well plate was used and each well had 3 seedlings per condition.

Silicon Nanowire Presence in ½ MS Plates and Hydroponics

In some cases, ½ MS plates were prepared with silicon nanowires. Nanowires were removed from their silicon chip substrate by 30 -60 s sonication. 6-well plates were utilized for hydroponics/use of liquid ½ MS supplemented with sucrose and vitamins and one plant was grown in each well. All plants used for subsequent experiments were 14 days old. These plants

were grown in the presence of Si nanowires or without nanowires for this entire period. All plants were grown in a growth chamber at 22°C in long day (16 h light, 8 h dark).

Silicon Nanowire Growth

Silicon nanowires were produced using the protocol from Nair (2020). In brief, silicon nanowires were grown in a custom-built chemical vapor deposition machine via Au nanoparticle (20-100 nm in diameter, Ted Pella Inc.) catalyzed vapor-liquid-solid growth mechanism. Intrinsic nanowires were grown with the following conditions: 80 torr, 60 standard cubic centimeters per minute (SCCM) of hydrogen carrier gas, and 2 SCCM of silane for 20 minutes.

Production of Microfibers with Silicon Nanowire Bases

To make microfibers, a small piece of a Si substrate with SiNWs was made via VLS (vapor-liquid-solid) method in a custom-built chemical vapor deposition machine and sonicate it in isopropanol (IPA) for 60 s, until the SiNWs visibly fell off the chip. SiNWs were then dropcast into silicon nanoneedle molds 300 × 300-μm round base tapering to a height of 600 μm with a tip radius of around 10 μm (Blueacre Technology) (Yu et al., 2015). Molds with SiNWs were left at room temperature for the IPA to evaporate. The substrate was added to the device by melting polystyrene (PS, Mw: 100 k, PDI: 1.06, Polysciences) pellets in the mold at 180 °C for 4 h under vacuum. Fabricated microfiber arrays were assessed via scanning electron microscopy (Carl Zeiss Merlin SEM).

Electron microscopy

Plant roots were fixed in with 2.5% Glutaraldehyde in sodium cacodylate buffer and embedded in Spurrs resin (EMS) following the manufacturers protocol. A microtome was used to make 90 nm sections that were imaged on a Technai F30 twin scope at an accelerating voltage of 300 kV. For scanning electron microscopy (SEM), freeze-dried roots were adhered on vertical stub for cross-sectional imaging and sputtered with 5 nm Pd/Pt. SEM and EDS (energy dispersive spectroscopy) were performed using a Tescan lyra 3 field-emission scanning electron microscope.

Inductively coupled plasma-optical emission spectroscopy (ICP-OES)

Each two-week-old plant was freeze dried and digested in 400 μL of concentrated HNO_3 and 100 μL of 15% H_2O_2 and volume made up to 5 mL. Agilent 700 Series spectrometer was used to perform ICP-OES tests (Parvlovic et al., 2013; Persson et al., 2016; Quigley et al., 2016; Slomberg et al., 2012).

Molybdic Acid Assay for the Estimation of Silica SiO_2 Content in Agar

Molybdic acid assays were performed using the protocol from Coradin et al. (2004). In brief, a gram of agar from areas with plant roots was placed in 12.5 mLs of distilled water. The samples were microwaved for 2 minutes to melt the agar. Following this, the samples were placed at 4°C for about 20 minutes to cool them off. After cooling, 500 μL of Ammonium molybdate tetrahydrate solution and 500 μL of 1.5 M sulfuric acid was added to each of the samples and to the standards. High purity silica standards were purchased from Sigma Aldrich to prepare 0 ppm, 5 ppm, 10 ppm, 15 ppm, 20 ppm, 25 ppm, 50 ppm, and 100 ppm solutions. The samples were then left at RT for 10 minutes for a yellow color to develop. Following this, their

absorbances were measured at 400 nm using a 96-well plate in a Synergy Neo HST Plate Reader. Each sample had 2 biological replicates and 3 technical replicates.

Confocal Imaging

Confocal imaging of roots grown in the presence of silicon nanowires for 2 weeks were performed on a LEICA-SP5 confocal microscope. The roots were imaged using the DIC differential interference contrast. The nanowires were imaged using their reflection via an acousto-optical beam splitter in the microscope that separated the fluorescence channels from reflection channels (Parameswaran et al., 2018).

Statistical analysis

T-tests were performed using Origin Pro 9.0 and Prism (GraphPad).

RESULTS

Biological Impact of Nanowires on Arabidopsis Seedlings

To test the impact of SiNWs on Arabidopsis, plants were grown in the presence of two concentrations of silicon nanowires (low and high) for 2 weeks. There was no significant difference in the weight of plants between those grown with silicon nanowires and those without silicon nanowires in terms of both wet weight and primary root length. The root length of the seedlings grown with low concentrations of SiNWs was significantly different from the controls and those grown with high concentrations of nanowires according to the one-way ANOVA test performed (Figure 2.1). There was a wide range of values for both the weights and primary root lengths for the samples (Figure 2.1 D-E). Furthermore, all plants visually looked the same

(Figure 2.1). The takeaway from this preliminary data was that the SiNWs do not cause cytotoxic effects on young Arabidopsis seedlings.

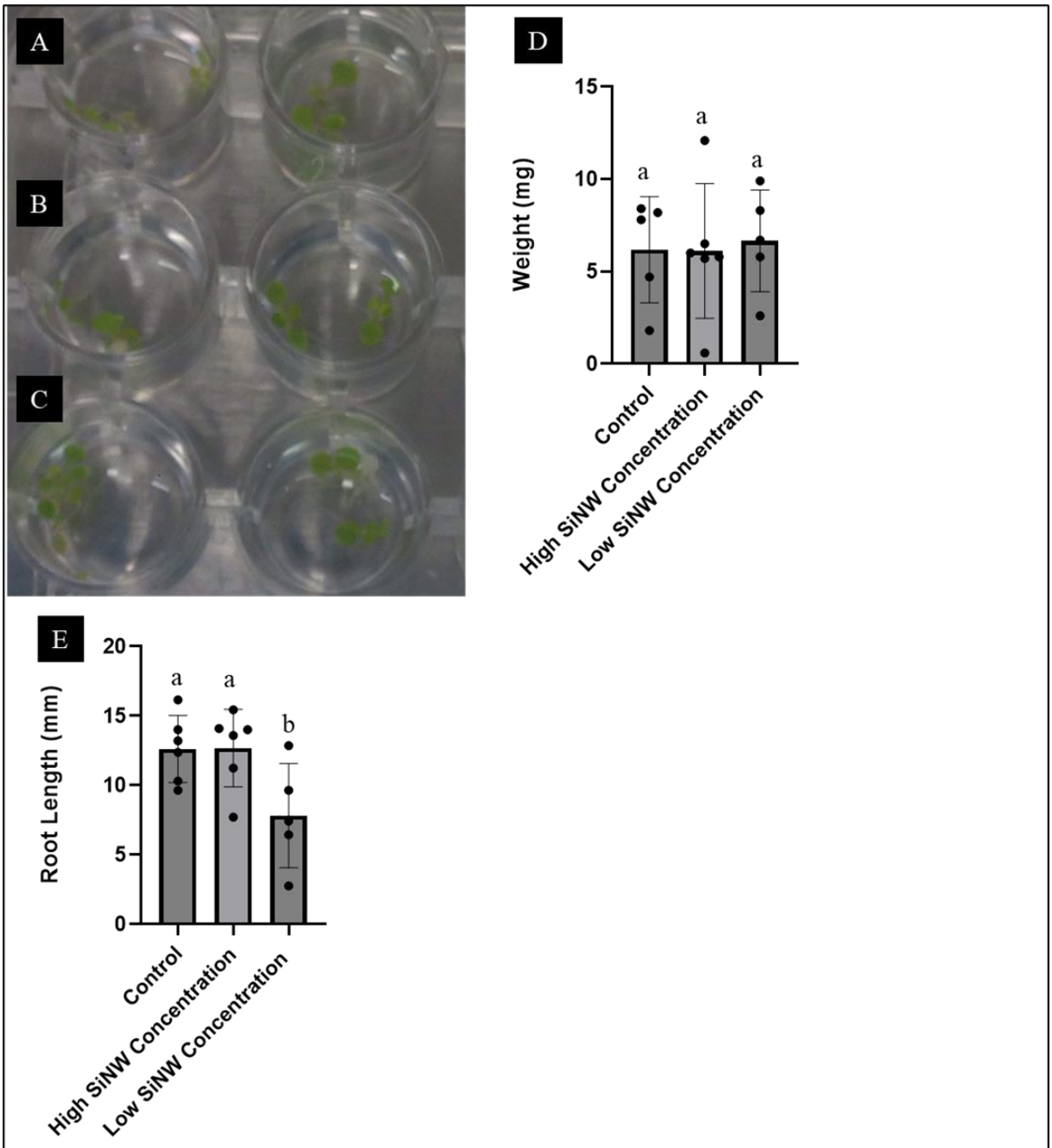

Figure 2.1: Different silicon nanowire concentrations and their affect on developing Arabidopsis seedlings. (A) High nanowire concentration. (B) Low nanowire concentration. (C) Control with no nanowires (1/2 MS media only). Used SiNWs 100 nm in diameter; length of SiNWs varied. (D) Weight of Arabidopsis seedlings 2 weeks post exposure to SiNWs. (E) Length of primary roots after 2-week exposure to SiNWs. N=5-6 per condition. 1-way ANOVA was used for significance testing. Different letters show significant differences between treatments. Each dot represents measurements for 1 seedling.

SiNW Uptake via Arabidopsis Roots

For SiNWs to be useful delivery vehicles for plants, we first needed to know if they would be able to enter plant roots. To test this, we imaged the root of an Arabidopsis seedling grown in the presence of silicon nanowires using confocal microscopy. Figure 2.4 shows that SiNWs were potentially attached to root hairs/cuticles (Figure 2.2). A three-dimensional stack performed on a nanowire suspected to be internalized revealed confinement of the nanowire reflection signal within the root hair boundaries (Figure 2.2). For this experiment, only one root was examined that was grown in the presence of wires and a control grown without wires.

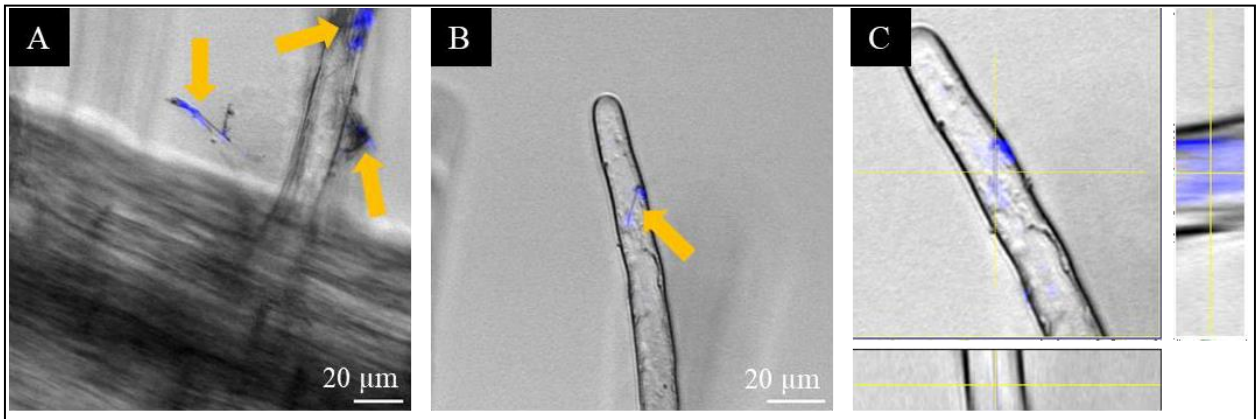

Figure 2.2: Nanowire uptake in Arabidopsis root hairs. (A) DIC confocal image of a root with nanowires attached. (B) A root hair with a nanowire suspected to be internalized. (C) A z-stack orthographic projection (77.40 µm x 77.40 µm x 16.07 µm) of root hair and nanowire in (B), suggesting internalization. Arabidopsis seedlings were 14 d old and grown in the presence of SINWs for 14 d. Arrows point to SiNWs.

Further electron microscopy was carried out on roots with and without nanowire treatment. The roots were embedded in resin and sectioned using a microtome (Figure 2.3). Micrographs of the vascular bundle showed that nanowires were fragmented and attached to the epidermal cells of roots (Figure 2.3). Further analysis revealed the presence of a degraded nanowire within a xylem vessel (Figure 2.4), which was identified based-on the lack of nuclei and the presence of thickened corners- typical for xylem vessels (Casimiro et al., 2003; Baum et

al., 2002). The nanowires present in the xylem vessel appeared degraded, and it looked as though there were gel-like structures surrounding it (Figure 2.4). Root sections prepared for electron microscopy were completed by the core facility at the University of Chicago. Sections were randomly taken from the root sections, so we cannot know from which part of the root or developmental zone that the root section was taken from. A control block, Arabidopsis seedlings grown without nanowires, was prepared. However, useful images of the control could not be obtained due to poor sample quality after embedding and staining.

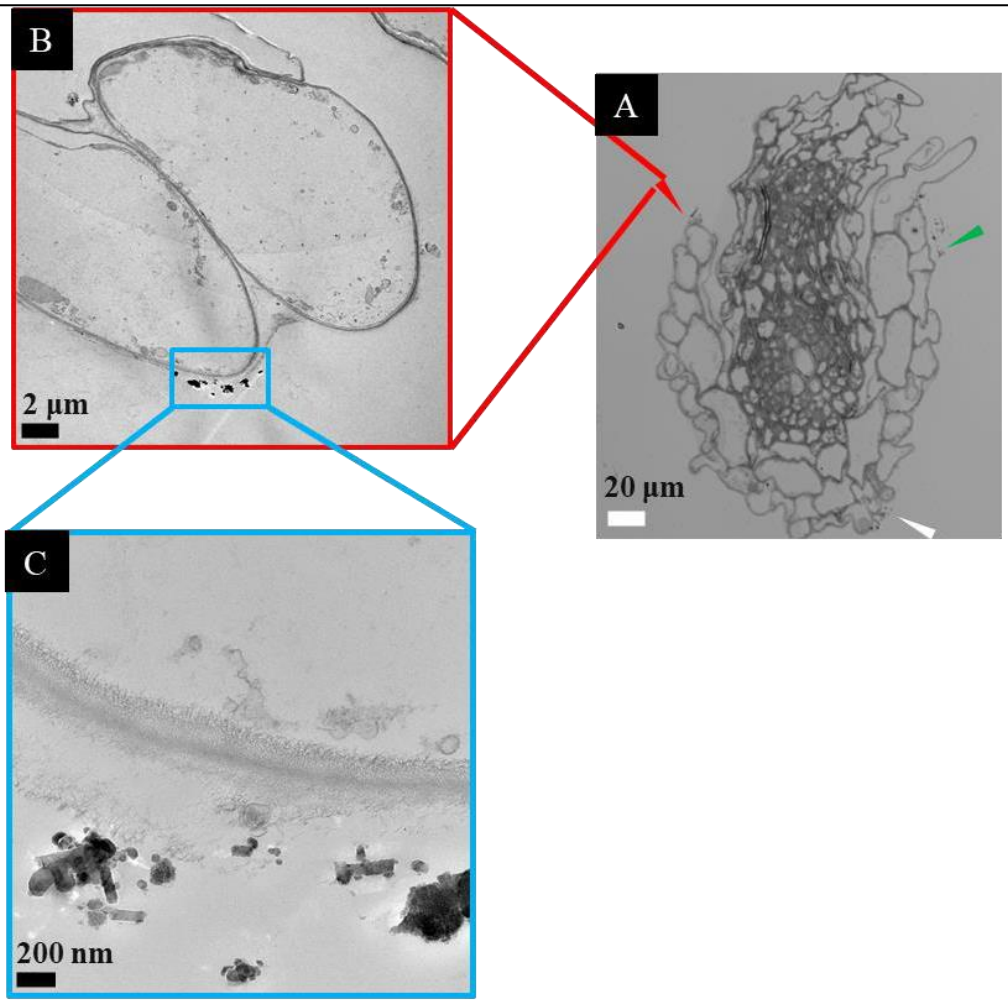

Figure 2.3: Nanowire attachment to root epidermis. (A) An optical microscopy image of a cross-section of a resin embedded two-week old plant root, treated with nanowires for 14 d. Arrows marks regions where SiNW fragments were attached to root epidermis. (B) TEM of the region in A corresponding to red arrow showing attached nanowire. (C) A magnified electron microscopy view of B confirming nanowires attaching to root epidermis. N=3

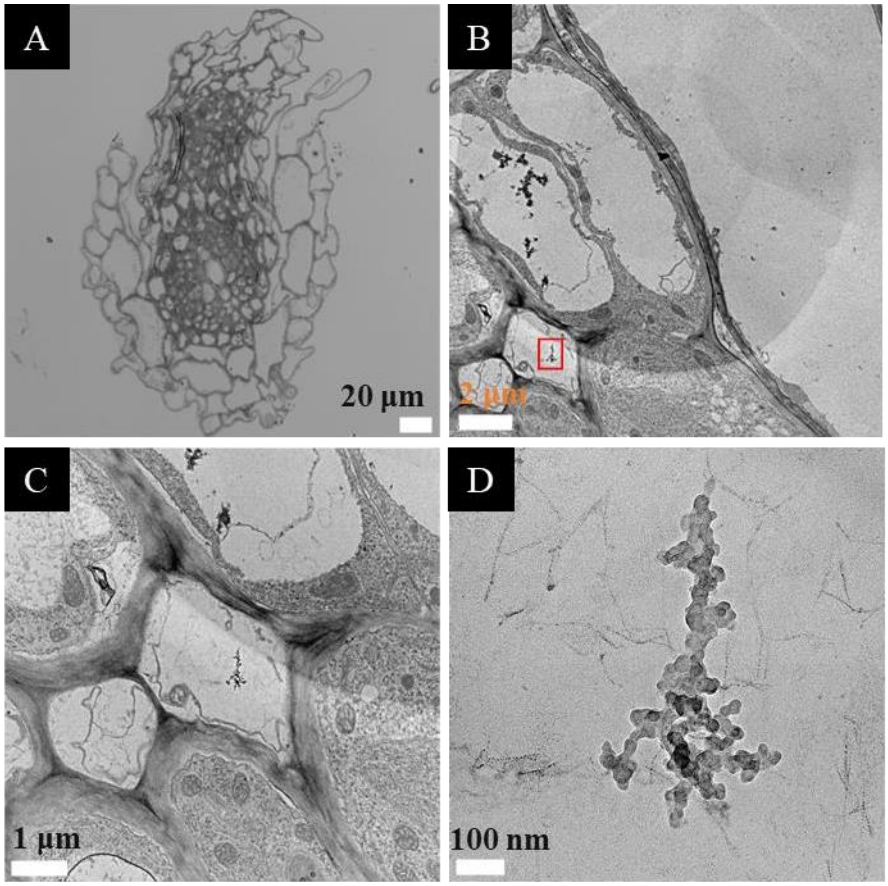

Figure 2.4: Degradation of SiNWs within roots. (A) An optical microscopy image of a cross-section of a resin-embedded 14-day old Arabidopsis root treated with nanowires for 2 weeks. (B) A cell within a vascular bundle with nanowire (red box). It is an optical microscopy image of the cross-section where EM image of a is taken. (C) A magnified view of (b) showing the location of nanowire in a xylem vessel. (D) A magnified view of (c) showing nanowire degradation with gel like structures around it. N=3

Porous Gel-like Deposits in Cell Walls and Vacuoles

Examination of low magnification (nanometer scale) TEM images revealed deposits with higher phase contrast in the apoplastic region and vacuoles of cortical cells and vascular bundle (Figure 2.5 A, G, D and Figure 2.6 A, D). These deposits were further examined at higher magnification (micron scale) (Figure 2.5 B, C, E, F, H, I and Figure 2.7 B, C, E, F respectfully). All of the deposits showed a porous gel structure as observed in three separate samples in

Figures 2,5-6, resembling chemically synthesized silica aerogels (Rao et al., 2006; Ge et al., 2009; He et al., 2017).

In one instance (Figure 2.6) the gels formed were globular, resembling synthetic aerogels (Rao et al., 2006; Ge et al., 2009; He et al., 2017). Though most of the gels had non-periodic structure, there was one instance in which a mesoporous structure was observed (Figure 2.6). These experiments were conducted using plants grown in the presence of SiNWs for 2 weeks. Controls, plants without exposure to nanowires, are needed. A control block, Arabidopsis seedlings grown without nanowires, was prepared. However, useful images of the control could not be obtained due to a problem with embedding and staining the sample.

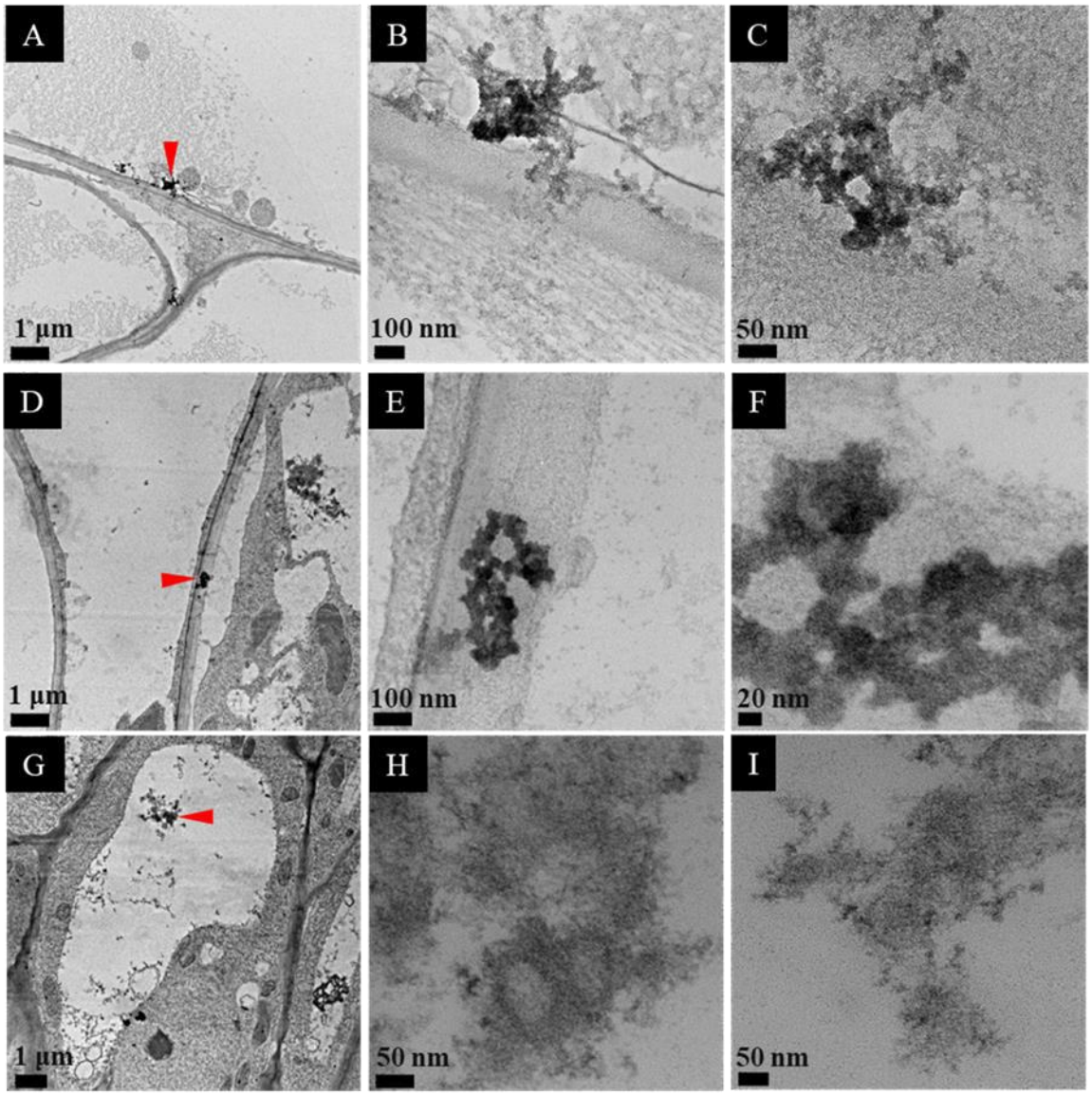

Figure 2.5: Porous silicon structures in root cells. Low magnification electron microscopy image of cells in a cross-section showing a dense deposit in root cell walls (A,D) and in a vacuole (G). Magnified view of (A, D, G) revealing porous structure (B,E, H-respectively). High resolution TEM images showing porous gel like structures (C, F, I) potentially from silica aggregates formed from nanowire uptake degradation. N=3

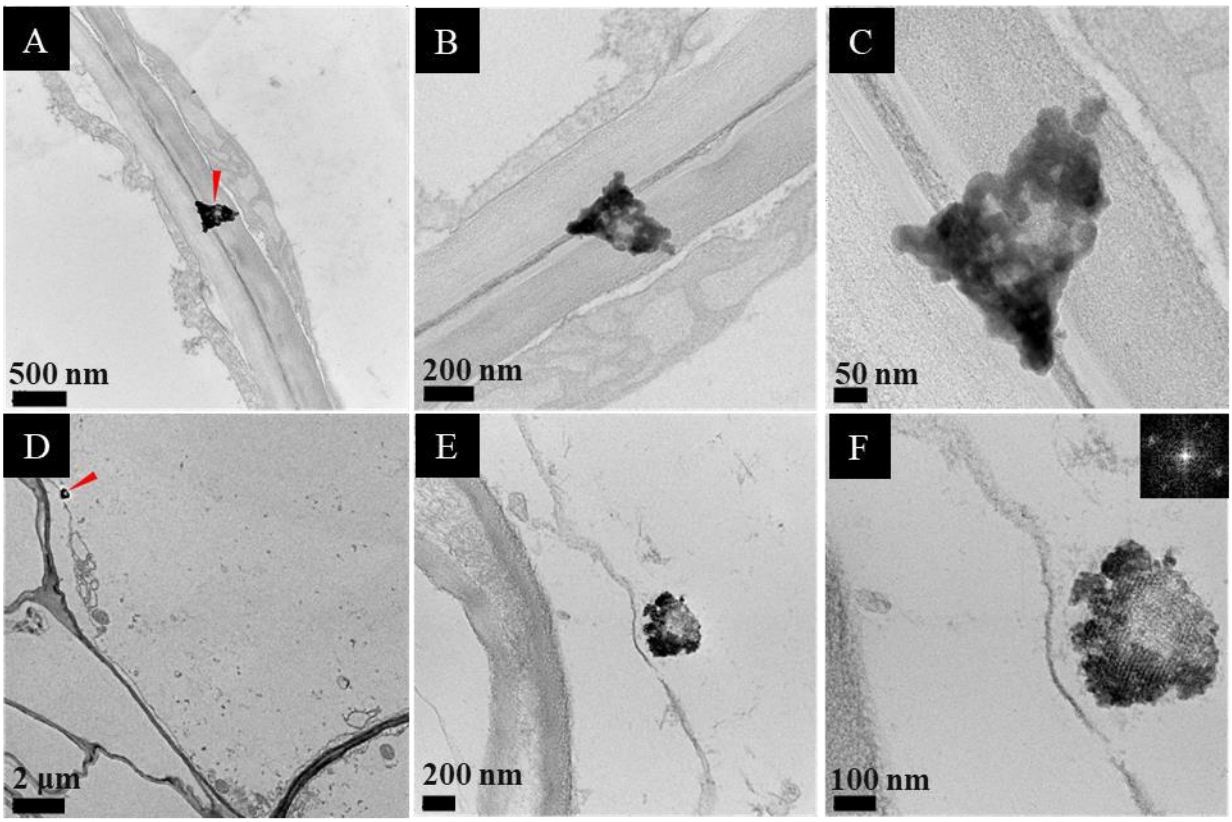

Figure 2.6: Differences in observed porous silicon structures. (A) A silica fragment trapped in the cell wall with magnified view (B-C) revealing its porous-gel like nature. (D) Another silica fragment closely attached to a cell wall revealing its mesoporous nature in its magnified view (E-F) and Fourier transform (Inset of F). These images suggest that besides the foam like structure observed in Figure 5, other structures of silicates could potentially form from nanowire degradation. Electron microscopy results are from three independent plant root. The mesoporous like structure was observed in once. Gel like structures were found in all roots imaged. Electron microscopy results are from root sections taken from 3 different plants.

Quantitative Estimation of Silicon Content

We used ICP-OES, an analytical method, to quantify silicon content of plants cultured with or without nanowires. We observed a quantitative increase in the silicon content of a plant cultured with nanowires suggesting the uptake and processing of silicon, corroborating the TEM investigation (Figure 2.7A). ICP-OES done on agar gel around the plants roots also suggested an increase in silicon concentration verifying the addition of nanowire to media (Figure 2.7B).

However, the silica concentration of agar estimated using molybdic acid assay, the colorimetric assay, remain unchanged (Figure 2.7C). These results indicate that the agar contains crystalline silicon nanowires that have not degraded into silica or silicic acid. The MS media used to make the agar plates is acidic (pH 5.7) and silicon degrades at basic pH levels (Lee et al., 2017). Therefore, we infer that the degradation of the silicon nanowires that resulted in the silica structures in the EM images happened within compartments of the plant roots with basic pH.

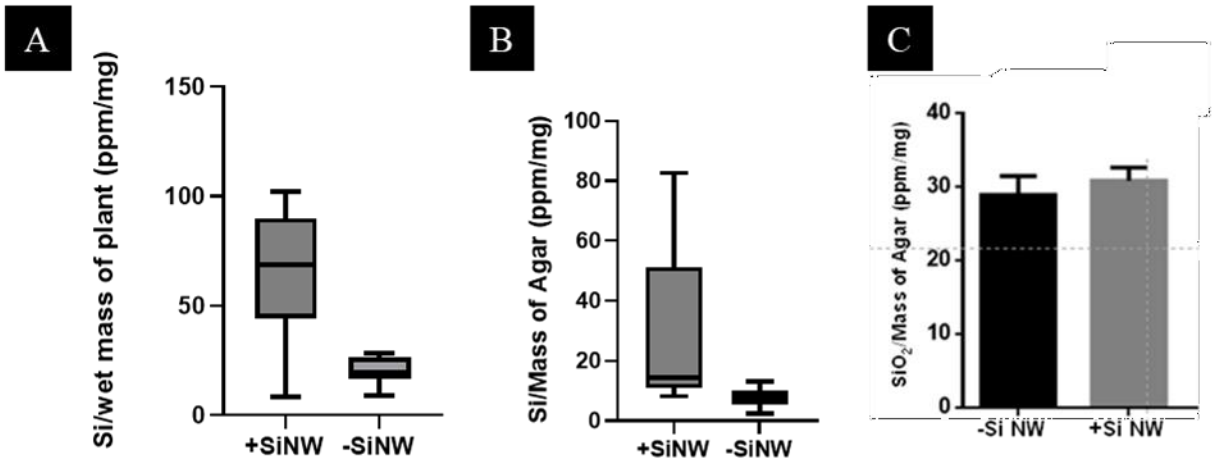

Figure 2.7: Quantitative estimation of silicon content via ICP-OES and molybdic acid assay. (A) ICP-OES measured silicon concentration in two-week old plants treated with and without silicon nanowires (unpaired two-tailed T-test, n=5-10, p-value <0.005) grown in ½ MS agar. (B) ICP-AES measured silicon concentration in two-week plant grown agar with and without silicon nanowires (unpaired one-tailed T-Test, n=5-10, p-value<0.05). (C) Molybdic acid assay estimation of silica concentration in two-week plant grown agar with and without silicon nanowires (n=1-2). A & B are box and whisker plots, the line represent the smallest and greatest values of the graphed data.

To further verify silicon content, two-week old plants cultured in liquid media with and without SiNWs were freeze dried, sectioned, and were subjected to elemental mapping for silicon. The ones treated without nanowires did not show any localized increase in the concentration of silicon (Figure 2.8A-D) including root hairs (Figure 2.9A-B). However, the ones treated with SiNWs showed an overall increase in silicon concentration (Figure 2.8G-H) besides localization in a vascular bundle and the cortex (Figure 2.8I-K). Similar results were

obtained from EDS mapping on root hairs (Figure 2.9C-D). Quantitatively estimating from the EDS spectra, the untreated roots have around < 0.5 atomic % of silicon whereas the ones treated have > 1.2 atomic % of silicon.

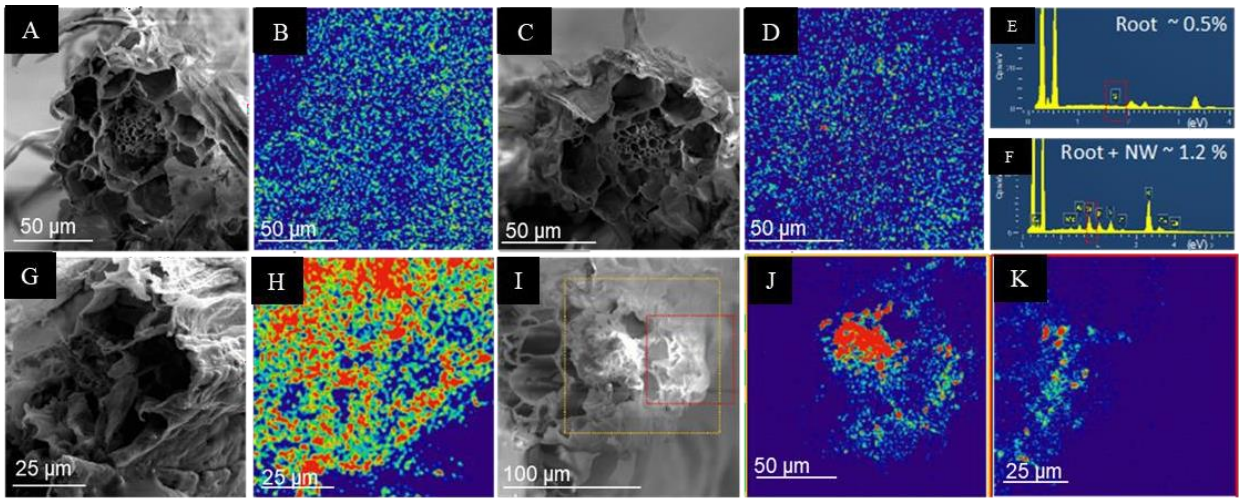

Figure 2.8: Elemental silicon mapping in Arabidopsis roots. (A) Electron microscopy of a freeze-dried section of two-week old plant roots along with silicon EDS map in (B) with heat map representation. (C) Electron microscopy of freeze-dried section of two-week old plant roots treated with silicon nanowire, along with silicon EDS map in (D) with heat map representation. Representative EDS spectra (One out of three roots under a condition scanned) of root section without silicon nanowire treatment (E) and with silicon nanowire treatment (F) along with approximate silicon concentration in those root sections. (G) Electron microscopy of freeze-dried section of two-week old plant roots treated with silicon nanowires along with silicon EDS map in (H) with heat map representation. (I) Electron microscopy of freeze-dried section of two-week old plant roots treated with silicon nanowires along with regional silicon EDS maps in (J,K) with heat map representation. The root sections treated with silicon nanowire show enhanced silicon concentration in the cross-sections (H) and localized silicon-based deposits in the vascular bundle and the epidermis (J,K). Three independent samples were scanned for the EDS spectra under each condition.

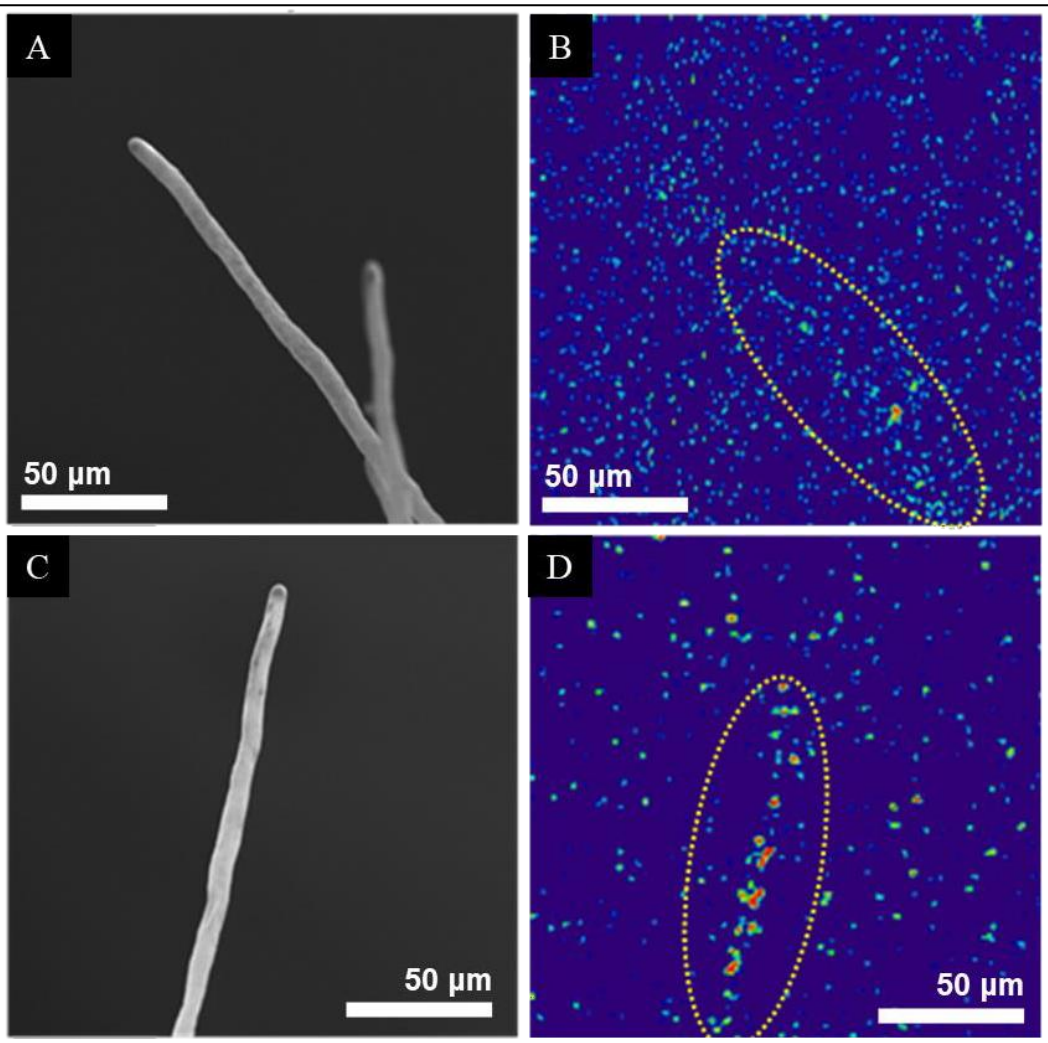

Figure 2.9: Elemental mapping of Arabidopsis roots exposed to SiNWs for 2 weeks. (A) SEM image of root hair without nanowire treatment and (B) its silicon EDS map showing no silicon-based densification in the root hair. (C) SEM image of root hair with nanowire treatment and (D) its silicon EDS map showing silicon-based densification in the root hair. Three independent samples were scanned for the EDS spectra under each condition.

SiNW Microneedle Fabrication

SiNW microneedles were generated as an alternative material to use for delivery of dye and DNA in plants. They were generated using a mold from Blue Acre Technology. In short, freestanding nanowires were placed at the needle tip in the mold. It was thought that the SiNWs would form the sharp tip of these microneedles and would aid in penetrating plant tissue for delivery (Figure 10). However, it was found that some tips broke off in the mold and the SiNW

tips were left behind. In other cases, it was observed that the SiNWs were mixed in with the polystyrene material rather than all being present at the tips (Figure 2.11). The takeaway from this was that the SiNW microneedles were not useful.

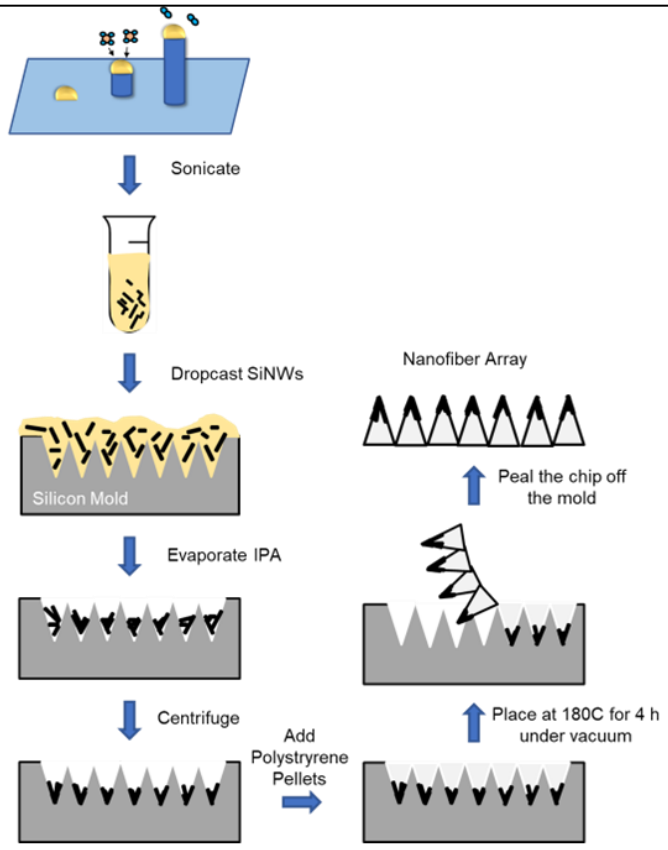

Figure 2.10: Workflow for producing microfibers with silicon nanowires at the tips. First silicon nanowires are grown via vapor-liquid-solid growth mechanism in a custom build CVD machine using Au nanoparticles as the catalyst. A small portion of the silicon substrate is broken off of the main wafer with the SiNWs and placed in a conical tube with IPA. The tube is then sonicated (~60 s) until the wires come off of the substrate, resulting in a large color burst in the tube. After this, SiNWs in IPA are dropcast onto a microfiber/microneedle mold and left to evaporate. The mold with the wires is then centrifuged to help get the SiNWs to concentrate at the tips of the mold. Polystyrene pellets are then added. The mold with the SiNWs and polystyrene pellets is placed at 180°C for 4 h under vacuum. Finally, the microneedles attached to this flexible based are removed from the mold.

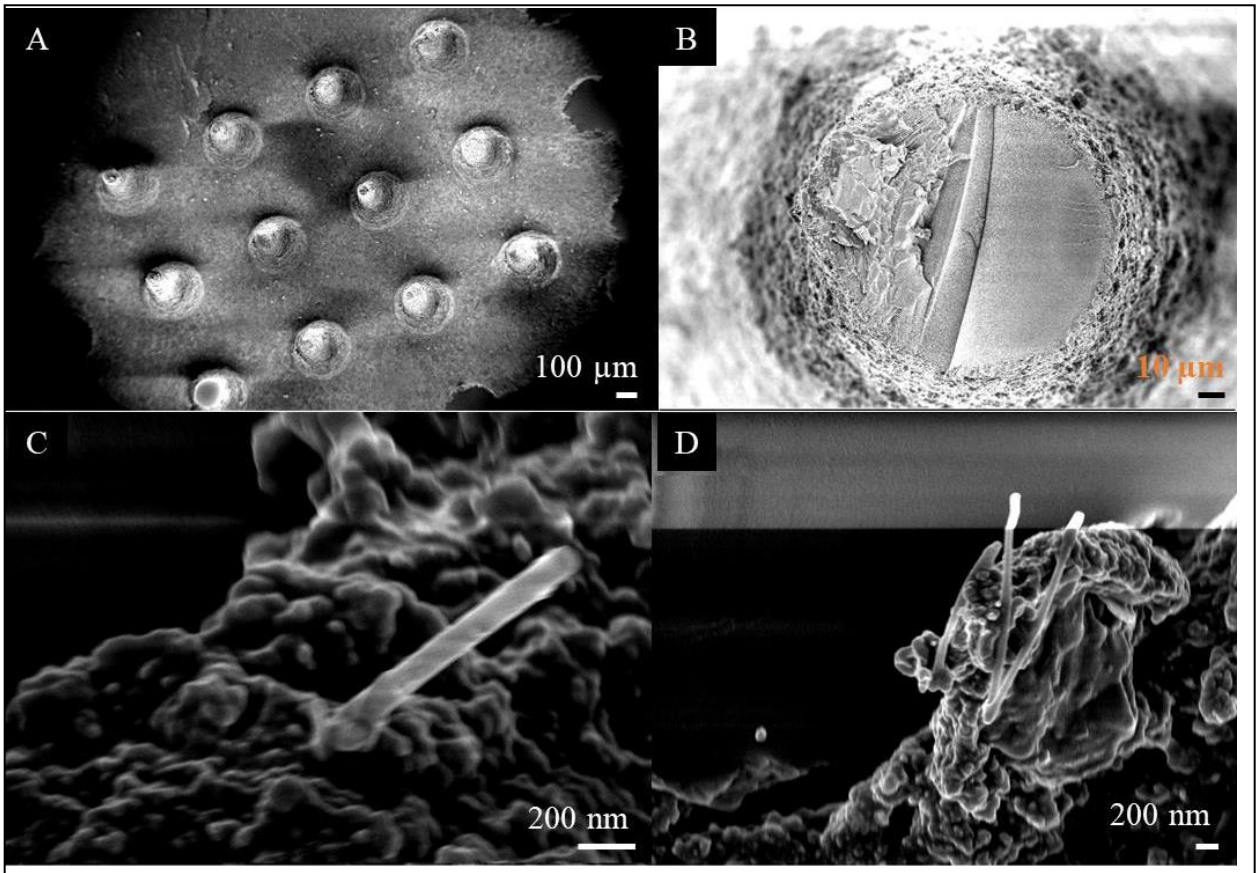

Figure 2.11: SEM Images of SiNW microfibers. (A) Top view of microfiber array. (B) Zoom in of the top of a fiber with no SINWs present. (C& D) SiNWs within the polystyrene base. They are mixed in with the polystyrene and did not form the tips of the microfibers.

DISCUSSION

In this chapter, I investigated whether or not free-standing silicon nanowires are tolerated by plants and can enter plant cells. This is a necessary step if SiNWs are to be used as nanovehicles for delivery in plants. We discuss how these materials are eventually broken down from crystalline silicon to silicate particles and incorporated into plant cell walls using electron microscopy, molybdic acid assays, and ICP-OES.

As evidenced by the TEM, the degradation of silicon nanowires occurs along the potential transport pathway of the silicon nanowires. Chemically, silicon can convert to silicic

acid at pH values ranging from neutral to basic (Lee et al., 2017). This process is accelerated with increasing pH (Lee et al., 2017). Silicic acid when sustained in a basic environment is known to deprotonate and undergo condensation with other silicic acid molecules to form polysilicic acid (PSA) (Annenkov et al., 2017). Polysilicic acid can also undergo Ostwald ripening with increasing concentration. Ostwald ripening is the phenomenon in which solid solutions change into inhomogeneous structures over time. In this case, smaller PSA colloidal particles dissolve and then redeposit onto larger particles. This is a spontaneous thermodynamic process as larger particles possess higher surface energy. PSA forms negatively charged colloidal particles, which are stable in a basic environment. These particles when transferred to an acidic environment undergo protonation and become unstable. Such a loss of colloidal stability can cause PSA particles to aggregate into gels (Annenkov et al., 2017). However, if the PSA particles are treated with polysaccharides like cellulose and callose (β-1,3-glucan) the hydroxyl groups on the polysaccharides could stabilize the deprotonated hydroxyls of PSA under basic conditions. This is because the pKas for hydroxyl groups on either species are different. The stability of PSA-associated polysaccharides also subsequently leads to their modified molecular structure, which can act as a template for gelation when the pH shifts to an acidic range (Annenkov et al., 2017). Hence there is a very clear understanding of how non-enzymatically pH can control the transformation of silicon to various essential forms that could exist in nature (Figure 2.12).

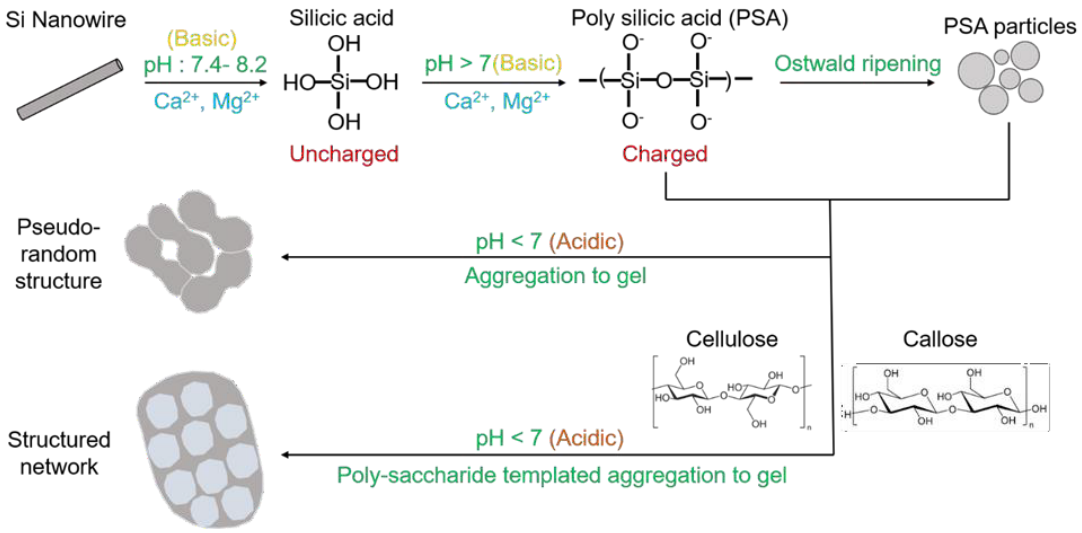

Figure 2.12. Schematic illustration of crystalline silicon nanowires undergoing degradation. First, they can change to silicic acid under neutral to basic pH conditions in the presence of calcium and magnesium **ions.** Silicic acid can further undergo base assisted polymerization to polysilicic acid (PSA) structures which are negatively charged due to de-protonation of hydroxyl groups. When the concentration of PSA grows to a critical concentration it can facilitates nucleation of PSA particles by Ostwald ripening. PSA or its particles when transformed from a basic environment to an acidic environment can cause the charged hydroxyl groups to get protonated, causing them to aggregate into random gel like structures. However, if the gelation happens in the presence of cellulose or callose which can complex with PSA under basic conditions, the gels will have an underlying structure.

The pH variations along the symplastic and apoplastic pathways are significantly different, which can be detected by using pH sensitive probes in Arabidopsis thaliana (Martiniere et al., 2018). The symplastic pathway includes cell-to-cell cytoplasmic transport via plasmodesmata. In this route, the basic pH ranges from 7.4 to 8 along the epidermis to the xylem vessels. The apoplastic pathway on the other hand happens via the intercellular spaces with acidic pH in the range of 6.5 to 6, along the epidermis to the xylem vessels (Martiniere et al., 2018). Thus, in line with the chemistry required for processing, we expect the transport via the symplastic pathway to result in conversion of crystalline nanowires to silicic acid or PSA. They can be further converted to silica gels in the vacuole (pH= 5.2-5.6) or the apoplastic region (pH= 6.0-6.5) (Martiniere et al., 2018; Shen et al., 2013). Presently, we cannot conclude where in the transport pathway each observed structure forms. To determine this, degradation studies of

silicon nanowires are needed to explore the chemistry behind the conversion of silicon nanowires to gels in plants (Figure 2.12).

Silicon nanowires are an auspicious material to use for delivery in plants. In terms of trying to use them to fabricate the tips of microneedles, they present some challenges. One of the biggest obstacles with trying to use them to form the tips of microneedles was that they would often get stuck in the mold. With the current method utilized for growing silicon nanowires (VLS with dropcasted Au catalyst particles), it is hard to control for the concentration of nanowires utilized. Presently, there is no way to measure SiNW concentration with high confidence. Zimmerman and colleagues (2016) would cut SiNW wafers of different sizes (1mm x 2mm or 2mm x 2mm) and sonicated them in specific volumes of media. They would then dropcast a known volume onto a glass slide and cover the droplet with a coverslip. Following this they took several pictures and counted the number of SiNWs in each image to determine the number of wires per volume (Zimmerman et al., 2016). The issue with this is that there is no way to control the number of wires grown on each silicon substrate. Additionally, the amount of wires present is somewhat arbitrary, and the number of free wires produced during sonication cannot be controlled. We tried to measure the weight of silicon nanowire chips before and after sonication (sonication is necessary to remove SiNWs) using a micro-balance Soft Matter Characterization Facility at the University of Chicago. Unfortunately, the micro-balance did not have the ability to detect the change in size before and after sonication. Additionally, some wires were lost during transport of the sample to the facility. For the aforementioned reasons, nanowire concentration could only be deduced visually and not quantitatively.

The data presented here are preliminary, but they offer insight into how silicon nanowires could be used with plants. Future studies are needed to determine the specific transport route of silicon nanowires from roots hairs to being distributed throughout a plant if that happens.

Understanding the chemistry behind the observed silicon processing in plant roots can lead to bioinspired material synthesis. Additionally, it provides clarity about what happens to SiNWs after they are taken up into plants. SiNWs are minimally invasive and have much promise as a future nanovehicle for delivery in plants.

WORKS CITED

Asad, S., Mukhtar, Z., Nazir, F., Hashmi, J. A., Mansoor, S., Zafar, Y., & Arshad, M. (2008). Silicon carbide whisker-mediated embryogenic callus transformation of cotton (Gossypium hirsutum L.) and regeneration of salt tolerant plants. *Molecular Biotechnology*, *40,* 161-169.

Banerjee, K., Pramanik, P., Maity, A., Joshi, D. C., Wani, S. H., & Krishnan, P. (2019). Methods of using nanomaterials to plant systems and their delivery to plants (Mode of entry, uptake, translocation, accumulation, biotransformation and barriers). In *Advances in Phytonanotechnology* (pp. 123-152). Academic Press.

Baum, S. F., Dubrovsky, J. G., & Rost, T. L. (2002). Apical organization and maturation of the cortex and vascular cylinder inArabidopsis thaliana (Brassicaceae) roots. *American Journal of Botany*, *89*(6), 908-920.

Casimiro, I., Beeckman, T., Graham, N., Bhalerao, R., Zhang, H., Casero, P., ... & Bennett, M. J. (2003). Dissecting Arabidopsis lateral root development. *Trends in Plant Science*, *8*(4), 165-171.

Coradin, T., Eglin, D., & Livage, J. (2004). The silicomolybdic acid spectrophotometric method and its application to silicate/biopolymer interaction studies. *Spectroscopy*, *18*(4), 567-576.

Fincheira, P., Tortella, G., Seabra, A. B., Quiroz, A., Diez, M. C., & Rubilar, O. (2021). Nanotechnology advances for sustainable agriculture: current knowledge and prospects in plant growth modulation and nutrition. *Planta*, *254*, 1-25.

Davern, S. M., McKnight, T. E., Standaert, R. F., Morrell-Falvey, J. L., Shpak, E. D., Kalluri, U. C., ... & Mirzadeh, S. (2016). Carbon nanofiber arrays: a novel tool for microdelivery of biomolecules to plants. *PLoS One*, *11*(4), e0153621.

Ge, D., Yang, L., Li, Y., & Zhao, J. (2009). Hydrophobic and thermal insulation properties of silica aerogel/epoxy composite. *Journal of Non-Crystalline Solids*, *355*(52-54), 2610-2615.

He, S., Yang, H., & Chen, X. (2017). Facile synthesis of highly porous silica aerogel granules and its burning behavior under radiation. *Journal of Sol-Gel Science and Technology*, *82*, 407-416.

Hussain, H. I., Yi, Z., Rookes, J. E., Kong, L. X., & Cahill, D. M. (2013). Mesoporous silica nanoparticles as a biomolecule delivery vehicle in plants. *Journal of Nanoparticle Research*, *15*, 1-15.

Kim, W., Ng, J. K., Kunitake, M. E., Conklin, B. R., & Yang, P. (2007). Interfacing silicon nanowires with mammalian cells. *Journal of the American Chemical Society*, 129(23), 7228-7229.

Lee, Y. K., Yu, K. J., Song, E., Barati Farimani, A., Vitale, F., Xie, Z., ... & Rogers, J. A. (2017).

Dissolution of monocrystalline silicon nanomembranes and their use as encapsulation layers and electrical interfaces in water-soluble electronics. *ACS Nano*, *11*(12), 12562-12572.

Martinière, A., Gibrat, R., Sentenac, H., Dumont, X., Gaillard, I., & Paris, N. (2018). Uncovering pH at both sides of the root plasma membrane interface using noninvasive imaging. *Proceedings of the National Academy of Sciences*, *115*(25), 6488-6493.

Morgan, J. M., Jelenska, J., Hensley, D., Retterer, S. T., Morrell-Falvey, J. L., Standaert, R. F., & Greenberg, J. T. (2022). An efficient and broadly applicable method for transient transformation of plants using vertically aligned carbon nanofiber arrays.

Nair, V. (2020). *Design of Semiconductor Biointerfaces for Modulation of Cellular Signalling and Neuronal Networks* (Doctoral dissertation, The University of Chicago).

Parameswaran, R., Koehler, K., Rotenberg, M. Y., Burke, M. J., Kim, J., Jeong, K. Y., ... & Tian, B. (2019). Optical stimulation of cardiac cells with a polymer-supported silicon nanowire matrix. *Proceedings of the National Academy of Sciences*, *116*(2), 413-421.

Pavlovic, J., Samardzic, J., Maksimović, V., Timotijevic, G., Stevic, N., Laursen, K. H., ... & Nikolic, M. (2013). Silicon alleviates iron deficiency in cucumber by promoting mobilization of iron in the root apoplast. *New Phytologist*, *198*(4), 1096-1107.

Persson, D. P., Chen, A., Aarts, M. G., Salt, D. E., Schjoerring, J. K., & Husted, S. (2016). Multi-element bioimaging of Arabidopsis thaliana roots. *Plant Physiology*, *172*(2), 835-847.

Quigley, K. Q. (2016). The Ecological Drivers and Consequences of Grass Silicon Accumulation (Doctoral dissertation, Wake Forest University).

Ramkumar, T. R., Lenka, S. K., Arya, S. S., & Bansal, K. C. (2020). A short history and

perspectives on plant genetic transformation. *Biolistic DNA Delivery in Plants: Methods and Protocols*, 39-68.

Rotenberg, M. Y., Elbaz, B., Nair, V., Schaumann, E. N., Yamamoto, N., Sarma, N., ... & Tian, B. (2020). Silicon nanowires for intracellular optical interrogation with subcellular resolution. *Nano Letters*, *20*(2), 1226-1232.

Safdar, M., Kim, W., Park, S., Gwon, Y., Kim, Y. O., & Kim, J. (2022). Engineering plants with carbon nanotubes: a sustainable agriculture approach. *Journal of Nanobiotechnology*, *20*(1), 1-30.

Shalek, A. K., Robinson, J. T., Karp, E. S., Lee, J. S., Ahn, D. R., Yoon, M. H., ... & Park, H. (2010). Vertical silicon nanowires as a universal platform for delivering biomolecules into living cells. *Proceedings of the National Academy of Sciences*, *107*(5), 1870-1875.

Shen, J., Zeng, Y., Zhuang, X., Sun, L., Yao, X., Pimpl, P., & Jiang, L. (2013). Organelle pH in the Arabidopsis endomembrane system. *Molecular Plant*, *6*(5), 1419-1437.

Slomberg, D. L., & Schoenfisch, M. H. (2012). Silica nanoparticle phytotoxicity to *Arabidopsis thaliana*. *Environmental Science & Technology*, *46*(18), 10247-10254.

Souri, Z., Khanna, K., Karimi, N., & Ahmad, P. (2021). Silicon and plants: current knowledge and future prospects. *Journal of Plant Growth Regulation*, *40*, 906-925.

Torney, F., Trewyn, B. G., Lin, V. S. Y., & Wang, K. (2007). Mesoporous silica nanoparticles deliver DNA and chemicals into plants. *Nature Nanotechnology*, *2*(5), 295-300.

Rao, A. V., Bhagat, S. D., Hirashima, H., & Pajonk, G. M. (2006). Synthesis of flexible silica aerogels using methyltrimethoxysilane (MTMS) precursor. *Journal of Colloid and Interface Science*, *300*(1), 279-285.

Verma, S. K., Das, A. K., Gantait, S., Kumar, V., & Gurel, E. (2019). Applications of carbon

nanomaterials in the plant system: A perspective view on the pros and cons. *Science of the Total Environment*, *667*, 485-499.

Yu, J., Zhang, Y., Ye, Y., DiSanto, R., Sun, W., Ranson, D., ... & Gu, Z. (2015). Microneedle-array patches loaded with hypoxia-sensitive vesicles provide fast glucose-responsive insulin delivery. *Proceedings of the National Academy of Sciences*, *112*(27), 8260-8265.

Zimmerman, J. F., Parameswaran, R., Murray, G., Wang, Y., Burke, M., & Tian, B. (2016). Cellular uptake and dynamics of unlabeled freestanding silicon nanowires. *Science Advances*, *2*(12), e1601039.

CHAPTER 3:

An Efficient and Broadly Applicable Method for Transient Transformation of Plants Using Vertically Aligned Carbon Nanofiber Arrays

PREFACE:

This chapter contains a paper published from the collaborative work completed under the supervision of Dr. Jean T. Greenberg (Doi:10.3389/fpls.2022.1051340). The article was published in *Frontiers in Plant Science* under the Creative Commons License. My contributions to the study are as follows: I worked with members of Oak Ridge National Laboratory, the University of Chicago, and East Tennessee State University to draft and submit user proposal applications to work at the Center for Nanophase Materials at Oak Ridge National Laboratory to design and fabricate carbon nanofibers of varying length and pitch. Furthermore, I performed experiments in which I used carbon nanofibers of different pitches and lengths to transiently transform Arabidopsis leaves, poplar leaves, and tomato fruit with a fluorescent marker that localizes to plant vacuoles. I also used the fibers in rigid substrates to deliver dye to apples, strawberries, and peaches and demonstrated that fibers in rigid substrates could be used to deliver biosensors in roots. In collaboration with Dr. Joanna Jelenska and Dr. Jean Greenberg, I edited and revised the manuscript, cover letter, and responses to editors.

ABSTRACT

We pioneered and demonstrated the use of vertically aligned carbon nanofiber (VACNF) arrays to efficiently perform transient transformation of different tissues with DNA constructs in multiple plant species. The VACNFs permeabilize plant tissue transiently to allow molecules into cells without causing a detectable stress response. We successfully delivered DNA into

leaves, roots, and fruit of five plant species (Arabidopsis, poplar, lettuce, *Nicotiana benthamiana*, and tomato) and confirmed accumulation of the encoded fluorescent proteins by confocal microscopy. Using this system, it is possible to transiently transform plant cells with both small and large plasmids. The method is successful for species recalcitrant to *Agrobacterium*−mediated transformation. VACNFs provide simple, reliable means of DNA delivery into a variety of plant organs and species.

INTRODUCTION

The ability to introduce DNA into plants and achieve plant transformation has radically changed agriculture and provided a means to study fundamental processes in plants. Transformations can involve the integration of DNA into a plant genome (stable transformation) or the introduction of DNA into plant cells without the incorporation of transgenes into the genome (transient transformation) (Alteper et al., 2016). Additionally, plastids, cellular organelles in plants with their own genomes, can be stably and transiently transformed (Maliga, 2004; Yu et al., 2020). Transient transformation is faster than stable transformation. It provides the opportunity to study the functions and regulation of genes either in single cells or within the context of plant organs (Birch,1997; Krenek et al., 2015; Sheen, 2001). For example, reporters can be introduced to monitor transcriptional activation, the subcellular localization of proteins, and subcellular processes through the delivery of different molecular probes (Levy et al., 2018).

Three of the main methods employed for transient transformation in plants involve *Agrobacteria*, protoplast transfection, and particle bombardment. *Agrobacterium*−mediated transformation is limited to plant species, cultivars, and tissue types (roots, leaves, and seedlings) that are susceptible to this bacterium (Hwang et al., 2017). High cell densities of *Agrobacteria*

are required to perform transient transformation (agroinfiltration), which can be harmful to plants (Karami, 2008; Li et al., 2009). For protoplast transfection, protoplasts are made via enzymatic breakdown of the cell wall after grinding up tissue. DNA is then delivered to the protoplasts via electroporation or polyethylene glycol using small vectors that are easy to manipulate. This process is advantageous because transient transformation can be achieved with a high frequency. Like *Agrobacterium*−mediated transformation, however, protoplast transfection is labor intensive, it requires optimization for each species (Gou et al., 2020; Baltes et al., 2017; Ren et al., 2020), and it does not allow studies of intact tissues. Finally, particle bombardment can be used to deliver DNA into a broader range of plants and tissues than agroinfiltration and protoplast transformation. The tissues to which particle bombardment can be applied include meristems, embryos, leaves, callus, stems, roots, pollen, styles, and petals (Lacroix and Citovsky, 2020). Particle bombardment, however, causes plant tissue damage when high bombardment pressures are used. Other limitations arise from the need to position plant material in the biolistic chamber or to align it with a gene gun, which limit the size of the specimen and the accessible sites (Mohan et al., 2019; Haque et al., 2018, Ozyigit and Yucebilgili Kurtoglu, 2020). Notably, all these methods affect plant physiology by inducing stress responses that may interfere with subsequent experiments using transiently transformed cells.

Nanomaterials are being developed for the delivery of biomolecules into plants because of their applicability to several different plant species and for their ability to increase transformation efficiency *in planta* (Kumar et al., 2020). The use of nanomaterials as vehicles for biomolecules has been widely studied in animal cells and tissues for drug delivery, but not in plants (Cunningham et al., 2018; Sanzari et al., 2019; Jain and Thareja, 2019; Jat et al., 2020; McKnight et al., 2004; McKnight et al., 2005). This may be due in part to the barriers presented

by the cell wall and the fact that different plant species have varying physiologies, which need to be considered when addressing the interactions between the host environment and the nanomaterial (Pérez−de−Luque, 2017). To overcome the hurdles presented by plants, the size of the nanoparticles has been tuned, and surface modifications have been made to enable attachment of cargo to nanovehicles (Kumar et al., 2020). Some examples of these nanovehicles include: surface functionalized and pristine single walled carbon nanotubes (Demirer et al., 2019; Liu et al., 2009), mesoporous silica nanoparticles (MSNs) (Torney et al., 2007; Chang et al., 2013), gold nanoparticles and nanoparticles made of other materials coated with gold, polymeric nanoparticles (Zhang et al., 2019b), DNA nanostructures (Zhang et al., 2019), layered double hydroxide clay nanosheets (Mitter et al., 2017), magnetic nanoparticles (used for pollen magnetofection (Zhao et al., 2017)), silicon carbide whiskers (Arshad et al., 2013), and peptides as carriers for nucleic acids (Zheng et al., 2017; Jat et al., 2020). Of the nanovehicles used to deliver genes/DNA into plants, acicular shaped materials (carbon nanotubes) account for a large portion of the studies conducted. These materials have been delivered into plants through passive delivery, a needleless syringe, or with the aid of ultrasound, a magnetic field, or a gene gun (Jat et al., 2020).

A promising approach used for delivering biomolecules into cultured animal cells was the application of vertically aligned carbon nanofibers (VACNFs; McKnight et al., 2004; McKnight et al., 2005). Since these fibers are similar in scale to aphid stylets but with closed tips, they were assessed by Davern et al. (2016) for their potential to permit delivery of different sized molecules such as dyes, proteins, and dextrans to plant leaves. For this method, molecules dissolved in water were pipetted onto a leaf surface, and overlayed with the fiber array that was then gently tapped to promote penetration of the nanofibers and molecules into the leaf tissue. Importantly,

the VACNFs enabled delivery of a variety of molecules into leaf tissue without causing a detectable stress response (Davern et al., 2016). Furthermore, fibers broke away from the backing and remained embedded in cells without causing loss of cell viability, providing markers for which cells potentially received molecules of interest.

In this work, we have pioneered the use of VACNF arrays for the purpose of delivering DNA−encoded probes to plants to enable transient transformation (impalefection). We show the flexibility of the method by using it to transiently transform plant organs in several species with DNA encoding fluorescent proteins that can be detected by confocal microscopy. By examining the plant with a minimally invasive method, this approach will provide a more physiologically accurate picture of signaling pathways than most other studies that rely on detached tissues.

METHODS

Plants

Arabidopsis thaliana (Columbia−0 accession) plants 3−4 weeks post vernalization were used for leaf transformations and grown in long day conditions (16 h of light, 8 h of dark) in soil at 19−20°C, 35−75% relative humidity (RH), and 150−200 μmol m^{-2} s^{-1} light in a growth room. Seeds were vernalized in the dark at 4°C for 4 d prior to planting. *Populus trichocarpa* (Nisq−1 genotype) (poplar) plants were grown in soil in long day conditions at 30−60 % RH, 150−200 μmol m^{-2} s^{-1} light intensity, 22°C in a greenhouse. Lettuce (*Lactuca sativa* cultivar Salinas) was grown in long day conditions at 19°C in a greenhouse. Second to fourth true leaves of young (20−30 day old) lettuce plants were used for transformation. For experiments with roots, lettuce seeds were germinated at 22°C (long day conditions) for 7−14 days in petri dishes with filter paper and 0.5 g/L MaxiGro (General Hydroponics). *Nicotiana benthamiana* was grown for 4−5 weeks in long day conditions at 24°C in a growth chamber. Tomato fruits, strawberries, apples,

and peaches were purchased from a grocery store and were stored at room temperature prior to use. Roots used for VACNF delivery experiments came from Arabidopsis seedlings 5−6 d post planting grown on ½ MS plates supplemented with vitamins, grown under long day light conditions. Seeds for Arabidopsis seedlings were sterilized (70% ethanol for 5 min, 50% chlorine laundry bleach supplemented with 0.5% Tween−20 for 10 min, and washed 4x with dH_2O) and vernalized in the dark at 4°C for 4 d prior to planting.

Production of the vertically aligned carbon nanofibers (VACNFs)

Carbon−based nanofibers with a lateral spacing (pitch) of 10, 20, or 35 μm and height ranging from 15−25 μm were made in the Center for Nanophase Material Science at Oak Ridge National Laboratory using nickel catalyst dots patterned across the top of a silicon wafer via electron beam lithography, metal evaporation, and conventional lift−off using the method described by (Melechko et al., 2009). For the lithography step, the silicon wafers were coated with polymethyl methacrylate resist and exposed using a JEOL 9300FS electron beam lithography system and developed in a solution of 1:3 methyl−isobutyl ketone: isopropyl alcohol (Nano MIBK/IPA 1:3 Developer, MicroChem, Newton, MA). Electron beam lithography was necessary to define the catalyst dots with diameters between 200 nm and 500 nm. After developing the resist and cleaning with a 6−second exposure to oxygen plasma, electron beam evaporation was used to deposit a thin nickel film (100−125 nm) on the patterned resist. Sequential sonication in acetone and isopropyl alcohol was used to remove the underlying resist layer, leaving catalyst dots in the desired pattern behind. Nanofiber growth was then conducted using a plasma−enhanced chemical vapor deposition chamber using an acetylene/ammonia mixture. Growth parameters were optimized to control the length and taper of the nanofibers

(tapering less than 200 nm). After fabricating the VACNFs, their geometry was assessed using scanning electron microscopy (Zeiss Merlin FE−SEM) at a 30° tilt with an acceleration potential of 1 kV (Figure 3.1).

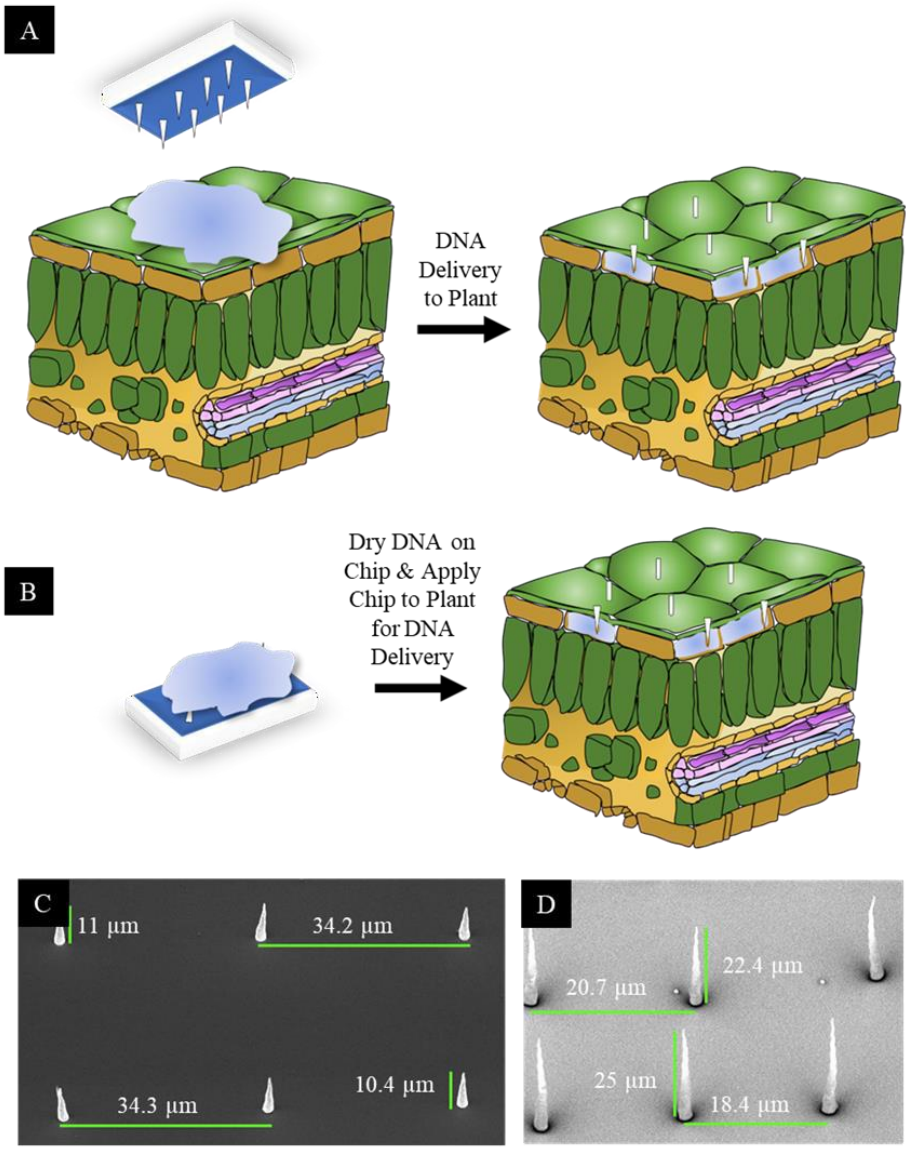

Figure 3.1. Design and application of carbon nanofibers. (A) On−plant of fiber delivery. A chip, placed on top of a leaf on which a 1 µL droplet of DNA solution is placed, is gently tapped to push the fibers into the leaf tissue. The chip is then removed, and nanofibers typically remain embedded in the tissue. (B) On−chip DNA method of fiber delivery. Fifteen minutes after a 1 µL drop of DNA is placed on a chip, it is placed on a plant organ surface and tapped with tweezers as in (A). After tapping, the chip was removed, and nanofibers were left embedded in the tissue. For both methods, −fiber controls utilized the flat (fiberless) side of the chip. (C) Electron micrograph of VANCFs with ~35 µm pitch, 10−15 µm height, and imaged at a 30° angle. (D) Electron micrograph of VANCFs with ~20µm pitch, 20−30 µm height, and imaged at a 30° angle. Due to the fact that the fibers were imaged at 30° angle, the apparent heights appear to be smaller than the actual height by a factor of sin(30°)=1/2. Fibers were grown using 200−500 nm e−beam dot sizes and taper to a diameter less than 200 nm. Growth parameters: plasma current 1 amp, C_2H_2: NH_3 = 0.55, 625°C, 10 torr.

DNA and dye delivery via VACNFs

Application to leaves, roots, and fruit "on−plant method"

Fiber delivery of DNA or dye to plant cells was conducted using a method modified from Davern et al. (2016). In brief, a 1 µL droplet containing fluorescein dye (1 mM), TAMRA dye (5(6)−Carboxytetramethylrhodamine, 10 µM), or of 200 ng/µl of plasmid DNA purified from liquid bacterial cultures was applied to the surface of a leaf or fruit. For Arabidopsis and poplar leaves, abaxial surfaces of detached leaves were impaled. For lettuce and *N. benthamiana*, adaxial surfaces of leaves attached to plants were impaled. A VACNF chip (3x3 mm) was placed on top of the droplet (with the fibers oriented such that they came into contact with the droplet), and the fibers were tapped into the plant tissue with a pair of forceps, using a hard surface to support the other side of the plant organ. For control experiments, the VACNF chip was applied with its smooth back to the leaf or fruit. Fibers applied without DNA or dye were anther control.

For dye delivery experiments, chips were left on the plants for 5 minutes and removed just before imaging. Chips were applied to roots of intact lettuce seedlings and roots were imaged 5 min – 1 h after dye delivery. After VACNF−mediated DNA delivery, Arabidopsis or Populus leaves were stored in a humid chamber for 48 h in long−day conditions (16 h of light, 8 h of dark) prior to imaging. Tomato fruits were kept in long day conditions as well for 40 h after DNA delivery. Arabidopsis leaves transformed with AALP:GFP were stored in the dark for 48 h prior to imaging (Tamura et al., 2003) unless otherwise specified. Lettuce plants were maintained in long day condition for 4 d after impalefection (the period effective for transient transformation via *Agrobacteria* (Wroblewski et al., 2005) and *N. benthamiana* plants for 3 d. Just before imaging, the plant tissues that came in contact with the chips were excised and placed on glass slides. In the case of the tomato fruit, the epidermal layer was removed to expose the top layer of

the pericarp. Both the epidermal layer and the pericarp were examined for fibers and transient−mediated protein accumulation.

Application to Arabidopsis leaves and roots "on−chip method"

When applying the chips to the Arabidopsis leaves using the "on−chip" method, 1 μL of 200 ng/μL DNA solution was drop−cast on to the fiber side of the chip and allowed to dry for 15 min prior to impaling tissue. When placing the droplet on the fibers, great effort was taken to ensure that the droplet was placed in the center of the chip and covering several fibers. Leaves were placed on a hard substrate and the fibers were applied on the abaxial side of the leaves using a pair of tweezers for the tapping. After VACNF−mediated delivery, plant leaves were stored in a humid chamber for 48 h in long−day conditions. For roots, the same method of drying DNA on VACNFs was applied. Roots were placed on agar plates and chips were applied to the organs while they were on top of the agar. Seedlings with roots transformed with biosensor FlincG (fluorescence indicator of cGMP) via VACNFs were kept on agar plates in long day light (16 h light, 8 h dark) conditions for 36 h prior to imaging.

Agrobacterium−mediated transformation

Lettuce (cultivar Salinas) and *N. benthamiana* leaves were infiltrated with *Agrobacterium tumefaciens* GV3101 carrying p35S−mCherry/pCambia (Kang et al., 2014) at OD_{600}=0.6. Plants were grown in the same way as for VACNFs experiments and kept in their growth conditions for 4 d post infection for lettuce and 3 d post infection for *N. benthamiana* before imaging.

Plasmids

The binary ~11,000 bp plasmid pUbiquitin$_{10}$:YFP−Gateway from Michniewicz et al. (2015), the ~3000 bp protoplast vector pUC with p35S:Arabidopsis Aleurain Like Protein (AALP):GFP from Kang et al. (2014), and the ~3000 bp vector pUC with p35S:mCherry, were used for VACNF−mediated transformation. pCambia with identical p35S:mCherry cassette (~10,000 bp) was used for *Agrobacterium*−mediated transformation (Kang et al., 2014). The binary vector pART: delta−FlincG (N2105633 Nottingham Arabidopsis Stock Centre), 6857 bp, with the cGMP biosensor FlincG (Isner and Maathuis, 2011) was also used.

Treatment of seedlings with Pep1

40 µL of Pep1 peptide (20 nM, Biomatik) was added to a glass slide on top of the root prior to imaging to trigger cGMP production in seedlings transiently transformed with the FlincG sensor.

Microscopy

Images were captured with Zeiss LSM 800 or LSM 710 confocal microscope. GFP and fluorescein signals were collected with an emission range of 510 and 545 nm, excitation was 488 nm. YFP signal was collected with an emission range of 491−573 nm, excitation was 488 nm. mCherry was imaged with 561 nm excitation and 570−628 emission.

Integrated density measures for fluorescent proteins

Fluorescence values for AALP:GFP, mCherry, and YFP were measured as total fluorescence (integrated density) in 20 µm × 20 µm confocal image areas (Jelenska et al., 2017) and quantified using ImageJ/FIJI (Schindelin et al., 2012).

Statistical analysis

Statistical analysis (ANOVA and Tukey's test) was performed using PRISM 9 (GraphPad). Statistically different categories ($P<0.05$) are marked by different letters.

RESULTS

Fiber design and application

Two approaches for introducing plasmid DNA into plant cells using VACNF chips were implemented: "on−plant" and "on−chip" methods (Figure 3.1A−B). For the on−plant method, a 1 µl droplet containing DNA was placed on the surface of a leaf. A VACNF chip was orientated such that the fibers came into contact with the droplet. Tweezers were then used to apply a force on the back side of the chip, driving the fibers into the tissue and delivering materials into the plant (Figure 3.1A). With the on−chip method, DNA was first applied to a chip, which was then used to impale the tissue (Figure 3.1B). In this work, we used 200 ng of plasmid DNA in 1 µL of water, after preliminary experiments using different concentrations and the on−plant method suggested this amount was optimal. Our conditions were similar to those used for successfully introducing DNA into mammalian cells using VACNF chips (McKnight et al., 2004; McKnight et al., 2005).

Previously, VACNFs were made to have the approximate diameter of aphid stylets (Davern et al., 2016) (Figure 3.1). These original nanofibers had a base diameter of 500 nm and tapered to 100 nm at the tip. Additionally, they had a lateral spacing (pitch) of 20 µm, to minimize the number of nanofibers penetrating individual epidermal cells in *Populus* leaves. We designed additional fiber arrays with longer (35 µm) or shorter (10 µm) pitch, reasoning that those additional geometries may be useful for a broad array of plant cells of various sizes and

shapes of plant cells (Figure 3.1C−D). In this study, fibers with 35 or 20 μm pitch were used for large Arabidopsis epidermal cells that have a jigsaw−like appearance and do not have a uniform shape; cells are 20 to 50 wide μm and can be as long as 100 μm. These fibers were also used for dye delivery in peaches, strawberries, and apples. Fibers with shorter pitch (10 μm and 20 μm) were used for tomato fruit, and leaves of poplar, lettuce, and *N. benthamiana*. All fibers were 10−25 μm in length and all designs were successful in transforming plants (Figures 3.1−6).

On−plant VACNF−mediated transformation of Arabidopsis leaves with a small plasmid

To test the applicability of VACNFs for transient transformation, we first employed a green fluorescent protein (GFP) fusion to the Arabidopsis aleurain−like protein (AALP) that transits through the endomembrane system and targets vacuoles (Sohn et al. 2003; Kim et al., 2005; Kang et al., 2014). We used a small (~3000 bp) pUC−based vector (used previously for protoplast transformation) and the VACNF on−plant method on excised leaves (Figure 3.1A). The accumulation of AALP:GFP was detected by confocal microscopy in Arabidopsis leaves 48 h after transformation (Figure 3.2A). We quantified success of delivery by comparing measurements of fluorescence that resulted from delivery of the vector (+DNA−AALP:GFP, +fibers) and the various controls (−DNA, +Fibers; +DNA−AALP:GFP, −Fibers (flat side of the chip); and −DNA, −Fibers (no treatment)). GFP signal was present only in leaf areas in which plasmid was delivered via fibers (+DNA−AALP:GFP, +Fibers) (Figure 3.2E) and was not observed in controls. Background signal in Figure 2 mainly comes from the stomatal guard cells, as indicated by asterisks, which were excluded from the analysis. When imaging the −DNA, +Fibers control, fields of view were selected such that fibers (which are autofluorescent) were present (Figure 3.2C). These data show successful VACNF−mediated transformation of

Arabidopsis leaves, resulting in expression of a fluorescent reporter at levels easy to image by florescence microscopy.

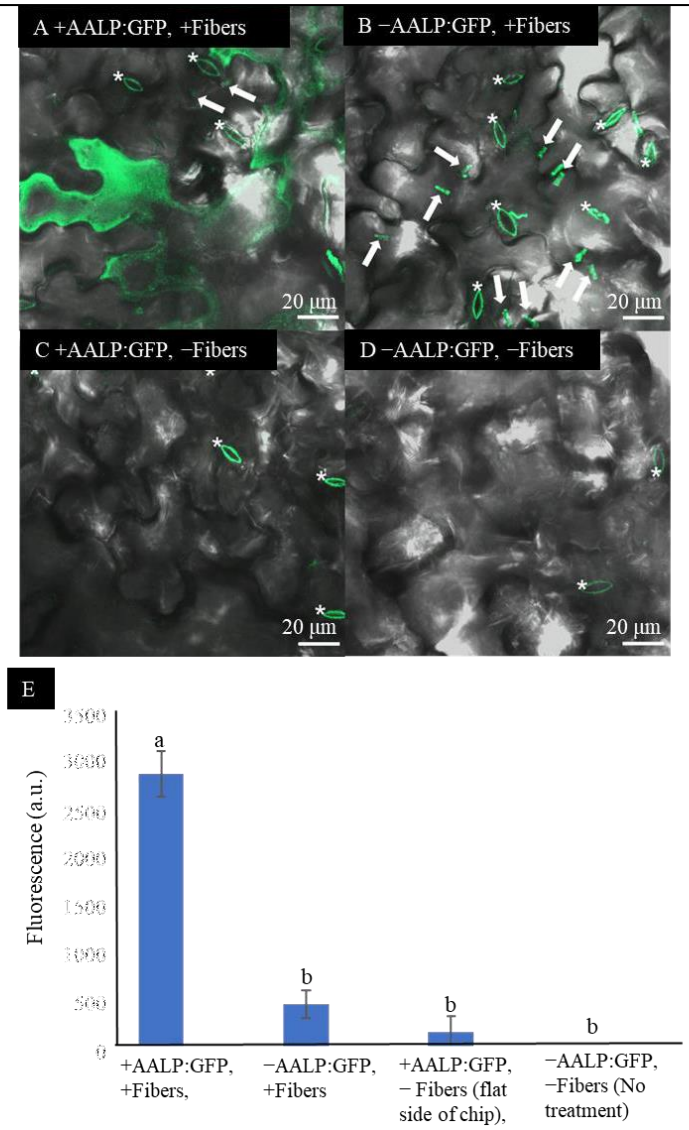

Figure 3.2. Fluorescent image analysis of Arabidopsis leaves transiently transformed with AALP:GFP 48 h after delivery via VACNF with a 35 µm pitch. (A) p35S:AALP:GFP/pUC plasmid delivery via VACNF using the on−plant method. GFP fluorescence is shown in green (+DNA−AALP:GFP, +fibers). (B) Fibers only (−DNA, +fibers). (C) AALP:GFP plasmid delivery without fibers (backside of chip with no fibers; +DNA−AALP:GFP, −fibers). (D) No treatment (−DNA, −fibers). (E) Graph of average integrated densities of GFP fluorescence (green channel) of defined 20×20 µm areas (n≥40 per condition, combined results from two experiments). Regions containing stomata (*) were excluded due to autofluorescence, and the average fluorescence signal intensity from the no −treatment condition was subtracted from each average. 2−way ANOVA (and Tukey test) was used for significance testing, and error bars represent the standard error of the mean. Different letters show significant differences between treatments ($P < 0.0001$). All images shown are maximum projections of 40 µm z−stacks. Scale bars are 20 µm and white arrows indicate fibers in the images.

On−plant and on−chip methods of VACNF−mediated transformation with a large plasmid

To further demonstrate the utility of the VACNF chips, we tested if a large plasmid encoding yellow fluorescent protein (YFP) could be used to transform leaves that were detached from plants. We used fibers with the on−plant method to transform Arabidopsis leaves with $pUBQ_{10}$:YFP carried on the ~11,000 bp Gateway plasmid, usually used for *Agrobacterium*−mediated transformation (Michniewicz et al., 2015) (Figure 3.3). The leaves to which the plasmid was delivered via fibers (+DNA-YFP, +Fibers,) had significantly greater signal in the YFP channel than the controls (−DNA, +Fibers; +DNA−YFP, −Fibers (flat side of the chip); −DNA, −Fibers (no treatment)) (Figure 3.3I). Similar to a small plasmid, the use of a large binary vector resulted in easily detectable reporter fluorescence. Background signals observed in Figure 3 again mainly came from the guard cells, as indicated by the asterisks in the figure. In this experiment, we also compared the on−plant and on−chip methods of VACNF−mediated impalefection. There was no observable difference in the expression pattern of YFP in leaves transformed (Figure 3.3A−B). Additionally, there was no significant difference in measured fluorescence values for the on−chip and on−plant methods (Figure 3.3I). Therefore, we used the on−plant method in most subsequent experiments. Accounting for various factors, including where force was applied to the chip as well as the number of fibers that penetrated the leaf tissue, observable expression was detected in different areas within the 3mm×3mm area of leaf tissue under the chip. As the leaf surface is not completely flat, not all cells came into contact with the chip. These experiments show that detached leaves can be transformed with a large plasmid using VACNFs.

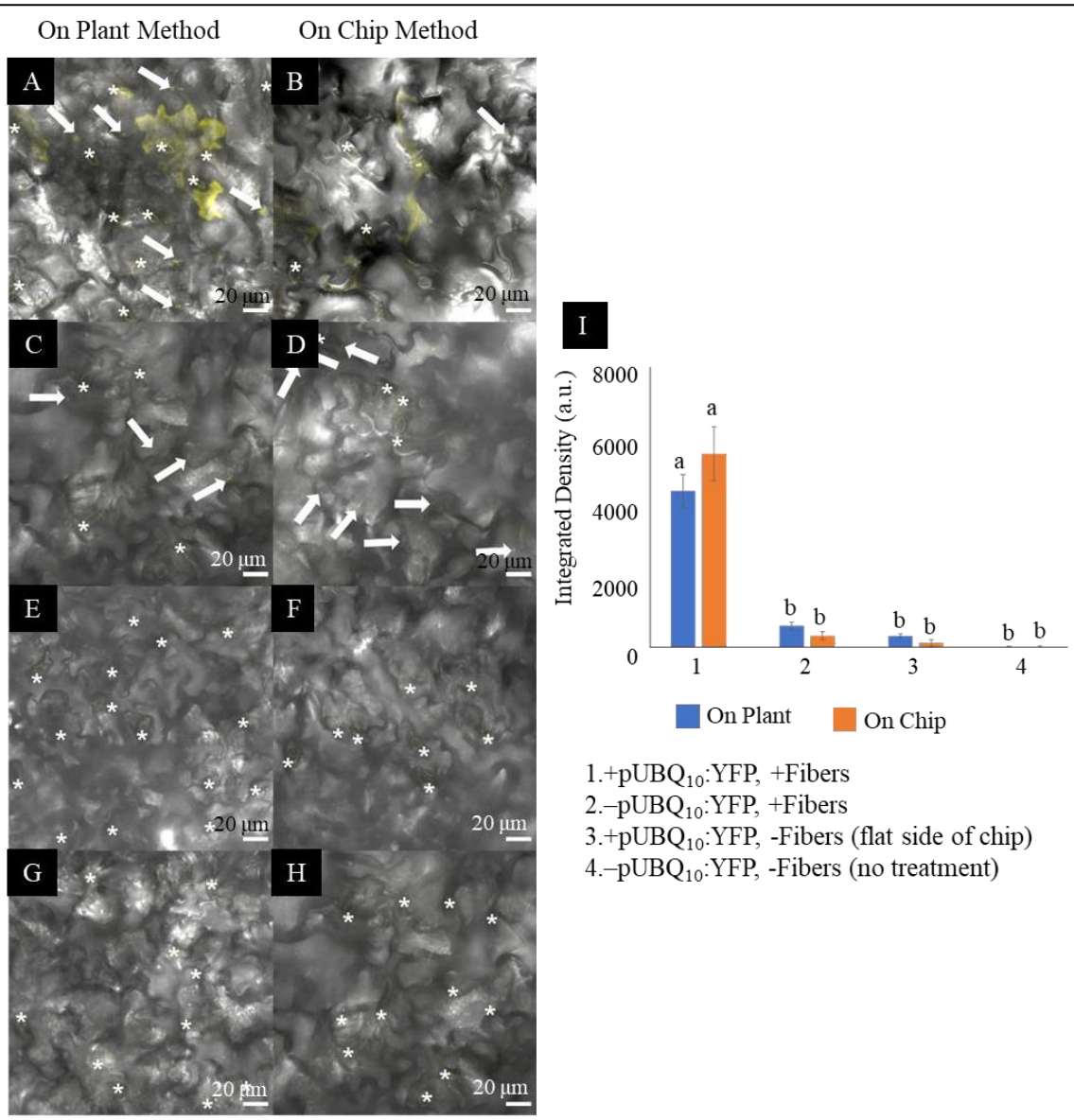

Figure 3.3. Fluorescent image analysis of Arabidopsis leaves transiently transformed with pUBQ$_{10}$:YFP 48 h after delivery via VACNF with a 35 µm pitch using the on−plant or on−chip methods. (A) and (B) DNA−YFP delivery via VACNF using the on−plant and on−chip methods, respectively (+DNA−YFP, +Fibers). (C) and (D) Fibers only (–DNA, + Fibers). (E) and (F) DNA−YFP delivery without fibers (flat chip: +DNA−YFP, −Fibers). (G) and (H) No treatment (−DNA, −Fibers). (I) Graph representing relative average fluorescence signal intensity of 25 20×20 µm areas from images of 5 biological replicates combined from 2–3 experiments using fluorescence from the YFP channel. Regions containing stomata (*) were excluded due to autofluorescence, and the average fluorescence intensity from the no−treatment condition was subtracted from each average. 2−way ANOVA (and Tukey test) was used for significance testing, and error bars represent the standard error of the mean. Different letters show significant differences between treatments ($P < 0.0001$). All images shown are maximum projections of 40 µm z−stacks. White arrows indicate fibers in the images.

VACNF−mediated transformation of different plant species

To further substantiate the applicability of VACNF chips, the on−plant method was applied to excised poplar leaves to deliver DNA encoding AALP:GFP in the pUC vector. Arabidopsis leaves served as a positive control in this experiment to show that the quality of DNA was suitable for delivery and expression (Figure 3.4A). GFP signals were observed in impaled regions 48 h post−delivery in Arabidopsis and poplar leaves (Figure 3.4A and C). The fibers were also used to successfully deliver p35S:mCherry/pUC vector to lettuce (*Lactuca sativa* cv. Salinas) and *Nicotiana benthamiana* leaves attached to plants (Figure 3.5A and B). These results show that nanofibers can deliver DNA to different plants for the production of encoded proteins.

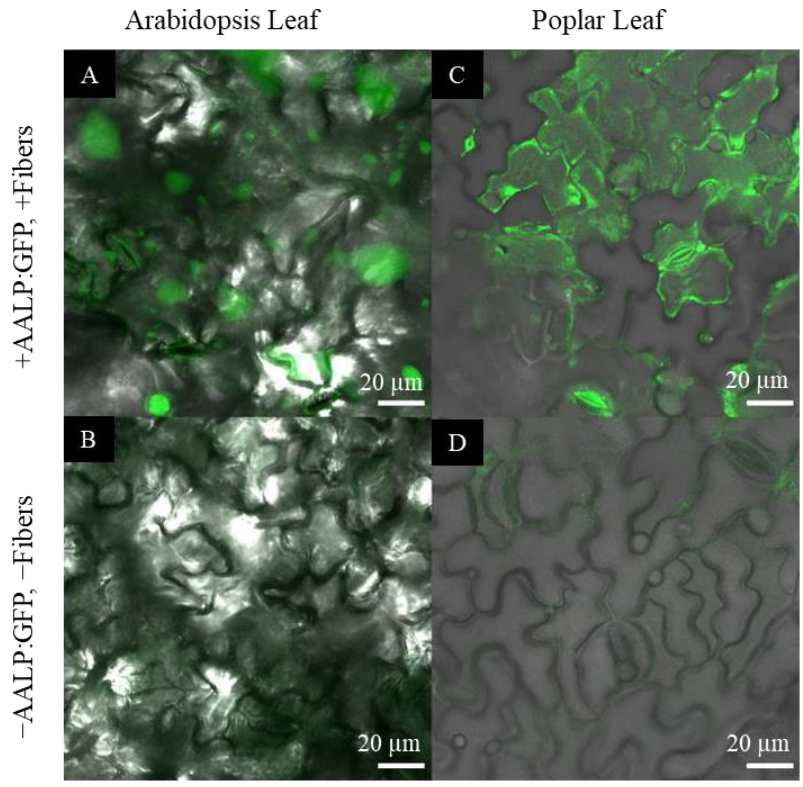

Figure 3.4. Use of VACNF to introduce DNA expression constructs into poplar leaves. Images were generated using confocal fluorescence microscopy. VACNFs delivered a small plasmid resulting in expression of a vacuolar marker, AALP:GFP (shown in green). (A) Arabidopsis leaf 48 h after delivery of p35S:AALP:GFP/pUC via fibers with 20 µm pitch (+DNA−AALP:GFP, + Fibers), (C) Poplar leaf 48 h after delivery via fibers with 10−µm pitch (+DNA−AALP:GFP, +Fibers). (B and D) Show untreated controls (−DNA, −Fibers). All images are maximum projections of 40 µm z−stacks.

Comparison of VACNF and *Agrobacterium*−mediated transient transformation

Agrobacterium is commonly used for transformation of intact plants. Therefore, we compared expression of mCherry resulting from *Agrobacterium*−mediated transformation, using pCambia binary vector, to our VACNF−mediated delivery of p35S:mCherry/pUC in lettuce and *N. benthamiana* leaves attached to plants (Figure 3.5). mCherry fluorescence in lettuce leaf was much higher using VACNF−mediated impalefection than was found using agroinfiltration (Figure 3.5A, C, and E). In contrast for *N. benthamiana*, which is highly amenable to transient transformation with *Agrobacteria*, mCherry fluorescence was higher after agroinfiltration than

after imaplefection, as observed by microscopy (Figures 3.5B and D) and quantified (Figure 3.5G).

For the experiments described above with lettuce, it was necessary to optimize the timing of observations after VACNF−mediated transient transformation. In contrast to other plant species, we did not detect fluorescence in lettuce 2 d after transformation either via VACNFs or *Agrobacteria*. Wroblewski et al. (2005) previously noted that the highest transient expression occurred in lettuce 4−5 d after agroinfiltration. We detected mCherry signals 3−5 d after transformation of lettuce with both methods, with highest signal at 4 d. In *N. benthamiana* fluorescence was highest 3 d post transformation. Our results stress the importance of optimalization of VACNFs protocols for different plants, which may require different times for transgene expression after impalefection. The experiments with lettuce show that VACNFs can be a superior method for plant species and tissues recalcitrant to *Agrobacterium*−mediated transformation.

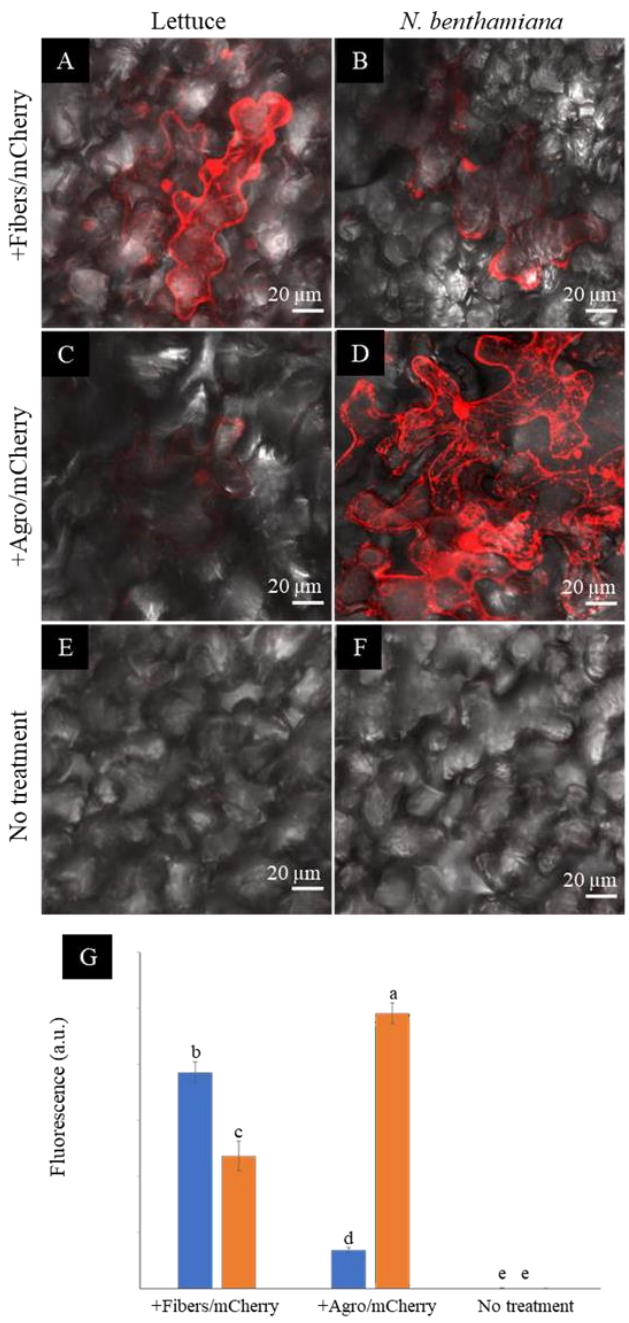

Figure 3.5: Comparison of VACNF− and *Agrobacterium*−mediated transient transformation. A) p35S:mCherry/pUC expression 4 d after delivery via VACNFs with 10 µm pitch using the on−plant method in lettuce and (B) 3 d after delivery in *N. benthamiana*. (C) *Agrobacterium*−mediated delivery of p35S:mCherry/pCambia in lettuce, 4 d after agroinfiltration. (D) p35S:mCherry/pCambia 3 d after agroinfiltration in *N. benthamiana*. (E) and (F) show background signal for no treatment samples in lettuce and *N. benthamiana*, respectively. (G) Graph representing average fluorescence signal intensity of the mCherry fluorescence of 20×20 µm areas (n≥40, combined results from 2–3 experiments). Background signal (no treatment) was subtracted, 2−way ANOVA (and Tukey test) was used for significance testing, and error bars represent the standard error of the mean. Different letters show significant differences between treatments ($P < 0.0002$). All images are maximum projections of 20 µm z−stacks.

VACNFs may be useful for cargo delivery and transformation of different plant organs

Curved organs present a challenge for transient transformation using VACNFs, where having a relatively flat surface to tap the chip with nanofibers into the tissue is an advantage. Nevertheless, to establish broader applicability of the method, we tried various tissues, including hypocotyl, roots, and fruit. While we did not get successful transformation of hypocotyls, we did have a few positive results with other curved organs. We found that it was useful as a first test to deliver a fluorescent dye (e.g., fluorescein or TAMRA) to the sample organ, as demonstrated by Davern et al. (2016). This permits a rapid assessment of whether the mechanics of the delivery method will work. In this way, we showed that VACNF arrays could successfully deliver dyes into fruit (store−bought strawberries, apples, and peaches) and lettuce roots (Figure 3.6A−H). In addition, we were able to transform tomato fruit with p35S:AALP:GFP/pUC using the on−plant method (Figure 3.6I). Specifically, after 40 h, GFP signals were observed in the tomato fruit pericarp when the chip contact area was excised from the fruit. We did not see significant GFP signals in the epidermal (skin) layer. For Arabidopsis roots, we used the on−chip method to deliver FlincG, a fluorescence−based reporter for cGMP. After delivery of the construct, we treated the roots with Pep1, a plant peptide that activates signaling, to induce cGMP, and monitored signal over time. We captured images of a transformed cell that showed increased fluorescence signal over time in response to Pep1 (Figure 3.6K), similar to what was previously reported (Ma et al., 2012). Controls for this experiment (+DNA−FlincG, +Fibers, +Water; and −DNA, +Fibers, +Pep1) did not show an increase in green fluorescence over time (Figure 3.6L−M). Thus, delivery of the biosensor and application of an elicitor are necessary for increased fluorescence signal over time. This experiment indicates that a functional probe can be expressed in cells transformed using VACNF.

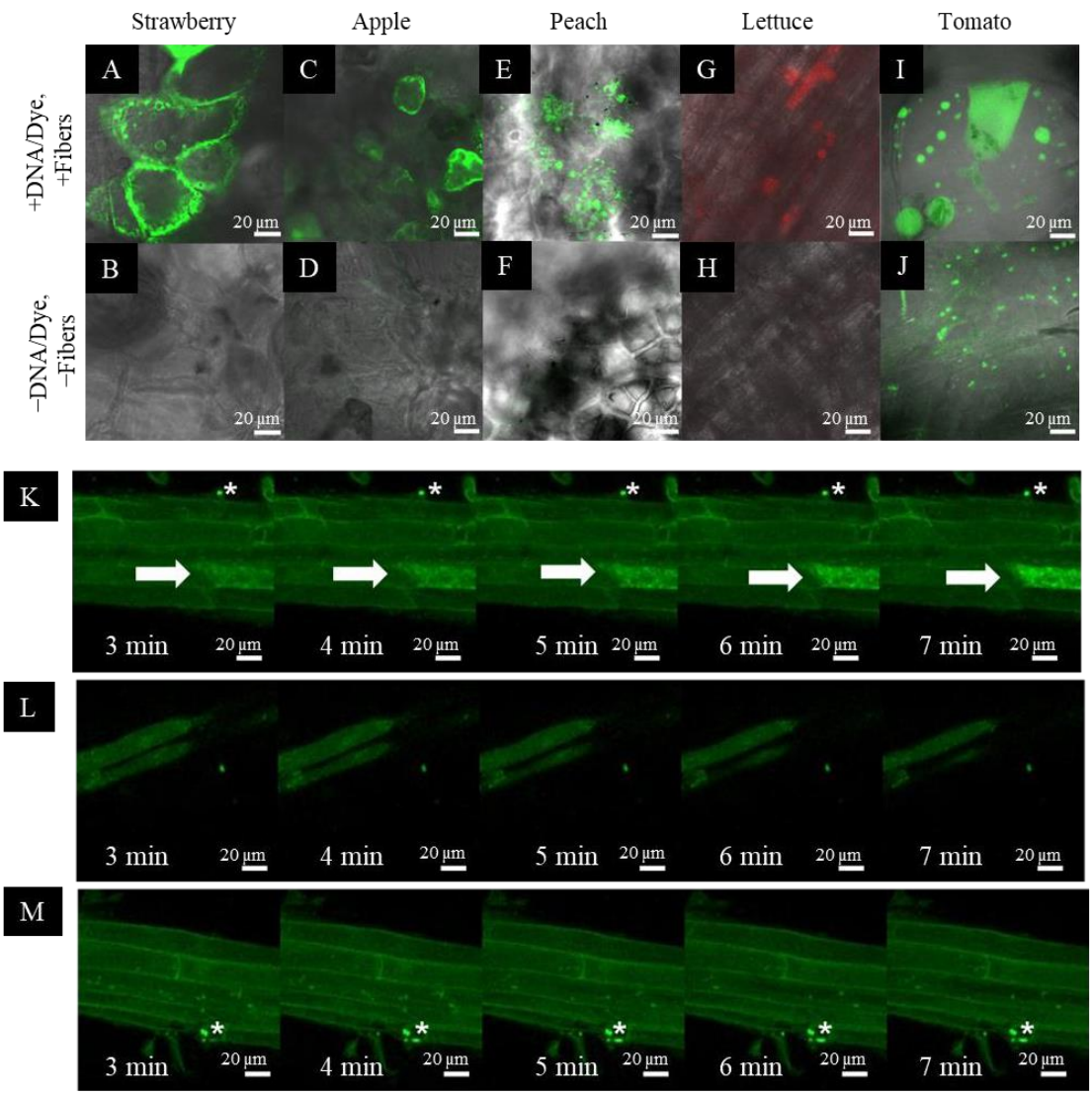

Figure 3.6: Application of VACNFs to curved organ surfaces. Images were generated using fluorescence confocal microscopy. Fluorescein dye was delivered to store bought strawberry (A), apple (C), and peach (E) via fibers with 35 µm pitch with the on−plant method. (G) TAMRA dye was delivered to lettuce roots using the on−plant method with fibers with 10 µm pitch. (I) DNA (p35S:AALP:GFP/pUC) was delivered to store−bought tomato fruit 40 h after delivery of via on−plant method with fibers with 20 µm pitch. The area shown is approximately one large cell. Panels B, D, F, H, and J show no−treatment controls of plant tissue for panels A, C, E, G, and I, respectively. (K-M) DNA encoding FlincG was delivered to Arabidopsis roots via VACNFs with 35 µm pitch (on−chip method), and expression was assessed after 36 h. (K) 36 h after FlincG delivery, Arabidopsis roots were treated with Pep1 peptide (panels show different time points after exposure to elicitor Pep1 (20 nM))(+DNA−FlincG, +Fibers, +Pep1). The white arrow points to the transformed cell with signal increasing over time. (L) 36 h after FlincG delivery, Arabidopsis roots were treated with water (panels show different time points after exposure to water, which does not trigger production of cGMP) (+DNA−FlincG, +Fibers, +water). (M) Arabidopsis roots with fibers without biosensor delivery treated with Pep1 (−DNA, +Fibers, +Pep1). A−F are single images (0.5 µm) captured via confocal microscopy. G−H are maximum projections of 118 µm z−stacks and I−M are maximum projections of 40 µm z−stacks. * denote regions with fibers.

DISCUSSION

In this work, two different VACNF chip impalefection protocols (on−plant and on−chip, Figure 3.1) were established for transient transformation of leaves, roots, and fruit in a number of plant species (Figures 3.2−6). VACNF chips can be used on intact plants or on organs detached from plants. This raises the possibilities of a number of interesting applications, such as studying the impact of environmental perturbation on reporter gene activity. Both the on−plant and on−chip methods rely on the fibers to make small punctures in the cell wall and membrane through an impulse force resulting from the tapping of the tweezers on the back of the chip. Using the fibers in this manner is minimally invasive and was not found to be toxic or damaging to the plant (Davern et al., 2016). Importantly, these methods do not require fibers to be surface functionalized, unlike other existing methods (Jat et al., 2020; Zhang et al., 2022b), and the fibers can be used to deliver different sized vectors. With the exception of hypocotyls, all plant organs that we tested could be transformed using VACNFs: leaves (Arabidopsis, poplar, lettuce, and *N. benthamiana*), roots (Arabidopsis) and fruit (tomato; Figures 3.2-6). Importantly, VACNF−mediated transformation may be successfully used in a species, such as lettuce, for which Agrobacterium−mediated transient transformation is inefficient (Figure 3.5).

A workflow summarizing important design, quality−control, and operational steps for impalefection is provided in Figure 3.7. Successful DNA delivery with the VACNFs in plants depends upon on the geometry of the fibers and the design of the chips. The fibers used herein were straight with a tapering diameter such that the tip was less than 200 nm and resembled an aphid stylet. It was found that sharp tips with smaller diameters were less damaging than blunt tips in Arabidopsis leaf epidermal cells (Forouzesh et al., 2014; Forouzesh, 2012) . In their study, Forouzesh et al. (2013) used single tips (or a single fiber equivalent) for nanoindentation studies

to quantify the failure stress of cell walls. If the fibers are bent, they are unable to make direct contact with the leaf tissue, hence unable to impale cells and achieve delivery. Straightness of fibers is one of the first things to check if VACNF−mediated transformation fails (Figure 3.7). Pitch is another consideration, although in our experience it did not impact delivery success. The chips used in our experiments were designed to limit the number of fibers penetrating each cell (limit 1−2 fibers) by varying the pitch. Another factor that did prove critical for protein expression after VACNF−mediated impalefection is the timing. Most fluorescent markers were detected after 2 d. However, in lettuce, expression took longer, 4 d (Figures 3.2−6).

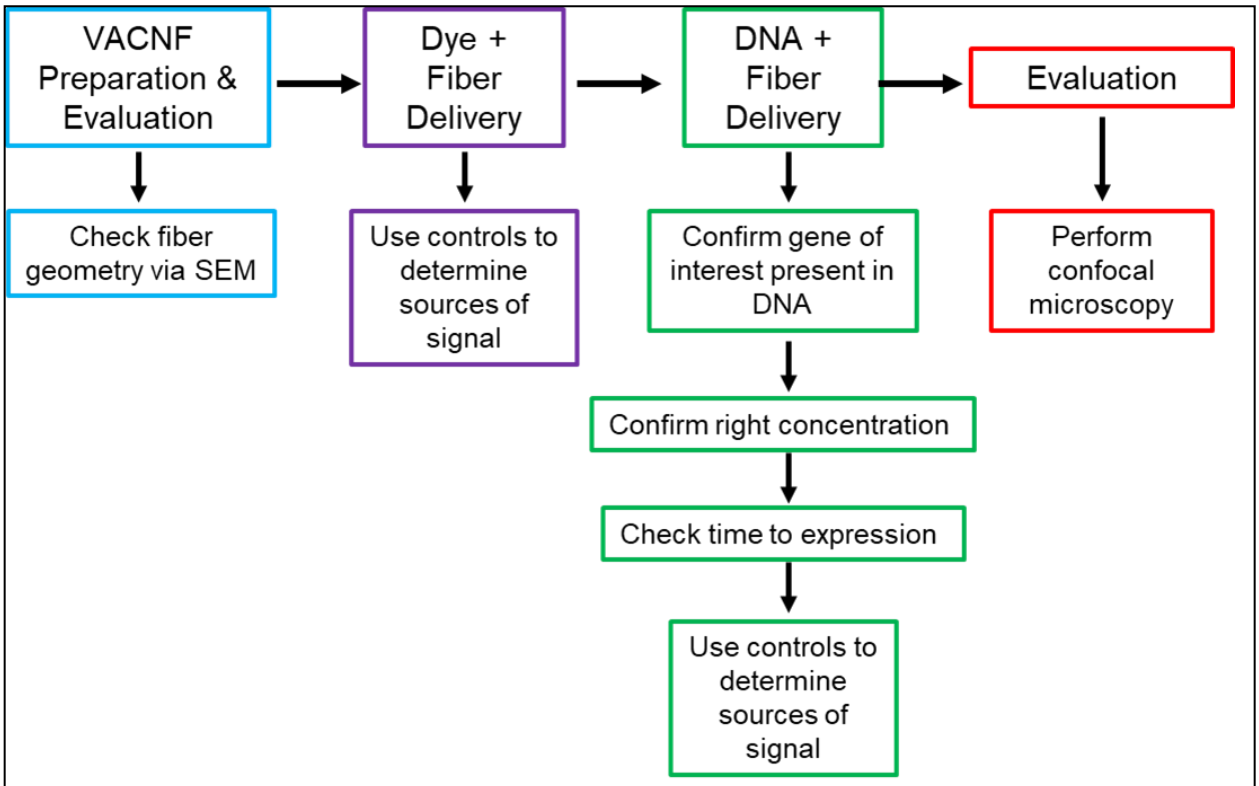

Figure 3.7. Workflow for VACNF mediated transient transformation of plants. When using the VACNFs for delivery of small molecules, there are a few problems that can arise. The first step in troubleshooting is to check the geometry of the fibers using scanning electron microscopy to ensure that the fibers are straight and have a sharp tip. After confirming the fiber geometry, the next step is to make sure that you are able to successfully deliver dye into your plant/organ of choice. For this purpose, place a 1 µL droplet on the plant surface and use the fibers to deliver the dye, checking for delivery with the microscope. With this step and all other steps moving forward, it is important to use appropriate controls (−Dye,−Fibers; −Dye, +Fibers; and +Dye,−Fibers,) to be confident that you are getting signal from dye delivery. If both steps are successful, the next step would be to ensure that your gene of interest is present in your plasmid, you are using the right concentration of DNA, and you are waiting the right amount of time after delivery to check expression. The last step is to check expression using confocal microscopy.

Both large (binary vectors utilized for *Agrobacterium*−mediated transformation) and small vectors (previously used for protoplast transformations) can be successfully delivered and expressed in plants (Figures 3.2−6). Smaller plasmids are easier to manipulate and tend to have a higher transient transformation efficiency in protoplast transfections and particle bombardment than the larger vectors used for *Agrobacterium*−mediated transformations (Sainsbury et al.,

2009). With fiber delivery, results using larger and smaller vectors were similar. Therefore, constructs designed for use with *Agrobacterium* can be successfully used with VACNFs.

Nanomaterials are increasingly being used for transient transformation. The most recent methods of nanoparticle−mediated transformation or delivery of nucleic acids to plants have relied upon using pressure infiltration to deliver nanoparticles into plants via a needleless syringe (Izuegbunam et al., 2021; Zhang et al., 2022; Zhang et al, 2019; Demirer et al., 2019). Together, these nanoparticle−mediated methods have enabled delivery of nucleic acids and other molecules into Arabidopsis, tobacco, onion, maize, wheat, rapeseed, mustard, carrot, cotton, tomato, spinach, arugula, watercress, cowpea, chamomile, barley, and moss (Kumar et al., 2020; Jat et al., 2020; Izuegbunam et al., 2021). Roots can take up nanoparticles through passive diffusion and plant leaves can easily be transformed with passive infiltration of nanoparticles entering through the stomata (Hubbard et al., 2020). To the knowledge of the authors, only one study previously used nanoparticles to transform other parts of a plants that were not leaves or roots. Specifically, in Izuegbunam et al. (2021), the authors used needleless syringes to deliver nanorods with anchored DNA to developing seed tissues in Arabidopsis, field mustard, barley, and wheat. This method requires the conjugation of DNA to nanorods and subsequent release of DNA once inside cells.

In summary, we have demonstrated the utility of using vertically aligned carbon nanofibers to overcome the challenges of crossing plant cell walls and plasma membranes to deliver DNA into cells. There is no release of cargo necessary, since nanofibers facilitate delivery through mechanical means into the plant, probably by forming transient channels around the fibers through which material can enter cells (Davern et al., 2016). The level of transgene expression readily allowed detection of several fluorescent reporters. Previously,

VACNFs were successfully used to deliver proteins to plants cells (Davern et al., 2016). In that study dextran and proteins were detected in plant cells as early as 5 minutes after introduction via VACNFs. Labeled peptides entered vascular tissues which allowed their distribution throughout the plant (Davern et al., 2016). In the present work, we have demonstrated the value of VACNF chips in delivering DNA into leaves, roots, and fruit, with the minimally invasive impalefection allowing subsequent expression of the intended gene products. Looking forward, VACNF chips could be utilized to deliver multiple types of biomolecules together (e.g., gene editing reagents) to plants via delivery to a meristem, plant cell culture, or plants undergoing early organogenesis.

ACKNOLWEDGMENTS

We thank Dr. Inhwan Hwang (Pohang University of Science and Technology) for CaMV p35S: AALP:GFP DNA and Dr. Jiyoung Lee (Korea Research Institute of Bioscience and Biotechnology) for p35S−mCherry constructs. We thank John Zdenek for assistance with plant growth and maintenance. We thank Mindy Clark from Oak Ridge National Laboratory and Dr. Gail Taylor from the University of California, Davis for *Populus trichocarpa* (Nisq−1 genotype). Nanofiber arrays were fabricated at the Center for Nanophase Materials Sciences (CNMS), which is a Department of Energy Office of Science User Facility (Proposal ID:CNMS2019−103). Support from CNMS is awarded through a peer−reviewed proposal system and is provided at no cost to successful applicants who intend to publish their results (http://www.cnms.ornl.gov/user/becoming_a_user.shtml). We thank the CNMS for assistance with the production of nanofiber arrays. We thank Dr. John Caughmen, Dr. Timothy McKnight, and Travis Bee for critical discussion about experimental design.

Contribution to the field

One of the biggest challenges that plant biologists face arises when they are trying to study microscale phenomena. In order to study specific problems on such a small scale, researchers will often need to add different markers to visualize proteins or compartments that they are trying to study, or different components of a pathway they will need to modulate. The challenge in doing these experiments arises when scientists try to deliver the markers or reagents necessary to turn on or off certain genes. Current methods of delivery can be time consuming, cause damage to the plant, or are prohibitively expensive. Using vertically aligned carbon nanofibers, we have negated these issues. Our method takes less than 5 minutes, the fibers are produced at Oak Ridge National Laboratory, and the fibers are minimally invasive to plants. The fibers are generally applicable to a variety of plant species for the purpose of delivering DNA or other biomolecules.

WORKS CITED

Altpeter, F., Springer, N.M., Bartley, L.E., Blechl, A.E., Brutnell, T.P., Citovsky, V., Conrad, L.J., Gelvin, S.B., Jackson, D.P., Kausch, A.P. & Lemaux, P.G., (2016). Advancing crop transformation in the era of genome editing. *The Plant Cell*, *28*(7), 1510−1520.

Arshad, M., Zafar, Y., & Asad, S. (2013). Silicon carbide whisker−mediated transformation of cotton (*Gossypium hirsutum L.).* In *Transgenic Cotton*, ed. B. Zhang (Totowa, NJ: Humana), 79−92.

Baltes, N.J., Gil−Humanes, J. & Voytas, D.F., (2017). Genome engineering and agriculture: opportunities and challenges. *Progress in Molecular Biology and Translational Science*, *149*, 1−26.

Birch, R.G., (1997). Plant transformation: problems and strategies for practical application. *Annual Review of Plant Biology*, *48*(1), 297−326.

Chang, F.P., Kuang, L.Y., Huang, C.A., Jane, W.N., Hung, Y., Yue−ie, C.H. & Mou, C.Y., (2013). A simple plant gene delivery system using mesoporous silica nanoparticles as carriers. *Journal of Materials Chemistry*, *1*(39), 5279−5287.

Cunningham, F. J., Goh, N. S., Demirer, G. S., Matos, J. L., & Landry, M. P. (2018). Nanoparticle−mediated delivery towards advancing plant genetic engineering. *Trends Biotechnology*, *36*(9), 882−897.

Davern, S.M., McKnight, T.E., Standaert, R.F., Morrell−Falvey, J.L., Shpak, E.D., Kalluri, U.C., Jelenska, J., Greenberg, J.T. & Mirzadeh, S., (2016). Carbon nanofiber arrays: a novel tool for microdelivery of biomolecules to plants. *PLoS One*, *11*(4), e0153621.

Demirer, G.S., Zhang, H., Matos, J.L., Goh, N.S., Cunningham, F.J., Sung, Y., Chang, R., Aditham, A.J., Chio, L., Cho, M.J. & Staskawicz, B., (2019). High aspect ratio nanomaterials enable delivery of functional genetic material without DNA integration in mature plants. *Nature Nanotechnology*, *14*(5), 456−464.

Forouzesh, E. (2012). *Nanoindentation−based Methods for Studying the Mechanical Behavior of Living Plant Cells* [Doctoral dissertation]. [Lincoln (NE)]: University of Nebraska−Lincoln.

Forouzesh, E., Goel, A., Mackenzie, S.A. & Turner, J.A., (2013). In vivo extraction of Arabidopsis cell turgor pressure using nanoindentation in conjunction with finite element modeling. *The Plant Journal*, *73*(3), 509−520.

Forouzesh, E., Goel, A.K. & Turner, J.A., (2014). Quantifying plant cell−wall failure in vivo using nanoindentation. *MRS Communications*, *4*(3), 107−111.

Gou, Y.J., Li, Y.L., Bi, P.P., Wang, D.J., Ma, Y.Y., Hu, Y., Zhou, H.C., Wen, Y.Q. & Feng, J.Y., (2020). Optimization of the protoplast transient expression system for gene functional studies in strawberry (*Fragaria vesca*). *Plant Cell, Tissue and Organ Culture, 141*, 41−53.

Haque, E., Taniguchi, H., Hassan, M., Bhowmik, P., Karim, M.R., Śmiech, M., Zhao, K., Rahman, M. & Islam, T., (2018). Application of CRISPR/Cas9 genome editing technology for the improvement of crops cultivated in tropical climates: recent progress, prospects, and challenges. *Frontiers in Plant Science, 9*, 617.

Hubbard, J.D., Lui, A. & Landry, M.P., (2020). Multiscale and multidisciplinary approach to understanding nanoparticle transport in plants. *Current Opinion Chemical Engineering, 30*, 135−143.

Hwang, H.H., Yu, M. and Lai, E.M., (2017). *Agrobacterium*−mediated plant transformation: biology and applications. *The Arabidopsis Book, 15,* e0186.

Isner, J. C., & Maathuis, F. J. (2011). Measurement of cellular cGMP in plant cells and tissues using the endogenous fluorescent reporter FlincG. *The Plant Journal, 65*(2), 329−334.

Izuegbunam, C.L., Wijewantha, N., Wone, B., Ariyarathne, M.A., Sereda, G. & Wone, B.W., (2021). A nano−biomimetic transformation system enables in planta expression of a reporter gene in mature plants and seeds. *Nanoscale Advances, 3*(11), 3240−3250.

Jain, A.K. & Thareja, S., (2019). In vitro and in vivo characterization of pharmaceutical nanocarriers used for drug delivery. *Artificial Cells, Nanomedicine, and Biotechnology, 47*(1), 524−539.

Jat, S.K., Bhattacharya, J. & Sharma, M.K., (2020). Nanomaterial based gene delivery: a

promising method for plant genome engineering. *Journal of Materials Chemistry B*, *8*(19), 4165−4175.

Jelenska, J., Davern, S.M., Standaert, R.F., Mirzadeh, S. & Greenberg, J.T., (2017). Flagellin peptide flg22 gains access to long−distance trafficking in Arabidopsis via its receptor, FLS2. *Journal of Experimental Botany*, *68*(7), 1769−1783.

Kang, Y., Jelenska, J., Cecchini, N.M., Li, Y., Lee, M.W., Kovar, D.R. & Greenberg, J.T., (2014). HopW1 from *Pseudomonas syringae* disrupts the actin cytoskeleton to promote virulence in Arabidopsis. *PLoS Pathogens*, *10*(6), e1004232.

Karami, O., (2008). Factors affecting *Agrobacterium*−mediated transformation of plants. *Transgenic Plant Journal*, *2*(2)**,** 127−137.

Kim, H., Park, M., Kim, S.J. & Hwang, I., (2005). Actin filaments play a critical role in vacuolar trafficking at the Golgi complex in plant cells. *The Plant Cell*, *17*(3), 888−902.

Krenek, P., Samajova, O., Luptovciak, I., Doskocilova, A., Komis, G. & Samaj, J., (2015). Transient plant transformation mediated by *Agrobacterium tumefaciens*: Principles, methods and applications. *Biotechnology Advances*, *33*(6)**,** 1024−1042.

Kumar, S., Nehra, M., Dilbaghi, N., Marrazza, G., Tuteja, S.K. & Kim, K.H., (2020). Nanovehicles for plant modifications towards pest−and disease−resistance traits. *Trends in Plant Science*, *25*(2), 198−212.

Lacroix, B. & Citovsky, V., (2020). Biolistic approach for transient gene expression studies in plants. In *Biolistic DNA Delivery in Plants*, eds. Rugstgi, S. & Luo, H., (New York, NY: Humana), 125−139.

Levy, A., El−Mochtar, C., Wang, C., Goodin, M. & Orbovic, V., (2018). A new toolset for

protein expression and subcellular localization studies in citrus and its application to citrus tristeza virus proteins. *Plant Methods, 14*(1), 1−11.

Li, J.F., Park, E., von Arnim, A.G. & Nebenführ, A., (2009). The FAST technique: a simplified *Agrobacterium*−based transformation method for transient gene expression analysis in seedlings of Arabidopsis and other plant species. *Plant Methods, 5*, 1−15.

Liu, Q., Chen, B., Wang, Q., Shi, X., Xiao, Z., Lin, J. & Fang, X., (2009). Carbon nanotubes as molecular transporters for walled plant cells. *Nano Letters, 9*(3), 1007−1010.

Ma, Y., Walker, R. K., Zhao, Y., & Berkowitz, G. A. (2012). Linking ligand perception by PEPR pattern recognition receptors to cytosolic Ca2+ elevation and downstream immune signaling in plants. *Proceedings of the National Academy of Sciences, 109*(48), 19852−19857.

Maliga, P., (2004). Plastid transformation in higher plants. *Annual Reviews Plant Biology, 55*, 289−313.

McKnight, T.E., Melechko, A.V., Hensley, D.K., Mann, D.G., Griffin, G.D. & Simpson, M.L., (2004). Tracking gene expression after DNA delivery using spatially indexed nanofiber arrays. *Nano Letters, 4*(7), 1213−1219.

McKnight, T.E., Melechko, A.V., Guillorn, M.A., Merkulov, V.I., Lowndes, D.H. & Simpson, M.L., (2005). Synthetic nanoscale elements for delivery of materials into viable cells. In *NanoBiotechnology Protocols*, eds. Rosenthal, S. and Wright, D.W., (Nashville, TN: Humana Press), 191−208.

Melechko, A.V., Desikan, R., McKnight, T.E., Klein, K.L. & Rack, P.D., (2009). Synthesis of vertically aligned carbon nanofibres for interfacing with live systems. *Journal of Physics D: Applied Physics, 42*(19), 193001.

Michniewicz, M., Frick, E.M. & Strader, L.C., (2015). Gateway−compatible tissue−specific vectors for plant transformation. *BMC Research Notes*, *8*(1), 1−8.

Mitter, N., Worrall, E.A., Robinson, K.E., Li, P., Jain, R.G., Taochy, C., Fletcher, S.J., Carroll, B.J., Lu, G.Q., & Xu, Z. P. (2017). Clay nanosheets for topical delivery of RNAi for sustained protection against plant viruses. *Nature Plants*, *3*(2), 1−10.

Mohan, C., Shibao, P. Y. T., & Silva, F. H. (2019). Applications of Genome Engineering/Editing Tools in Plants. In *Advances in Plant Transgenics: Methods and Applications*, eds. Sathiskkumar, R., Kumar, S.R., Hema, J., & Baskar, V., (Singapore: Springer), 143−165.

Ozyigit, I.I. & Yucebilgili Kurtoglu, K., (2020). Particle bombardment technology and its applications in plants. *Molecular Biology Reports*, *47*, 9831−9847.

Pérez−de−Luque, A., (2017). Interaction of nanomaterials with plants: what do we need for real applications in agriculture? *Frontiers in Environmental Science*, *5*, 12.

Ren, R., Gao, J., Lu, C., Wei, Y., Jin, J., Wong, S.M., Zhu, G. & Yang, F., (2020). Highly efficient protoplast isolation and transient expression system for functional characterization of flowering related genes in cymbidium orchids. *International Journal of Molecular Sciences*, *21*(7), 2264.

Sainsbury, F., Thuenemann, E.C. & Lomonossoff, G.P., (2009). pEAQ: versatile expression vectors for easy and quick transient expression of heterologous proteins in plants. *Plant Biotechnology Journal*, *7*(7), 682−693.

Sanzari, I., Leone, A. & Ambrosone, A., (2019). Nanotechnology in plant science: to make a long story short. *Frontiers in Bioengineering and Biotechnology*, *7*, 120.

Schindelin, J., Arganda−Carreras, I., Frise, E., Kaynig, V., Longair, M., Pietzsch, T., Preibisch,

S., Rueden, C., Saalfeld, S., Schmid, B. & Tinevez, J.Y., (2012). Fiji: an open−source platform for biological−image analysis. *Nature Methods*, *9*(7), 676−682.

Sohn, E.J., Kim, E.S., Zhao, M., Kim, S.J., Kim, H., Kim, Y.W., Lee, Y.J., Hillmer, S., Sohn, U., Jiang, L. & Hwang, I., (2003). Rha1, an Arabidopsis Rab5 homolog, plays a critical role in the vacuolar trafficking of soluble cargo proteins. *The Plant Cell*, *15*(5), 1057−1070.

Sheen, J., (2001). Signal transduction in maize and Arabidopsis mesophyll protoplasts. *Plant Physiology*, *127*(4), 1466−1475.

Tamura, K., Shimada, T., Ono, E., Tanaka, Y., Nagatani, A., Higashi, S.I., Watanabe, M., Nishimura, M. & Hara-Nishimura, I., (2003). Why green fluorescent fusion proteins have not been observed in the vacuoles of higher plants. *The Plant Journal*, *35*(4), 545−555.

Torney, F., Trewyn, B.G., Lin, V.S.Y. & Wang, K., (2007). Mesoporous silica nanoparticles deliver DNA and chemicals into plants. *Nature Nanotechnology*, *2*(5), 295−300.

Wroblewski, T., Tomczak, A. and Michelmore, R., (2005). Optimization of *Agrobacterium*-mediated transient assays of gene expression in lettuce, tomato and Arabidopsis. *Plant Biotechnology Journal*, *3*(2), 259−273.

Yu, Y., Yu, P.C., Chang, W.J., Yu, K. & Lin, C.S., (2020). Plastid transformation: how does it work? Can it be applied to crops? What can it offer?. *International Journal of Molecular Sciences*, *21*(14), 4854.

Zhang, H., Demirer, G.S., Zhang, H., Ye, T., Goh, N.S., Aditham, A.J., Cunningham, F.J., Fan, C. & Landry, M.P., (2019). DNA nanostructures coordinate gene silencing in mature plants. *Proceedings of the National Academy of Sciences*, *116*(15), 7543−7548.

Zhang, Z., Wan, T., Chen, Y., Chen, Y., Sun, H., Cao, T., Songyang, Z., Tang, G., Wu, C., Ping,

Y. & Xu, F.J., (2019b). Cationic polymer-mediated CRISPR/Cas9 plasmid delivery for genome editing. *Macromolecular Rapid Communications*, *40*(5), 1800068.

Zhang, H., Goh, N.S., Wang, J.W., Pinals, R.L., González−Grandío, E., Demirer, G.S., Butrus, S., Fakra, S.C., Del Rio Flores, A., Zhai, R. & Zhao, B., (2022). Nanoparticle cellular internalization is not required for RNA delivery to mature plant leaves. *Nature Nanotechnology*, *17*(2), 197−205.

Zhang, Q., Ying, Y. & Ping, J., (2022b). Recent Advances in Plant Nanoscience. *Advanced Science*, *9*(2), 2103414.

Zhao, X., Meng, Z., Wang, Y., Chen, W., Sun, C., Cui, B., Cui, J., Yu, M., Zeng, Z., Guo, S. & Luo, D., (2017). Pollen magnetofection for genetic modification with magnetic nanoparticles as gene carriers. *Nature Plants*, *3*(12), 956−964.

Zheng, N., Song, Z., Liu, Y., Yin, L. & Cheng, J., (2017). Gene delivery into isolated *Arabidopsis thaliana* protoplasts and intact leaves using cationic, α−helical polypeptide. *Frontiers of Chemical Science Engineering*, *11*, 521−528.

CHAPTER 4

Transfer of Vertically Aligned Carbon Nanofibers to a Flexible Substrate and Application to Curved Plant Surfaces

PREFACE:

This chapter describes the work conducted at Oak Ridge National Laboratory to create tall carbon nanofibers and transfer the fibers from a rigid substrate to a flexible substrate. It also includes examples of how fibers in flexible substrates could be applied to curved plant surfaces for dye and DNA delivery. This collaborative work completed under the supervision of Professor Jean Greenberg. I wrote the initial draft of this chapter and revised it with helpful comments from Professor Jean Greenberg, Dr. Joanna Jelenska, Dr. Jennifer Morrell-Falvey, Dale Hensley, Dr. Scott Retterer, and Dr. Bernadeta Srijanto. I worked with Dale Hensley, Dr. Scott Retterer, and Dr. Bernadeta to produce the carbon nanofibers and to transfer them to a flexible substrate. Additionally, I performed all plant delivery experiments.

ABSTRACT:

Delivery of biomolecules and impermeable dyes to intact plants is a major challenge. Nanomaterials are up-and-coming tools for delivery of DNA to plants. As exciting as these new tools are, they have yet to be widely applied. Nanomaterials fabricated on a rigid substrate (backing) are particularly difficult to successfully apply to curved plant structures. Here we describe the process for both microfabricating vertically aligned carbon nanofiber arrays and transferring them from a rigid to a flexible substrate. We detail and demonstrate how these fibers on flexible substrates can be utilized for transient transformation of or dye delivery to plants.

Using a modified version of a method developed by Fletcher et al. (2006), we show how VACNFs can be transferred from their rigid silicon substrate to a flexible SU-8 substrate to form flexible VACNF arrays. To overcome the hydrophobic nature of SU-8, fibers in the flexible film are coated with a thin silicon oxide layer (2-3 nm). To use these fibers for dye/DNA delivery to curved plant organs, we deposit a 1 μL droplet on the fiber side of VACNF films, wait 10 min, place the films on the plant organ and employ a swab with a rolling motion to drive fibers into plant cells. With this method we have achieved dye and DNA delivery in plant organs with curved surfaces.

INTRODUCTION:

Plant transformation (both transient and stable) has yet to become widely achievable in all plant tissues and species. Traditional methods that use particle bombardment, Agrobacteria, electroporation, or polyethylene glycol treatment of protoplasts are slow or cumbersome. Furthermore, they are not applicable to every plant species (Canto et al., 2016; Gou et al., 2020; Baltes et al., 2017; Ren et al., 2020). The use of nanomaterials for DNA delivery is a burgeoning field that is still in its infancy (Kumar et al., 2020). Nanomaterials, specifically carbon nanofibers, have also successfully been used to deliver proteins, dextrans and dyes to plant leaves without causing a wound response (Davern et al., 2016). The goal of this work is to provide a description of how to use one type of nanomaterial, carbon nanofibers, for delivering biomolecules or dye to plants. Herein I use DNA as the biomolecule of choice, which permits transient transformation of cells in various plant organs.

Previously, my collaborators and I (Morgan et al., 2022) demonstrated the use of carbon nanofibers affixed to a rigid silicon substrate to transiently transform leaves of lettuce, *N.*

benthamiana and poplar, and both leaves and roots of Arabidopsis. Although transformations were successful on a variety of organs, fibers were more difficult to apply to plant tissues with curved surfaces, such as roots or fruits. I reasoned that a flexible backing for nanofibers might improve their efficiency of delivery by conforming better to the shape of the organ.

Herein, I describe methods utilized for fabricating and designing vertically aligned carbon nanofibers, transferring VACNFs to flexible substrates, and applying VACNFs on flexible substrates to plants for delivery of biomolecules and dyes. A more detailed procedure can be found in the Appendix B. Carbon nanofibers were produced using a direct current catalytic plasma-enhanced chemical-vapor deposition (dc C-PECVD) with Ni catalyst. The position, diameter, and the length of Ni catalyst were controlled using a combination of electron beam lithography, metal evaporation, and lift-off processes as described by Melechko et al. (2005; 2009). Using double layer e-beam resist, a thicker Ni catalyst can be deposited on the substrate, to give longer fibers (Nelson-Fitzpatrick, 2009). To produce of the desired length, the amount of Ni within the catalyst must be sufficient to last the entirety of the growth period (Melechko, 2009). The Ni catalyst protects the nanostructure from etching. If the catalyst disappears before the nanofibers reach the desired height, the fiber will no longer be protected and etch back while the PECVD chamber (Melechko, 2009). The majority of reported heights for nanofibers produced at the CNMS at Oak Ridge National Laboratory were less than 10 μm long. There are a few examples in which fiber production at ORNL exceeded 10 μm (Morgan et al., 2022; Davern et al., 2016; Fletcher et al., 2006; Fletcher et al., 2004; Fowlkes et al., 2005; Wood et al., 2016).

Fiber transfer from a rigid to a flexible substrate is based on a modification of methods described in Fletcher et al. (2006), with the current methods forgoing the use of an amorphous

carbon layer or a sacrificial photoresist layer. SU-8 lift-off with fiber transfer is achieved by utilizing the intrinsic tensile stress resulting from underbaking and underexposing the SU-8 (Keller et al., 2008; Jamal et al., 2011; Wouters et al., 2010). SU-8, a complex polymer, is naturally hydrophobic, which makes using it for facilitating DNA delivery difficult. To counteract the hydrophobic nature of the SU-8, we apply a thin layer of silicon oxide via atomic layer deposition (Williams and Goodman, 1974). Application of fibers on a rigid substrate for biomolecule/dye delivery utilizes the impact force of tweezer tapping described in Davern et al. (2016) and the on-plant and on-chip methods described in Morgan et al. (2022). Flexible VACNF films are applied to curved plant surfaces by first semi-drying DNA or dye droplets on the film as with the on-chip method from Morgan et al. (2022) and then rolling the films on curved plant surfaces using a small makeup applicator (Kundu et al., 2019; Acanda et al., 2021).

METHODS:

VACNF Production (Figure 4.1)

Figure 4.1 shows the altered steps for making VACNFs. Carbon-based nanofibers with a lateral spacing (pitch) 35 μm and height ranging from 40-50 μm were made in the Center for Nanophase Material Science (CNMS) at Oak Ridge National Laboratory using nickel catalyst dots patterned across the top of a silicon wafer via electron beam lithography, metal evaporation, and conventional lift-off using the method described by (Melechko et al., 2005; Melechko et al., 2009). For the lithography step, the silicon wafers were coated with double layers of polymethyl methacrylate resist (PMMA 495 A4 and PMMA 950 A2) and exposed using a JEOL 9300FS electron beam lithography system and developed in a solution of 1:3 methyl-isobutyl ketone: isopropyl alcohol (Nano MIBK/IPA 1:3 Developer, MicroChem, Newton, MA). Electron beam

lithography was necessary to define the catalyst dots with diameters of 300 nm. After developing the resist and cleaning with a 6-second exposure to oxygen plasma, electron beam evaporation was used to deposit an adhesive layer of Ti (10nm) and a thin nickel film (130 or 150 nm) on the patterned resist. Sequential sonication in acetone and isopropyl alcohol was used to remove the underlying resist layer, leaving catalyst dots in the desired pattern behind. Nanofiber growth was then conducted using a direct current plasma-enhanced chemical vapor deposition chamber using an acetylene/ammonia mixture. Growth parameters were optimized to control the length and taper of the nanofibers (tapering less than 200 nm). After fabricating the VACNFs, their geometry was assessed using scanning electron microscopy (Zeiss Merlin FE-SEM) at a 30° tilt with an acceleration potential of 1 or 3 kV.

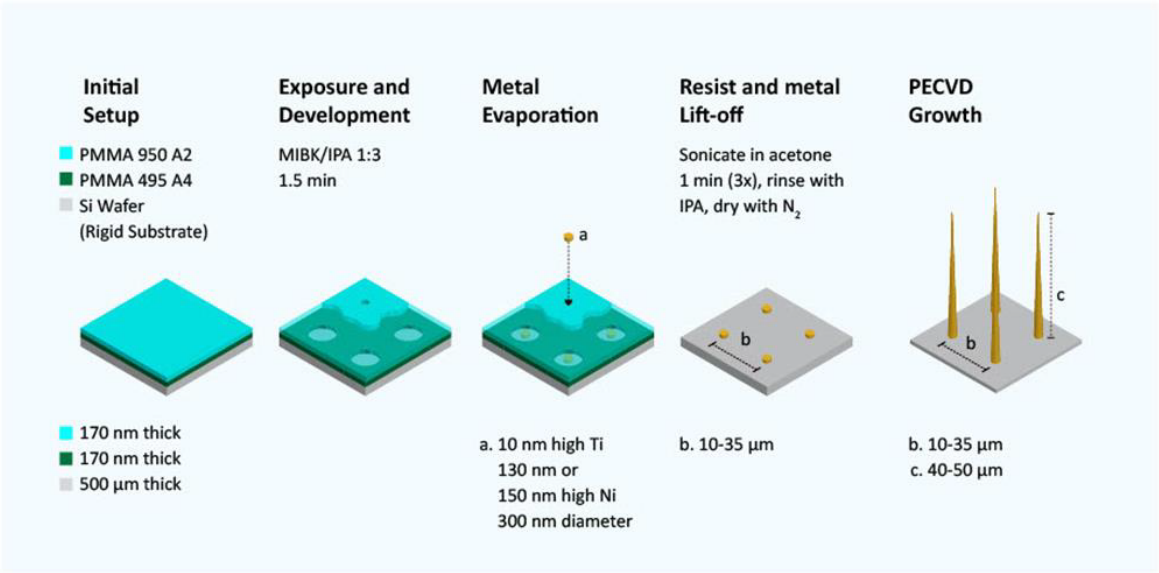

Figure 4.1: Workflow for making vertically aligned carbon nanofiber arrays. To produce VACNFs, a double layer of polymethyl methacrylate (PMMA 495 A4, 950 A2) is spin-coated onto a silicon wafer. Electron beam lithography is used to define an array of dots 300 nm in diameter. The resist is then developed in methyl isobutyl ketone/isopropanol (MIBK/IPA), 1:3 for 1.5 min. Using a metal evaporator, an adhesive layer of Ti (10 nm) is applied to the wafer, followed by a second layer of Ni (130 nm or 150 nm). The remaining resist is then removed via lift-off (sonication baths of acetone). The geometry of the catalyst dots is inspected via SEM. If the catalysts resemble hockey pucks and are flat, then they are placed in the plasma enhanced chemical vapor deposition (PECVD) machine and fibers are grown. Fibers are then inspected using SEM.

Transfer of VACNF To Flexible Substrate (Figure 4.2)

After nanofiber synthesis and inspection, each wafer was spun with SU-8 2015 at 4000 rpms for 45 s. The wafer was then soft baked for 3 min at 95°C. Following this, the wafer was patterned with a SUSS MicroTec MA6/BA6 Gen3 mask aligner at 95 mJ/cm^2 and post-baked for 6 min at 95°C. The pattern was developed in SU-8 developer for 15 seconds, rinsed with IPA, and dried with N_2 gas. A protective layer of Shipley SPR 955 CM 0.7 was spun on the wafer at 3000 rpm and softbaked at 90°C for 30 s. A silicon oxide layer (2-3 nm) was then added to the wafer via atomic layer deposition (Oxford FlexAl Atomic Layer Deposition; 22 cycles at 100°C)

to make the flexible substrate hydrophilic (Williams and Goodman, 1974). The wafer was then diced into 3 mm x 3 mm squares with the dicing saw. Geometry of the fibers was assessed using electron microscopy (Zeiss Merlin FE-SEM) at a 30° tilt with an acceleration potential of 3 kV. Individual chips were then placed in acetone until the SU-8 started to curl and looked like it was concaving. At this time, the SU-8 layer on most chips could be grabbed at the edge with sharp tweezers peeled from the underlying silicon substrate as an intact 3 mm square film. The VACNF SU-8 film was then washed in IPA for 5 min and ddH_2O for 5 min. To determine if the VACNF SU-8 films were hydrophilic or hydrophobic, it was noted whether the flexible substrates would sink or float in water. If the substrates floated, then they were still hydrophobic; if they sank it was assumed that they were hydrophilic.

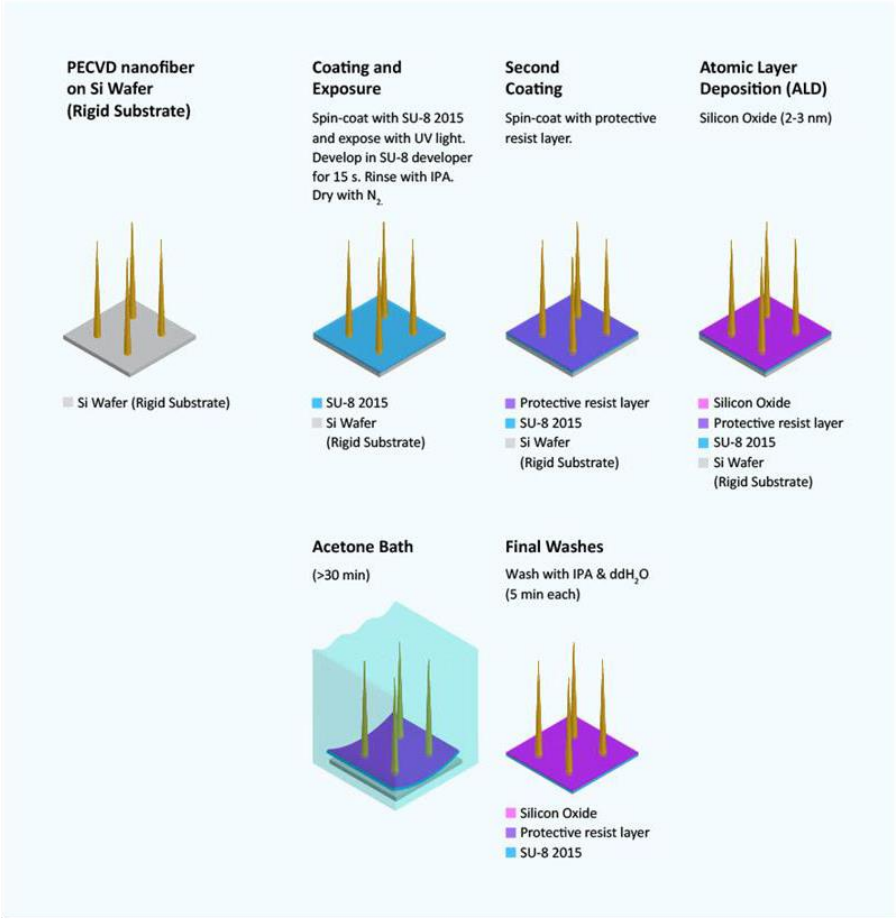

Figure 4.2: Workflow for transferring fibers from a rigid substrate to a flexible substrate. After nanofiber synthesis and inspection, each wafer is spun with SU-8 2015 at 4000 rpms for 45 s. The wafer is then soft baked for 3 min at 95 °C. Following this, the wafer is exposed to UV light and patterned in a mask aligner at 95 mJ/cm^2. It is then post-baked for 6 min at 95 °C. The pattern is developed in SU-8 developer for 15 s, rinsed with IPA, and dried with N_2 gas. A protective resist layer of SPR 955 CM 0.7 is spun on the wafer at 3000 rpm and softbaked at 90 °C for 30 s. A silicon oxide layer (2-3 nm) is then added to the wafer via atomic layer deposition (ALD) (22 cycles at 100 °C) to make the flexible substrate hydrophilic[15]. The wafer is then diced into 3 mm x 3 mm squares with the dicing saw. Individual chips are then placed in acetone until the SU-8 starts to curl and looks like it is concaving (>30 min). At this time the SU-8 layer on most chips can be grabbed at the edge with sharp tweezers and peeled from the underlying silicon substrate as an intact 3 mm square film. The film is then washed in IPA for 5 min and ddH_2O for 5 min.

Applying VACNFs in SU-8 Films to Plant Tissue Using the On-Chip Method

VACNF flexible substrate delivery of dye (10 μM) or DNA (200 ng) to plant cells was conducted using the "on-chip" method from Morgan et al. (2022). In brief, 1 μl was placed on

the fiber side of the chip and allowed to dry for 10 min prior to impaling tissue. The VACNF on the flexible substrate was then placed on the surface of the plant organ. A small make-up applicator (Disposable Micro Applicators Brush for Makeup and Personal Care (Head Diameter: 1.5 mm), Amazon) was then rolled over the SU-8 square like a paint roller and provided the force necessary for the fibers to penetrate the plant cells and achieve delivery (Kundu et al., 2019; Acanda et al., 2021). Flexible substrates were removed from plant surfaces using labeling tape.

Microscopy

Fluorescent images were captured with Zeiss LSM 800 or LSM 710 confocal microscopes. GFP, YFP, and fluorescein signals were collected with an emission range of 510 and 545 nm, excitation was 488 nm.

RESULTS:

Making Longer Carbon Nanofibers

The overall geometry of VACNF is controlled by different components of the microfabrication process. In general, the location of individual fibers is controlled by defining an array of dots, in which the catalyst material is deposited. The diameter of the VACNF base is much larger than the original 300 nm Ni dot because of the deposition of silicon nitride (SiN) onto the sidewalls. The Si comes from the etching of the Si substrate. The N comes from the ammonia (NH_3) when the plasma disassociates the ammonia. The height of the nanofiber is determined by the growth rate which varies depending on the ratio of acetylene (C_2H_2) to ammonia and time. The Ni catalysis is always being etched by the hydrogen. The process must

stop before the Ni is etched to nothing or the nanofiber starts to etch away, this determines the tapering/tip size. The shape and sidewall chemical composition is controlled by the ratio of gases utilized during the PECVD process (Melechko et al., 2011).

To produce an array of single carbon nanofibers longer than 25 μm used by Morgan et al. (2022) and Daven et al. (2016), we altered several factors. First we increased the amount of Ni catalyst to 130 or 150 nm Ni (Davern et al. (2016) used 50 nm Ni and Morgan et al. (2022) used 100-125 nm Ni). Second, we altered the acetylene: ammonia ratio, and increased the current and the growth time. Additionally, we paid more attention to the geometry of the catalyst material. To produce tall straight single fibers, the deposited catalyst needed to have a hockey puck shape (Melechko et al., 2005) rather than a shape that resembles a volcano (Figure 4.2). We overcame this by using a double layer of PMMA to create an undercut to aid in the liftoff of excess material (Figures 4.1 and 4.3). Any attempts to create fibers longer than 50 μm resulted in the fibers bending/becoming curved (Figure 4.4). The various parameters that were used to try and make fibers longer than 50 μm are listed in the Appendix A.

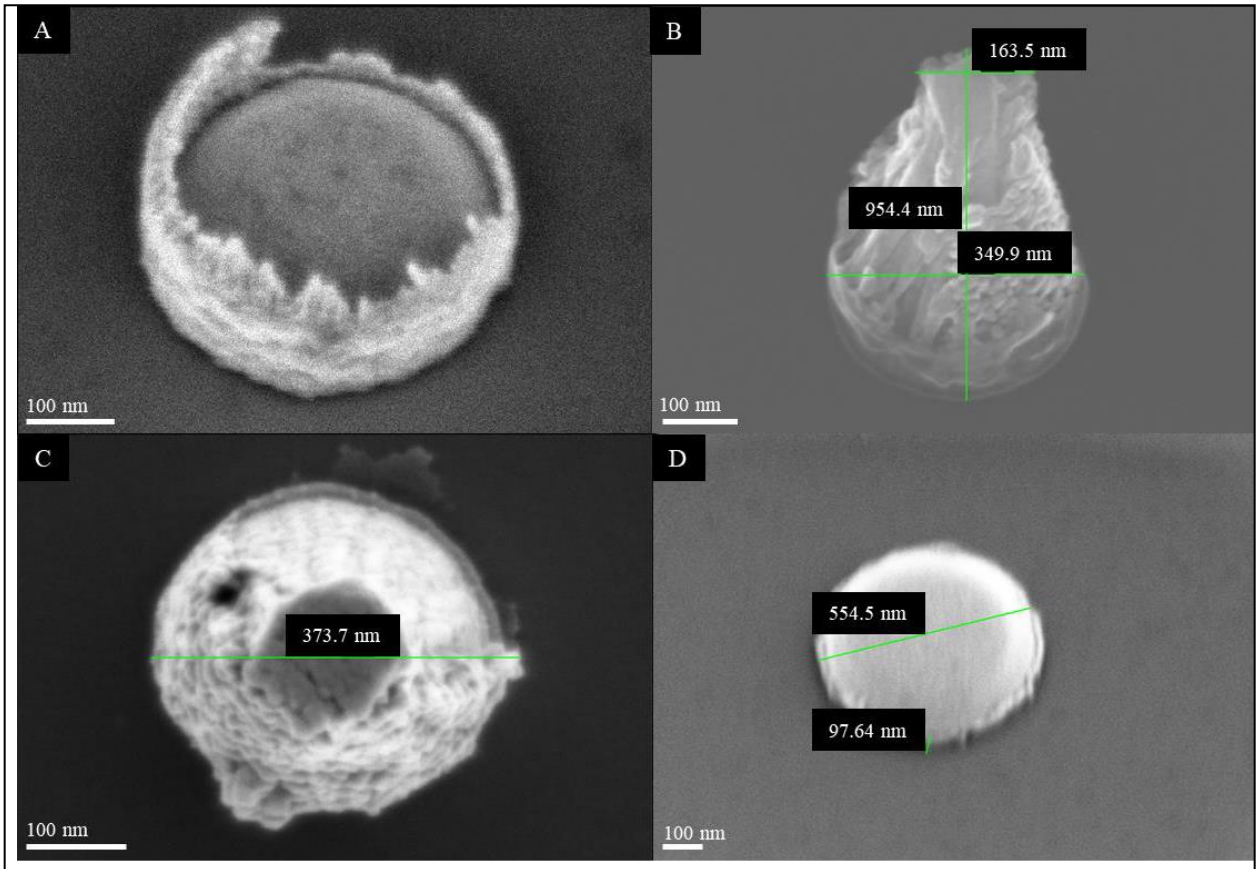

Figure 4.3: Catalyst shape. (A) SEM image of catalyst after lift-off.; photoresist present on the sides. (B) and (C) using single layer PMMA resist and the resulting volcano shape. (D) Desired hockey-puck catalyst shape made from double layers of PMMA. (A), (B), and (D) were all imaged at 30°. Because of this the apparent heights appear to be smaller than the actual height by a factor of sin(30°)=1/2.

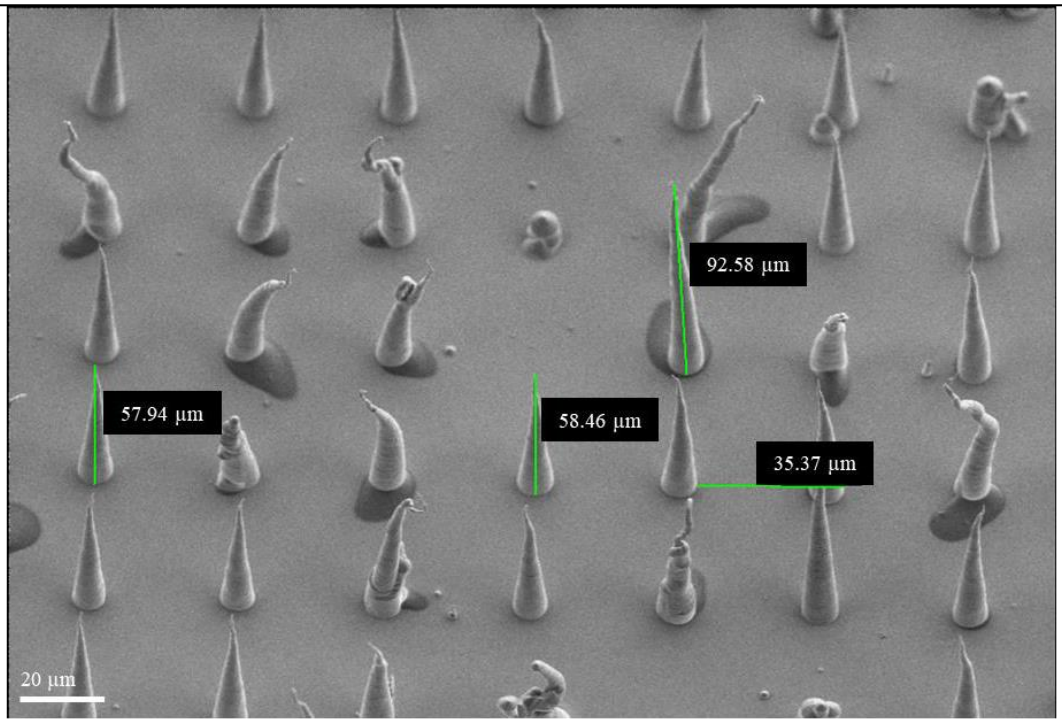

Figure 4.4: Attempt to make longer fibers. These fibers were made using 300 nm dots defined by e-beam lithography in double layers of PMMA resist. After e-beam lithography, 10 nm of Ti and 130 nm of Ni was deposited on the wafer. After lift-off and descumb the Si wafer was placed in the ECVD chamber. The following parameters were used for PECVD growth: growth time of 80 min, current of 1.5 A., acetylene: ammonia ratio of 48 sccm to 100 sccm, and a growth temperature of 620 °C. SEM image was taken at a 30° angle. Due to the fact that the fibers were imaged at 30° angle, the apparent heights appear to be smaller than the actual height by a factor of sin(30°)=1/2. Fibers have a 35 µm pitch.

Transfer of Fibers from Rigid Substrate to Flexible Substrate

Fiber transfer from a rigid to a flexible substrate was achieved by modifying the methods described in Fletcher et al. (2006). It relies on the intrinsic tensile stress resulting from underbaking and underexposing the SU-8 (Keller et al., 2008; Wouters et al., 2010; Jamal et al., 2011). Successful fiber transfer is demonstrated in Figure 4.5; in which small nubs of fibers are left on the silicon substrate (Figure 4.5B) and the top portion of fibers are visible in the SU-8 (Figure 4.5C).

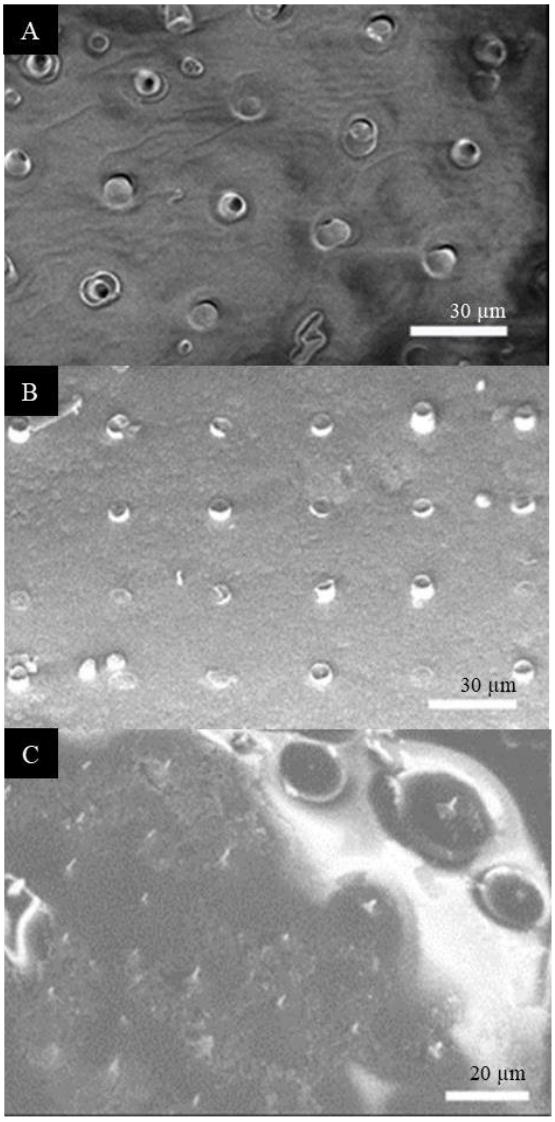

Figure 4.5: VACNF transfer to SU-8. (A) Back side of Su-8 square with VACNFs. (B) Silicon substrate after SU-8 lift-off and fiber transfer. (C) Fibers in SU-8 film after transfer. Images captured on SEM at a 30° tilt.

Application of Flexible VACNF Films to Plants

The distinct advantage of VACNF chips is the ability to deliver biomolecules or dyes to specific locations on a plant (Figure 4.6). Here we have used fluorescence readouts to assess delivery. Using different plants, substrates, and delivery methods (on-chip or on-plant) there can be differences in the timing of the appearance of fluorescein (Morgan et al., 2023).

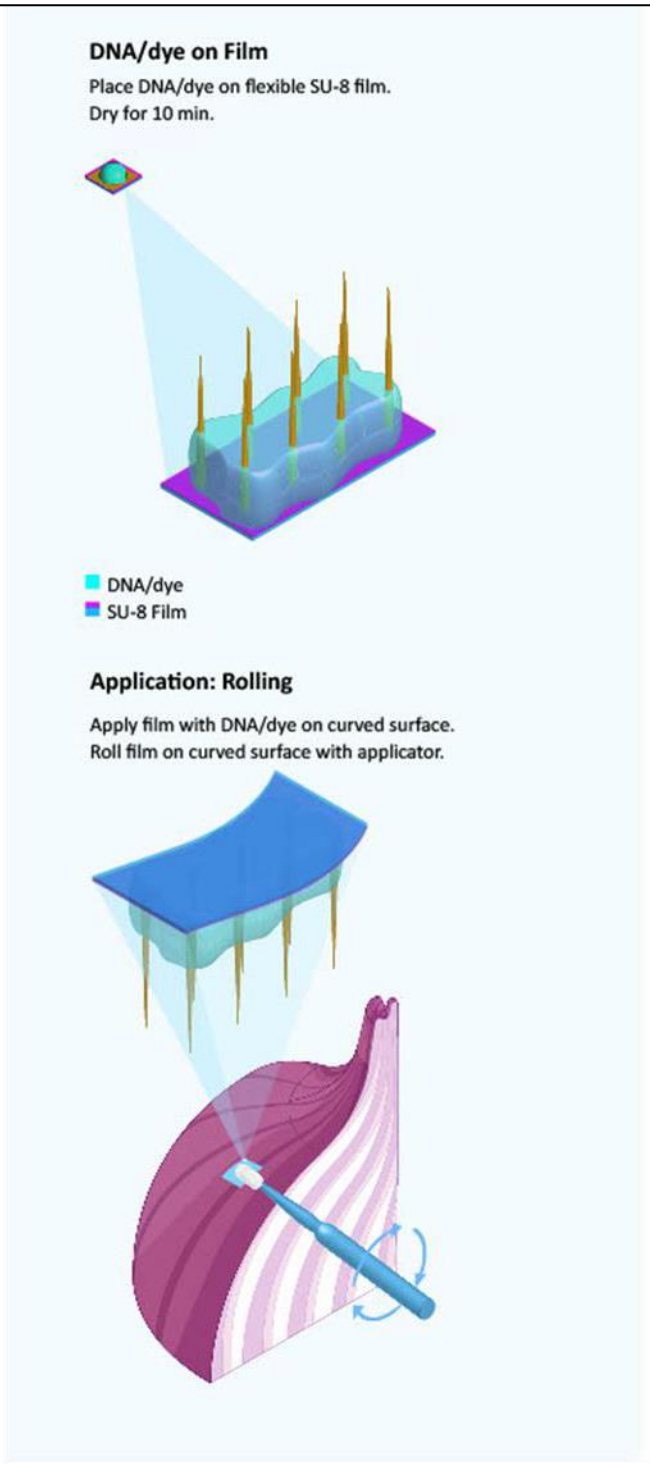

Figure 4.6: Schematic of dye/DNA delivery to plant tissue using fibers in flexible substrates. On-chip SU-8 film dye or DNA delivery. Fibers are transferred from the rigid silicon substrate to flexible SU-8 substrate. A 1 µL droplet of dye/DNA solution is dropcast on the VACNF film and dried for 10 min. The VACNF film with the semi-dried dye/DNA is then rolled onto a curved plant surface using a makeup applicator.

Fibers in the flexible substrate were suitable for dye delivery to curved surfaces, such as strawberries and apples (Figures 4.7 and 4.8), via a make-up applicator. Using a flexible substrate with strawberries, a strong fluorescein signal was observed right away (Figure 4.7), whereas it took 2 h to see a strong fluorescein signal in apples (Figure 4.8B, D). Successful delivery of plasmids encoding fluorescent markers can be determined by using fluorescence microscopy and finding the resulting signal (Figures 4.8-4.9). Controls are necessary to determine if the plant of choice has autofluorescence like the fluorescent marker encoded within the plasmid being delivered by fibers. Using fibers alone is helpful to determine if the impact force applied with tweezers results in damage to the plant tissue or if the observed fluorescence within the sample is due to the VACNFs, which are inherently fluorescent because of their silicon nitride layer (Pearce et al., 2012) (Figure 4.8C-D). Fibers impaled in plant tissue do not induce wound response, as assessed by H_2O_2 production (Davern et al., 2016). Lastly, using the control of +DNA, –Fibers is necessary to determine if the DNA is not entering into the plant through tapping alone and confirms that the fibers are necessary for delivery into plant cells (Figure 4.9C). Using the flexible VACNF films with the on-chip DNA delivery resulted in successful transient transformation of epidermal cells in store-bought apples and onions (Figures 4.8 and 4.9).

Failed experiments may have fibers broken off in the different fields of view, but there will be no resulting fluorescence signal from the attempt to deliver plasmid DNA or dye. If too much pressure is applied to the plant, there will be apparent tissue damage (Figure 4.10). This mechanical damage may look like small holes or transparent areas in the plant, as if a layer of cells has been removed when looking at the plant under a microscope. Sometimes imprints of the chip will be visible. An experiment in which fluorescent protein expression is not detected after

DNA delivery may also be due to the use of low-quality DNA, so it may be useful to make fresh DNA preparations.

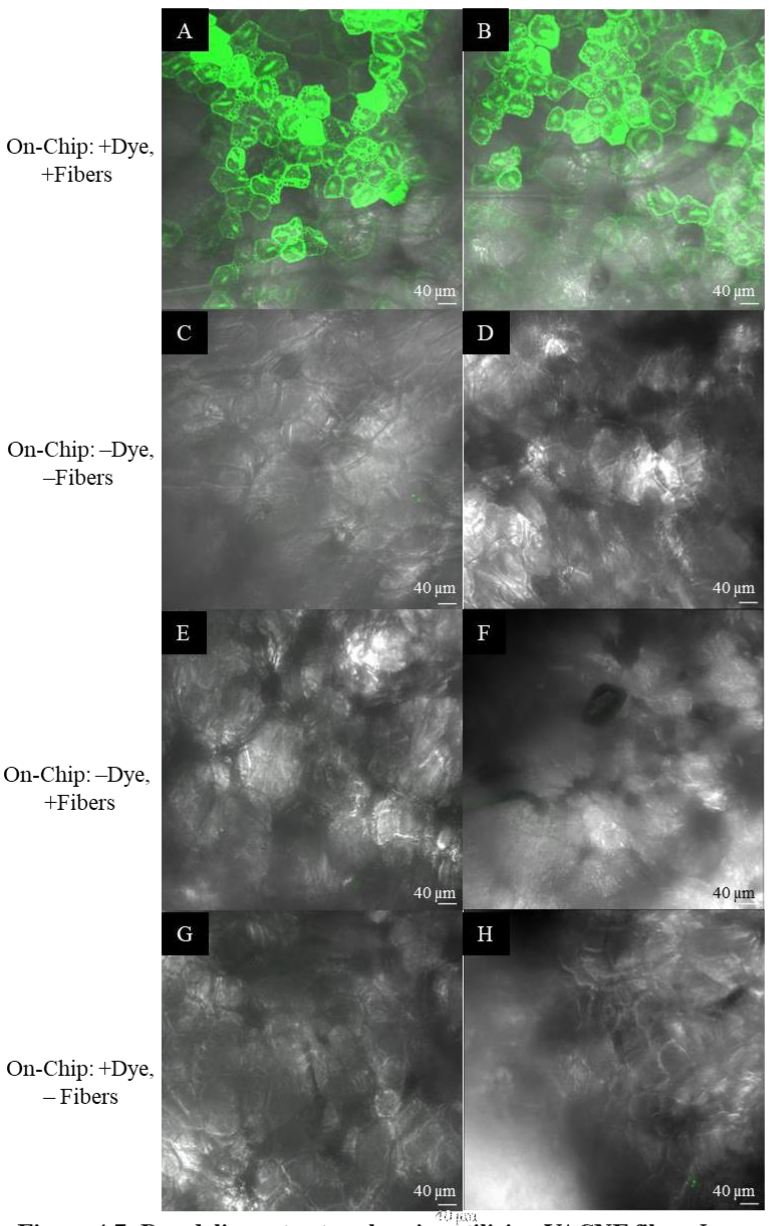

Figure 4.7: Dye delivery to strawberries utilizing VACNF films. Images were acquired using confocal microscopy. Using the on-chip method, dye droplets were dried on VACNF films, which were then rolled onto fruit surfaces using a makeup applicator. Fluorescein dye (10 µM) was delivered to strawberry cells and imaged after 10 min (A) and 1 h (B). Panels (C and D) show no treatment controls (–Dye, –Fibers). Panels (E and F) show –Dye, +Fibers controls after 10 min and 1 h, respectively. Panels (G and H) show +Dye, -Fibers controls after 10 min and 1 h, respectively. (A-H) are maximum projections of 188 µm z-stacks. Fibers have a 35 µm pitch.

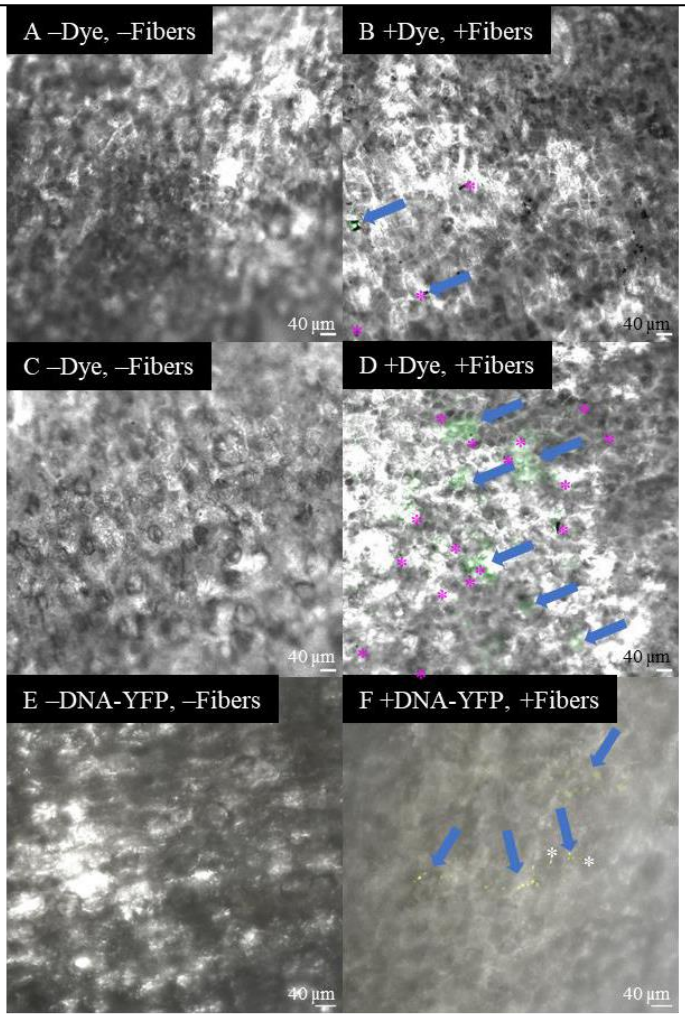

Figure 4.8: Dye delivery and transient transformation of apples via VACNF films. Images were generated using confocal microscopy. Using the on-chip method, 1 µL droplets of fluorescein dye (10 µM, B and D) or 1 µL of plasmid encoding pUBQ$_{10}$:YFP (DNA−YFP) (200 ng) were dried on VACNF films, which were then rolled onto fruit surfaces using a makeup applicator. Fluorescein dye was delivered to apple epidermis and imaged after 10 min (B) and 2 h (D). The dye took some time to diffuse into the cells after delivery (D). DNA-YFP delivery and expression via VACNF films after 48 h (F). Panels (A, C, and E) show no treatment controls (–Dye/DNA-YFP, –Fibers). The scale bars are 40 µm. (A-D) are single planer images from z-stacks. (E and F) are maximum projection of 53 µm z-stacks. Fiber pitch is 35 µm. Arrows denote fluorescein signal or YFP signal. * indicates a VACNF.

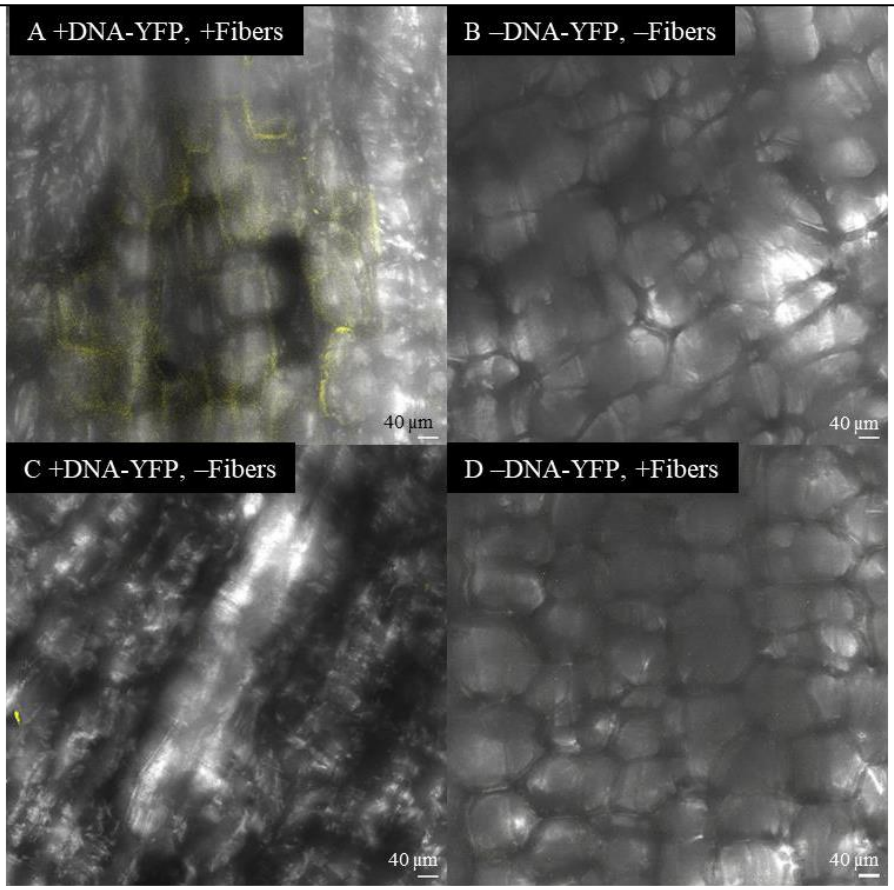

Figure 4.9: Transient transformation of onions using VACNF films. Images were acquired using confocal microscopy 48 h after DNA delivery. Using the on-chip method, 1 µL plasmid DNA encoding $pUBQ_{10}$:YFP (DNA-YFP) (200 ng) droplets were dried on VACNF films for 10 min, which were then rolled onto plant organ surfaces. (A) DNA-YFP was delivered to and YFP expressed in onion epidermis. Panel (B) shows no treatment control; (C) shows (–DNA-YFP, +Fibers) control and (D) shows the (–DNA-YFP, +Fibers) control. The scale bars are 40 µm. Fibers have a 35 µm pitch. Images are maximum projections of 115 µm z-stacks.

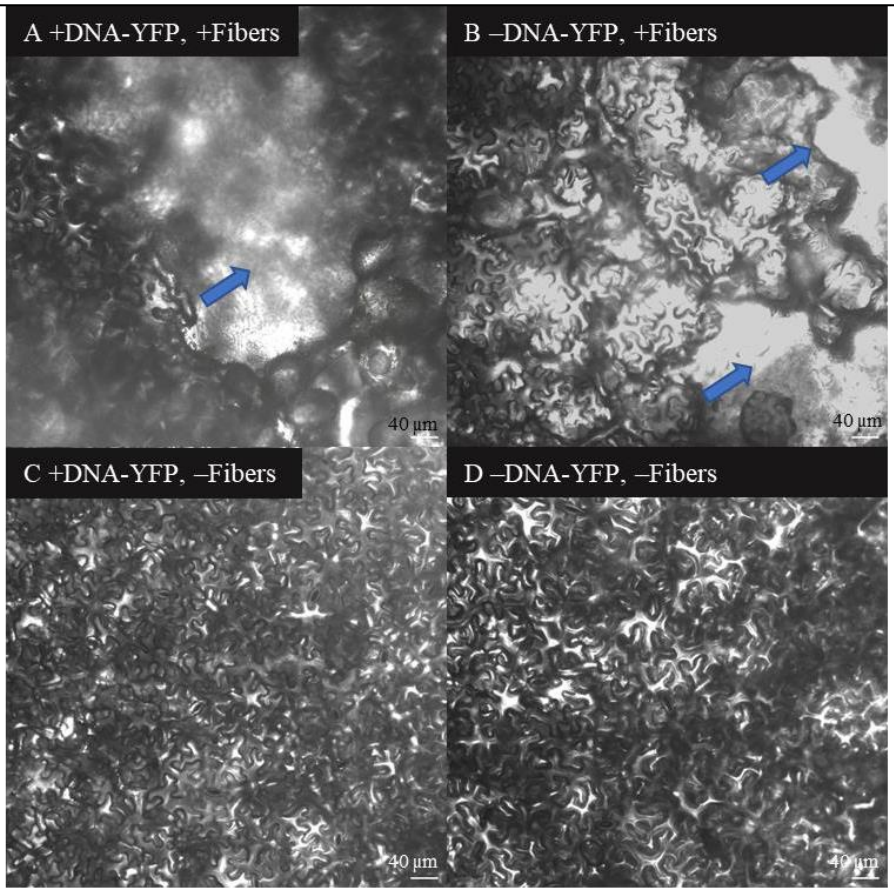

Figure 4.10: Tissue damage in lettuce from VACNF film application. Images were generated using confocal microscopy. On-chip method was used to deliver DNA to lettuce leaves. pUBQ$_{10}$:YFP DNA (200 ng) droplets were dried for 10 min on VACNF films, which were then rolled onto the abaxial side of detached lettuce leaves and stored in a humidity chamber for 4 d (A). (B) shows the (–DNA-YFP, +Fibers) control. (C) shows the (+DNA-YFP, –Fibers) control, and (D) is the no treatment (–DNA-YFP, –Fibers). Scale bars are 40 µm. VACNFs have a 35 µm pitch. Arrows point to plant damage resulting from rolling of the flexible substrate with too much force. Note that successful VACNF-mediated DNA delivery in lettuce was achieved in other experiments (Morgan et al., 2022).

DISCUSSION:

In this chapter, I presented methods for how to construct vertically aligned carbon nanofibers, transfer these fibers to a flexible substrate, and apply fibers in either a rigid or flexible substate to plants to use for delivery of biomolecules or dyes to plants. I also described and showed results from impalefection using the on-chip with fibers in flexible substrates. The application of using these fibers is simpler in practice and theory than traditional plant transformation methods (particle bombardment, protoplast transformation via PEG or

electroporation) and may be used for plants recalcitrant to Agrobacterium-mediated transformation. However, only a small number of cells are transformed.

Vertically aligned carbon nanofibers were produced at Oak Ridge National Laboratory Center for Nanophase Materials Sciences through their user program. Users can apply to use this facility. Alternatively, VACNF chips can be produced in clean rooms with direct current plasma enhanced chemical vapor deposition machines with a carbon source (Liu et al., 2010; Saleem et al., 2015). With the methods described, there are a few steps that are critical to the production of the fibers, fiber transfer, and application of the VACNF chips/films. For fiber application to work, fibers must be straight and have a tapering diameter of <200 nm at the tip for delivery in plant cells to be successful (Davern et al., 2016; Morgan et al., 2022). Additionally, the fibers need to be a certain minimum length to achieve delivery within plant cells. In theory, the carbon nanofibers can be made to have different pitches (lateral spacing) and lengths. The importance of producing fibers of different lengths is that longer fibers could be used to penetrate deeper tissue layers. Having longer fibers (greater than >40 μm in length) is important for flexible films, as the fiber transfer works by breaking the fibers from their base and requires layering SU-8 on top of the fibers. The working thickness of the SU-8 layer utilized for this protocol is 20-35 μm; any thinner and the flexible substrate would be very difficult to handle. The minimum height necessary to accomplish delivery within the epidermis of various plants (curved or flat) is approximately 10-15 μm (Davern et al., 2016; Morgan et al., 2022). With this knowledge in mind, fibers with lengths >40 μm are necessary for VACNF films.

Within the scope of this study, attempts were made to produce fibers greater than 50 μm. As evidenced in Figure 4.4, it is difficult to produce fibers with the same lengths on the same chip/substrate because of not being able to control the Ni crystal orientation (Fowlkes et al.,

2006). Fibers greater than 50 μm start to bend, potentially because of the Ni catalyst moving while in the PECVD chamber. The Ni catalyst at the tip of the fiber may start to bend because of the plasma electric fields as the fibers grow taller. This could cause the fiber to grow in a different direction. The alignment of the VACNFs is controlled by the plasmsa electric fields generated during fiber synthesis (Merkulov et al., 2002). Growth times for fibers are variable and are estimated based on the amount of Ni catalyst left on individual fibers. It is possible that fibers are being etched back after they run out of Ni catalyst resulting in shorter fibers. It is hard to estimate when individual fibers will run out of Ni and start to etch back.

There are several different parameters to consider when producing carbon nanofibers: choice of catalyst material, catalyst geometry, thickness of catalyst material as well as factors when growing fibers in a PECVD chamber (gas ratio, pressure, temperature, current, showerhead height, and growth time) (Melechko et al., 2005; Melechko et al., 2009; Merkulov et al., 2000; Retterer et al., 2008). To produce carbon nanofibers longer than 25 μm used by Morgan et al. (2022) and Daven et al.(2016), I increased the amount of Ni catalyst, altered the acetylene: ammonia ratio, and increased the current and the growth time. Additionally, I paid more attention to the geometry of the catalyst material. To produce tall straight fibers, the deposited catalyst needed to have a hockey puck shape rather than a shape that resembles a volcano. Volcano structures arise from deposition of Ni on the sidewalls of the resist, and the remnants of Ni after lift-off (Figure 4.3). To prevent the formation of volcanos, a double layer of PMMA was utilized to create an undercut during electron beam lithography (Rooks et al., 1987). The undercut aids in lift-off of the deposited metal catalyst (Figure 4.1).

In addition to fiber height, another critical step for successful fiber transfer is the amount of time spent in the acetone bath. The VACNF films need to be left in the acetone bath long

enough until their edges begin to curl; if they are left in the acetone bath for too little time, they are more difficult to lift off the chips and may break. The older the chips are, the longer they will have to remain in the acetone bath. Following the acetone bath, the films/chips are placed in isopropanol and then rinsed with water; the purpose of these baths is to remove access acetone as well as to remove the protective photoresist on the fibers.

Another step within the process that is of vital importance to the success of fiber mediated delivery is ensuring that the right amount of force is applied to VACNF chips/films. The delivery mechanism is dependent upon fibers making small punctures in cell walls via the impulse force of tweezer tapping on rigid substrates (Morgan et al., 2022; Davern et al., 2016) or rolling with of the mini-makeup applicator on flexible substrates. Fibers may break off and remain imbedded in plant cells (Morgan et al., 2022; Davern et al., 2016). Additionally, it is important to choose appropriate imaging time points after DNA delivery with VACNF chips/films, as time to detectable expression varies between plant species and the types of vectors being delivered (Morgan et al., 2022) (Figure 4.11).

With the on-chip approach, a 1 µl of solution was drop-casted on to the fiber side of the flexible VACNF film and allowed to dry for 10 minutes. When placing the droplet on the fibers great effort was taken to ensure that the droplet was placed in the center of the chip and covering several fibers. At the end of the drying period a “coffee ring” was present. With this formation of the ring, DNA is thought to be concentrated at the edges of the ring formation. Smalyukh et al. (2006) investigated the formation of ring-like deposits in drying drops of DNA. They dried DNA on surfaces with different hydrophilicity (clean glass plates, SiO, and indium tin oxide coatings). It was noted that as the DNA droplet evaporated, DNA chains were transported outward by water flow to the rim of the droplet and over time formed a liquid crystal. In the final stages of drying,

which for their study was ~45 minutes, zigzag patterns formed through the rim to the liquid crystal. Ten minutes, the drying time utilized in this manuscript, was enough time for the coffee ring pattern to form. Further studies are needed to quantify how much DNA is present at each region of the perimeter and if any liquid crystals formed as well as the impact that the fibers would have on the previously observed structures using the method from Mann et al. (2007).

As broadly applicable as this method is to plants, it has a few limitations. For example, adding a thin layer of silicon oxide to the VACNF films does not always result in films being completely hydrophilic because of the protective layer of photoresist added on top of the SU-8. To overcome this, thicker layers of silicon oxide could be applied to the VACNFs. To test if the films are hydrophobic or hydrophilic, they can be placed in water. If the films sink, they are hydrophilic and if they float, they are hydrophobic. Additionally, there can be variation between the batches of fibers produced (Melechko et al., 2011). There are several parameters that can be altered when growing the fibers in the plasma enhanced chemical vapor deposition machine; what is described in this protocol is a set of parameters for two different amount of Ni catalyst. Additionally, when the C_2H_2 ratio to NH_3 was too high, this would affect the potential for branching (multi-head CNF) in the fibers. In addition to variable chip features, there can be person to person variation in the application method, meaning that each person will apply a different amount of force when tapping rigid substrates into the plants or rolling the VACNF films onto the plants. This is typically overcome with practice and ensuring that dye delivery is achievable without apparent tissue damage.

Flexible VACNF films were used to demonstrate dye and DNA delivery to plant cells in this paper. However, they should be broadly applicable for RNAi silencing for plant systems like apples or other fruits where it would take years to produce stable transgenic lines. Moreover,

these fibers could also be used to deliver genetic editing materials or for stable transformations in plants.

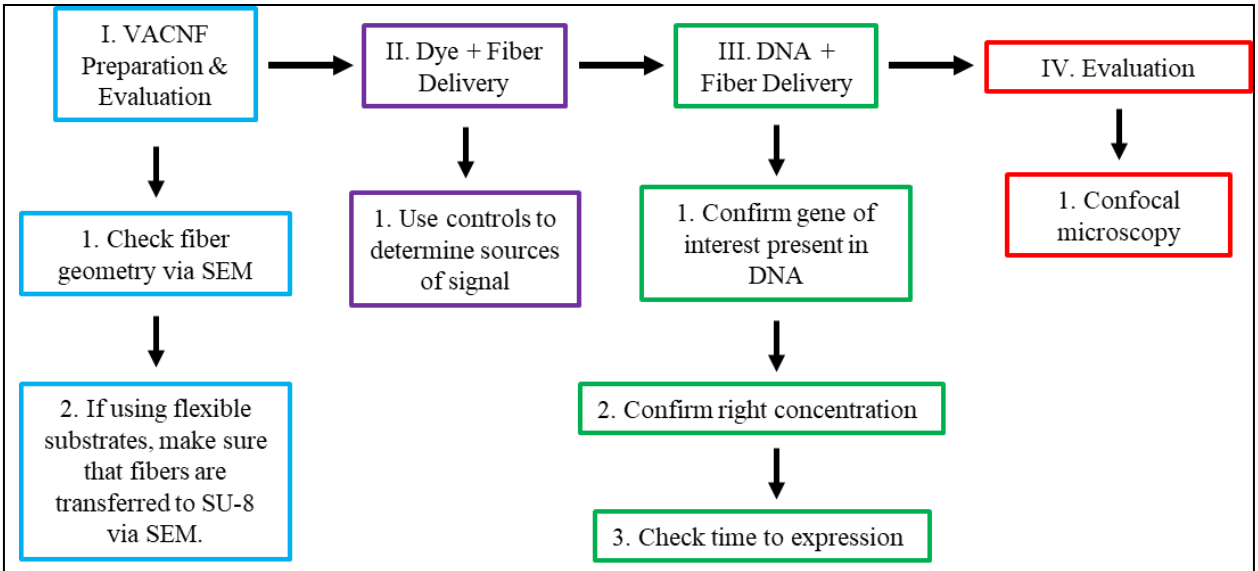

Figure 4.11: Workflow of VACNF-mediated delivery in plants. First, check the geometry of the fibers using SEM. For proper delivery, fibers need a tip with a diameter <200 nm. If using fibers on a flexible substrate, the next step would be to confirm that fibers are being transferred to SU-8 and to check the height of the exposed fibers via SEM. Next, test the usefulness of the fibers by trying to deliver dye into the plant/organ of choice using the rigid or flexible substrate. Use 1 µL droplet either placing it on the plant surface or briefly drying it on the chip/film. With this step and all other steps, it is imperative to use the proper controls (–Dye,–Fibers; –Dye, +Fibers; and +Dye,–Fibers), to be confident that signal comes from *bona fide* dye delivery. The third step is to confirm that the gene of interest is present in the plasmid, determine the concentration of DNA to deliver, and test the optimal amount of time after delivery to check expression. The final step is to use confocal microscopy to check expression of the delivered marker. Modified from reference (Morgan et al., 2022), *Frontiers in Plant Science* under the terms of the Creative Commons attribution license (CC BY).

ACKNOWLEDGMENTS:

Nanofiber arrays were fabricated at the Center for Nanophase Material Science, which is a Department of Energy Office of Science User Facility (Proposal ID: CNMS2019-103 and CNMS2022-A-1182). Support from CNMS is awarded through a peer-reviewed proposal system and is provided at no cost to successful applicants who intend to publish their results (http://www.cnms.ornl.gov/user/becoming_a_user.shtml). We thank Kevin Lester for assistance with the production of nanofiber arrays. We also thank Dr. John Caughmen, Dr. Timothy

McKnight, Dr. Amber Webb, Daryl Briggs, and Travis Bee for critical discussions about experimental design. We thank Leslie Carol for scientific illustrations. This work has been funded by the Bioimaging Science Program, U.S. Department of Energy, Office of Science, Biological and Environmental Research, DE-SC0019104 and the United States Department of Agriculture, 2021-67013-34835. JMM was supported by the United States Department of Agriculture: National Institute of Food and Agriculture: Agriculture and Food Research Initiative Predoctoral Fellowship 2021-67034-35167.

WORKS CITED:

Acanda, Y., Welker, S., Orbović, V., & Levy, A. (2021). A simple and efficient agroinfiltration method for transient gene expression in Citrus. *Plant Cell Reports*, *40*(7), 1171-1179.

Canto, T. (2016). Transient expression systems in plants: potentialities and constraints. *Advanced Technologies for Protein Complex Production and Characterization*, 287-301.

Davern, S. M., McKnight, T. E., Standaert, R. F., Morrell-Falvey, J. L., Shpak, E. D., Kalluri, U. C., ... & Mirzadeh, S. (2016). Carbon nanofiber arrays: a novel tool for microdelivery of biomolecules to plants. *PLoS One*, *11*(4), e0153621.

Fletcher, B. L., Hullander, E. D., Melechko, A. V., McKnight, T. E., Klein, K. L., Hensley, D. K., ... & Doktycz, M. J. (2004). Microarrays of biomimetic cells formed by the controlled synthesis of carbon nanofiber membranes. *Nano Letters*, *4*(10), 1809-1814.

Fletcher, B. L., McKnight, T. E., Melechko, A. V., Hensley, D. K., Thomas, D. K., Ericson, M. N., & Simpson, M. L. (2006). Transfer of Flexible Arrays of Vertically Aligned Carbon Nanofiber Electrodes to Temperature-Sensitive Substrates. *Advanced Materials*, *18*(13), 1689-1694.

Fowlkes, J. D., Fletcher, B. L., Hullander, E. D., Klein, K. L., Hensley, D. K., Melechko, A. V., ... & Doktycz, M. J. (2005). Tailored transport through vertically aligned carbon nanofibre membranes; controlled synthesis, modelling, and passive diffusion experiments. *Nanotechnology*, *16*(12), 3101. Fowlkes, J. D., Melechko, A. V., Klein, K. L., Rack, P. D., Smith, D. A., Hensley, D. K., ... & Simpson, M. L. (2006). Control of catalyst particle crystallographic orientation in vertically aligned carbon nanofiber synthesis. *Carbon*, *44*(8), 1503-1510.

Gou, Y. J., Li, Y. L., Bi, P. P., Wang, D. J., Ma, Y. Y., Hu, Y., ... & Feng, J. Y. (2020). Optimization of the protoplast transient expression system for gene functional studies in strawberry (Fragaria vesca). *Plant Cell, Tissue and Organ Culture (PCTOC)*, *141*, 41-53.

Jamal, M., Zarafshar, A. M., & Gracias, D. H. (2011). Differentially photo-crosslinked polymers enable self-assembling microfluidics. *Nature Communications*, *2*(1), 527.

Keller, S., Blagoi, G., Lillemose, M., Haefliger, D., & Boisen, A. (2008). Processing of thin SU-8 films. *Journal of Micromechanics and Microengineering*, *18*(12), 125020.

Kumar, S., Nehra, M., Dilbaghi, N., Marrazza, G., Tuteja, S. K., & Kim, K. H. (2020). Nanovehicles for plant modifications towards pest-and disease-resistance traits. *Trends in Plant Science*, *25*(2), 198-212.

Kundu, A., Nogueira Campos, M. G., Santra, S., & Rajaraman, S. (2019). Precision vascular delivery of agrochemicals with micromilled microneedles (μMMNs). *Scientific Reports*, *9*(1), 1-8.

Liu, J., Essner, J., & Li, J. (2010). Hybrid supercapacitor based on coaxially coated manganese oxide on vertically aligned carbon nanofiber arrays. *Chemistry of Materials*, *22*(17), 5022-5030.

Mann, D. G., McKnight, T. E., Melechko, A. V., Simpson, M. L., & Sayler, G. S. (2007). Quantitative analysis of EDC-condensed DNA on vertically aligned carbon nanofiber gene delivery arrays. *Biotechnology and Bioengineering*, *97*(4), 680-688.

Melechko, A. V., McKnight, T. E., Hensley, D. K., Guillorn, M. A., Borisevich, A. Y., Merkulov, V. I., ... & Simpson, M. L. (2003). Large-scale synthesis of arrays of high-aspect-ratio rigid vertically aligned carbon nanofibres. *Nanotechnology*, *14*(9), 1029.

Melechko, A. V., Merkulov, V. I., McKnight, T. E., Guillorn, M. A., Klein, K. L., Lowndes, D. H., & Simpson, M. L. (2005). Vertically aligned carbon nanofibers and related structures: Controlled synthesis and directed assembly. *Journal of Applied Physics*, *97*(4), 3.

Melechko, A. V., Desikan, R., McKnight, T. E., Klein, K. L., & Rack, P. D. (2009). Synthesis of vertically aligned carbon nanofibres for interfacing with live systems. *Journal of Physics D: Applied Physics*, *42*(19), 193001.

Melechko, A. V., Pearce, R. C., Hensley, D. K., Simpson, M. L., & McKnight, T. E. (2011). Challenges in process integration of catalytic DC plasma synthesis of vertically aligned carbon nanofibres. *Journal of Physics D: Applied Physics*, *44*(17), 174008.

Merkulov, V. I., Lowndes, D. H., Wei, Y. Y., Eres, G., & Voelkl, E. (2000). Patterned growth of individual and multiple vertically aligned carbon nanofibers. *Applied Physics Letters*, *76*(24), 3555-3557.

Merkulov, V. I., Melechko, A. V., Guillorn, M. A., Simpson, M. L., Lowndes, D. H., Whealton, J. H., & Raridon, R. J. (2002). Controlled alignment of carbon nanofibers in a large-scale synthesis process. *Applied Physics Letters*, *80*(25), 4816-4818.

Morgan, J. M., Jelenska, J., Hensley, D., Retterer, S. T., Morrell-Falvey, J. L., Standaert, R. F., &

Greenberg, J. T. (2022). *An efficient and broadly applicable method for transient transformation of plants using vertically aligned carbon nanofiber arrays*.

Morgan, J.M. Jelenska, J., Hensley, D., Retterer, S. T., Morrell-Falvey, J. L., Standaert, R. F., & Greenberg, J. T. (2023) Using vertically aligned carbon nanofiber arrays on rigid or flexible substrates fir delivery of biomolecules and dyes to plants. *JoVE.* In review.

Nelson-Fitzpatrick, N. (2011). Novel materials for the design of cantilever transducers.

Pearce, R., McKnight, T., Klein, K. L., Ivanov, I. N., Hensley, D., Meyer III, H., & Melechko, A. (2014). Synthesis and properties of SiNx coatings as stable fluorescent markers on vertically aligned carbon nanofibers. *AIMS Materials Science*, *1*(2), 87-102.

Ren, R., Gao, J., Lu, C., Wei, Y., Jin, J., Wong, S. M., ... & Yang, F. (2020). Highly efficient protoplast isolation and transient expression system for functional characterization of flowering related genes in Cymbidium orchids. *International Journal of Molecular Sciences*, *21*(7), 2264.

Retterer, S. T., Melechko, A., Hensley, D. K., Simpson, M. L., & Doktycz, M. J. (2008). Positional control of catalyst nanoparticles for the synthesis of high density carbon nanofiber arrays. *Carbon*, *46*(11), 1378-1383.

Rooks, M. J., Wind, S., McEuen, P., & Prober, D. E. (1987). Fabrication of 30-nm-scale structures for electron transport studies using a polymethylmethacrylate bilayer resist. *Journal of Vacuum Science & Technology B: Microelectronics Processing and Phenomena*, *5*(1), 318-321.

Saleem, A. M., Shafiee, S., Krasia-Christoforou, T., Savva, I., Göransson, G., Desmaris, V., &

Enoksson, P. (2015). Low temperature and cost-effective growth of vertically aligned carbon nanofibers using spin-coated polymer-stabilized palladium nanocatalysts. *Science and Technology of Advanced Materials*.

Williams, R., & Goodman, A. M. (1974). Wetting of thin layers of SiO2 by water. *Applied Physics Letters*, *25*(10), 531-532.

Wood, D. S., Hensley, D. K., & Roberts, N. A. (2016). Enhanced thermal conductance of polymer composites through embedding aligned carbon nanofibers. *AIMS Materials Science*, *3*(3), 851.

Wouters, K., & Puers, R. (2010). Diffusing and swelling in SU-8: insight in material properties and processing. *Journal of Micromechanics and Microengineering*, *20*(9), 095013.

Chapter 5
Conclusions and Future Directions

In this body of work I demonstrated how nanomaterials could be utilized for transient transformation of various plant species and plant organs. This is not the first time in which silicon- and carbon-based nanomaterials have been used as delivery vehicles for plants. Many nanomaterials have been used to achieve a similar feat (i.e. nanosheets, carbon nanotubes, mesoporous silica nanoparticles). The purpose of this study was to demonstrate the utility of different nanomaterials, provide detailed protocols and descriptions of the methods, and lay the groundwork for future works with these materials.

In chapter 2, I presented the biocompatibility of silicon nanowires with plants. This initial study showed that plants could grow in the presence of silicon nanowires without major health defects. Additionally, it showed the potential breakdown of silicon nanowires into silicic acid and where the SiNWs eventually ended up in plant roots. In mammalian cells, silicon nanowires breakdown/degrade over time (Zimmerman et al., 2016). Chemically, silicon can convert to silicic acid at pH values ranging from neutral to basic (Lee et al., 2017). This process is accelerated with increasing pH (Lee et al., 2017). Thus, in line with the chemistry required for processing, we expect the transport via the symplastic pathway to result in conversion of crystalline nanowires to silicic acid or PSA. They can be further converted to silica gels in the vacuole (pH= 5.2-5.6) or the apoplastic region (pH=6.0-6.5) (Martiniere et al., 2018; Shen et al., 2013). Further studies are needed to confirm if the proposed degradation pathway of silicon nanowires is correct. To explore the chemistry behind the conversion of silicon nanowires to gels in plants, nanowires could be placed in ½ MS media of varying pH values for two weeks. Resulting structures could be imaged with scanning electron microscopy. In addition to

investigating the chemical degradation of SiNWs, further verification of silicon content is needed.

Future studies are needed to see how silicon nanowires work for delivery in plants. For proof of principle experiments – demonstrating that SiNWs can be used for delivery—SiNWs could be labeled with dye and the labeled SiNWs could be added to an imaging chamber with roots from a young Arabidopsis seedling. Using confocal microscopy, the sample could be imaged over time. This experiment could help shed some light on how free-standing SiNWs are uptaken into plants and how they move once inside the plant. The free-standing SiNWs could be used to deliver DNA into plant roots or cells. To use the SiNWs with cells, they could be mixed with plant cell suspensions and the plasmid of choice to enable to deliver of the foreign DNA akin to the delivery method with SiC whiskers (Zhi et al., 2022). Previously, vertical arrays of SiNWs attached to their substrate have been used to deliver DNA into bacteria and mammalian cells (Becce et al., 2021; Elnathan et al., 2015). The SiNWs could be broadly applicable to plants.

In chapters 3 and 4, I demonstrated how vertically aligned carbon nanofiber arrays could be utilized for delivery of biomolecules in plants. Chapter 3 focuses more on the application of fibers in a rigid substrate to plants that are intact or to plant organs are detached. In chapter 4, I demonstrated how the fibers could be transferred from a rigid substrate to a flexible substrate and applied to curved plant surfaces. Furthermore, great effort was taken to produce longer fibers (>20 microns). There are very few examples in the literature where fibers created at Oak Ridge National Laboratory are greater than 20 microns. To achieve this feat, we examined the catalyst geometry and determined the experimental methods necessary to generate catalysts with the desired geometry. We found that there was an upper limit to grow straight, vertical fibers. Fibers

with a height greater than 60 microns would start to bend or curl. To achieve fiber transfer from a rigid substrate to a flexible substrate, I utilized the intrinsic tensile stress resulting from underbaking and underexposing the SU-8 (Keller et al., 2008; Jamal et al., 2011; Wouters et al., 2010).

All VACNF production took place in the Center for Nanophase Materials at Oak Ridge National Laboratory. This included the application of the protective photoresist layers, SU-8 2015, and dicing of the chips into 3 mm x 3 mm arrays. VACNF SU-8 film lift-off took place in the Greenberg lab at the University of Chicago. The VACNF chips coated with SU-8 and the protective resist layers were stored in the dark. To achieve lift-off, the underexposed, underbaked SU-8 coated chips were soaked in acetone until the SU-8 started to curl or completely lifted off from the rigid substrate. One of the disadvantages of storing the chips coated with SU-8 and the protective resist was that the longer the chips were stored in the dark, the longer they had to be soaked in acetone before lift-off occurred. One way to potentially overcome this issue would be to perform lift-off right away and transfer the VACNF SU-8 films to water-soluble tape or on top of silicon rubber with a polyethylene terephthalate backing as suggested in Appendix B. In theory, using an additional backing like this would help prevent the SU-8 from becoming rigid and fragile.

The advantage of using fibers in a flexible substrate is that they can be applied to any plant surface. SU-8 was utilized in chapter 4 as it was the first material that could used reproducibility for transferring fibers from a rigid substrate to a flexible substrate in my hands. PDMS was another contender. Pearce et al. (2013) used PDMS as their choice material for their flexible substrate. To achieve transfer of VACNFs from a rigid silicon substrate to PDMS, they first grew the fibers on a Si wafer. Then they coated the fibers with a thin layer of PDMS and

cured it. Finally, they dissolved the silicon substrate in 30% KOH at 80 °C. When I tried this protocol the fibers dissolved along with the Si substrate (Appendix C). Additional challenges with using PDMS, SU-8, and other flexible substrates is determining which thickness to use because the material will well-up in areas with fibers and be thicker than anticipated. In the work of Wood et al. (2016), they took advantage of this feature because they wanted to transfer fibers completely covered by PDMS.

Using VACNF arrays for DNA delivery is a fast and easy method. However, the method requires tapping of the VACNF chips (or rolling if in a flexible substrate/film) by the person performing the method. There will be variation in the amount of force applied by each person and between samples/experiments. To resolve this issue in the future, work could be done to create a device that could function to provide a consistent tapping/rolling force for the fibers. Currently, there are no studies in plants comparing the potential toxicological effects of carbon- and silicon- based nanomaterials. Such studies have been performed in sea urchins (Pikula et al., 2020), microalgae (Pikula et al., 2018; Pikkula et al., 2020b), and marine bivalves (Pikula et al., 2020c). To better determine which nanomaterials to use with plants long-term, toxicology studies are needed.

Another open question related to the application of VACNF arrays to plants is how they achieve delivery. Without wounding a plant via mechanical damage resulting from tapping/rolling the VACNF array; there are two proposed scenarios for how delivery is achieved (Davern et al., 2016). In the first scenario the plasma membrane is thought to tightly zip up around the fibers immediately after penetration. This would mean that delivery would be instantaneous. If the material of choice was dried onto the fibers, then material could be desorbed from the intracellular part of the fibers. In the second scenario, the plasma membrane would

imperfectly seal around the fibers after tapping. This would leave channels/pore open around the fibers through which molecules could diffuse into. Davern and colleagues (2016) claimed that the results from their experiments using fibers for dye delivery in poplar plants was rapid (<5 min) and that the duration of this fluorescence signal was finite. When they delivered fluorescently labeled proteins, the signal at the site of impalement peaked at ~30 min post delivery (Davern et al., 2016). Additionally, with they used the fibers to deliver radio-tracers and observed there was not an observable difference in movement of the radiotracer between 2 h and 20 h post-delivery. Only a small amount of the radio-tracer was excited and moved to distal tissue. Based on these results, Davern et al.(2016), theorized that permeabilization was transient, but could not determine if delivery from the fibers took place immediately after impalement, if molecules were desorbing from the surface of the fibers, or if there were some pores created in which molecules were leaking into plant cells.

In chapter 3, both the on-plant and on-chip methods worked for delivering plasmid DNA. There was no significant difference between the two. The results from chapter 3 support the notion of scenario one in which delivery is instantaneous if the material is wet or must desorb into the plant tissue if the material was dried/semi-dried onto the fibers. In chapter 4, the results are slightly more ambiguous. With the on-chip method, dye/DNA is semi-dried onto the VACNF SU-8 film for 10 minutes – 5 minutes shorter when using VACNFs on a rigid substrate. I found that different drying times were needed for different materials. In chapter 4 there were differences observed in how long it took to observe signal from the delivered fluorescein dye between plant species. With apples, it took ~ 2 h to see strong signal from the dye due to the desorption process. But with strawberries, the fluorescein signal could be observed right away. The following are possible explanations behind this observed difference. One reason there could

have been differences between the different fruit is that they have different water contents, strawberries are made up of 91% water and apples are made up of ~85% water (small differences between species of apples) (*Fooddata Central Search Results, n.d.)*. Since strawberries have a higher water content then apples, they could be causing the dried dye on the VACNF SU-8 film to rehydrate faster. Another potential explanation may be that the dye used for strawberries was more "wet" than the dye used with the apples. The same drying period of ten minutes was used for both apples and strawberries. The only difference was that the VACNF SU-8 films used with the strawberries were older than those used for the apple experiments. This means that a longer drying period for the on-chip method is needed when using older VACNF SU-8 films. The third explanation could be that the strawberries were damaged during the rolling of the VACNF SU-8 films for dye delivery, which may have created tissue damage allowing more dye molecules to diffuse or desorb into the cells. A fourth idea could be that the relative humidity in the environment in which the experiments are performed could affect the drying times. When trying to dry dye or DNA on VACNF films/chips, the goal is to achieve a coffee-ring appearance of the droplet; it is not completely dry. Taking the aforementioned results into account with the findings from Davern et al., it is hard to determine how exactly the fibers achieve delivery.

WORKS CITED

Becce, M., Klöckner, A., Higgins, S. G., Penders, J., Hachim, D., Bashor, C. J., ... & Stevens, M. M. (2021). Assessing the impact of silicon nanowires on bacterial transformation and viability of Escherichia coli. *Journal of Materials Chemistry B*, *9*(24), 4906-4914.

Davern, S. M., McKnight, T. E., Standaert, R. F., Morrell-Falvey, J. L., Shpak, E. D., Kalluri, U.

C., ... & Mirzadeh, S. (2016). Carbon nanofiber arrays: a novel tool for microdelivery of biomolecules to plants. *PLoS One*, *11*(4), e0153621.

Elnathan, R., Delalat, B., Brodoceanu, D., Alhmoud, H., Harding, F. J., Buehler, K., ... & Voelcker, N. H. (2015). Maximizing transfection efficiency of vertically aligned silicon nanowire arrays. *Advanced Functional Materials*, *25*(46), 7215-7225.

Fooddata Central Search Results. FoodData Central. (n.d.). Retrieved April 17, 2023, from https://fdc.nal.usda.gov/fdc-app.html#/

Jamal, M., Zarafshar, A. M., & Gracias, D. H. Differentially photo-crosslinked polymers enable self-assembling microfluidics. *Nature Communications*, *2*(1), 527 (2011).

Keller, S., Blagoi, G., Lillemose, M., Haefliger, D., & Boisen, A. Processing of thin SU-8 films. *Journal of Micromechanics and Microengineering*. *18*(12), 125020 (2008).

Lee, Y. K., Yu, K. J., Song, E., Barati Farimani, A., Vitale, F., Xie, Z., ... & Rogers, J. A. (2017). Dissolution of monocrystalline silicon nanomembranes and their use as encapsulation layers and electrical interfaces in water-soluble electronics. *ACS Nano*, 11(12), 12562-12572.

Martinière, A., Gibrat, R., Sentenac, H., Dumont, X., Gaillard, I., & Paris, N. (2018). Uncovering pH at both sides of the root plasma membrane interface using noninvasive imaging. *Proceedings of the National Academy of Sciences*, *115*(25), 6488-6493.

Pearce, R. C., Railsback, J. G., Anderson, B. D., Sarac, M. F., McKnight, T. E., Tracy, J. B., & Melechko, A. V. (2013). Transfer of vertically aligned carbon nanofibers to polydimethylsiloxane (PDMS) while maintaining their alignment and impalefection functionality. *ACS Applied Materials & Interfaces*, *5*(3), 878-882.

Pikula, K. S., Zakharenko, A. M., Chaika, V. V., Vedyagin, A. A., Orlova, T. Y., Mishakov, I.

V., ... & Golokhvast, K. S. (2018). Effects of carbon and silicon nanotubes and carbon nanofibers on marine microalgae Heterosigma akashiwo. *Environmental research*, *166*, 473-480.

Pikula, K., Zakharenko, A., Chaika, V., Em, I., Nikitina, A., Avtomonov, E., ... & Golokhvast, K. (2020). Toxicity of carbon, silicon, and metal-based nanoparticles to sea urchin strongylocentrotus intermedius. *Nanomaterials*, *10*(9), 1825.

Pikula, K., Chaika, V., Zakharenko, A., Markina, Z., Vedyagin, A., Kuznetsov, V., ... & Golokhvast, K. (2020b). Comparison of the level and mechanisms of toxicity of carbon nanotubes, carbon nanofibers, and silicon nanotubes in bioassay with four marine microalgae. *Nanomaterials*, *10*(3), 485.

Pikula, K., Chaika, V., Zakharenko, A., Savelyeva, A., Kirsanova, I., Anisimova, A., & Golokhvast, K. (2020c). Toxicity of carbon, silicon, and metal-based nanoparticles to the hemocytes of three marine bivalves. *Animals*, *10*(5), 827.

Shen, J.; Zeng, Y.; Zhuang, X.; Sun, L.; Yao, X.; Pimpl, P.; Jiang, L. Organelle PH in the Arabidopsis Endomembrane System. Molecular Plant 2013, 6 (5), 1419–1437.

Wouters, K., & Puers, R. (2010). Diffusing and swelling in SU-8: insight in material properties and processing. *Journal of Micromechanics and Microengineering*, *20*(9), 095013.

Wood, D. S., Hensley, D. K., & Roberts, N. A. (2016). Enhanced thermal conductance of polymer composites through embedding aligned carbon nanofibers. *AIMS Materials Science*, *3*(3), 851.

Zhi, H., Zhou, S., Pan, W., Shang, Y., Zeng, Z., & Zhang, H. (2022). The promising nanovectors for gene delivery in plant genome engineering. *International Journal of Molecular Sciences*, *23*(15), 8501.

Zimmerman, J. F., Parameswaran, R., Murray, G., Wang, Y., Burke, M., & Tian, B. (2016). Cellular uptake and dynamics of unlabeled freestanding silicon nanowires. *Science advances*, *2*(12), e1601039.

APPENDIX

Appendix A: PECVD Parameters for Attempting to Make Longer VACNFs.

Sample Number	Substrate	Catalyst(Å)	Buffer (Å)	Pattern	Pre-Etch NH3 (sccm)	Pre-Etch C2H2 (sccm)	Growth Temp (C)	Growth NH3 (sccm)	Growth C2H2 (sccm)	Pressure during growth (T)	Growth Current (A)	Growth Time (min)	Comments
1	1/4 Si	1200 Ni evaporator	50 Ti evaporator	20um pitch, 300nm dot size	100	56	620	100	56	10	1	65	arcing because it was just NH3, ran 4 minutes without C2H2
2	1/4 Si	1200 Ni evaporator	50 Ti evaporator	20um pitch, 300nm dot size	100	56	620	100	56	10	1	67	stable
3	1/4 Si, 200nmAi, 50nm Si evaporator	1300 Ni evaporator	100 Ti evaporator	300nm dots, 35um pitch	100	56	620	100	56	10	1	85	Some arcing,
4	1/4 Si	1300 Ni evaporator	100 Ti evaporator	300nm dots, 20um pitch	100	56	620 - 600	100	56	10	1	80	Stable, turned down temperature setpoint to 600C at 6 minutes to end.
5	1/4 Si	1300 Ni evaporator	100 Ti evaporator	300nm dots, 20um pitch	100	56	620	100	56	10	1	80	Some arcing at first
6	1/2 Si	1000 Ni evaporator	100 Ti evaporator	300nm dots, 35um pitch	100	56	623 - 600	100	56	10	1	66	Stable, 8 mintues left dropped to 600C
7	1/3 Si wafer with 220nm of evp Si	1300 Ni evaporator	100 Ti evaporator	300nm dots, 20um pitch	100	56	620	100	56	10	1	82	Some arcing at first
8	1/4 Si	1300 Ni evaporator	100 Ti evaporator	300nm dots, 20um pitch	100	56	620 - 620	100	56	10	1	80	some arcing, at 23 minutes turned down heat to 600C, reached 600C with 21 minutes left. Fibers need to be straighter.

9	1/3 Si wafer with 220nm of evp Si	1300 Ni evaporator	100 Ti evaporator	300nm dots, 20um pitch	100	56	620 - 600	100	56	10	1	80	Some arcing, reduced temperature to 600C for 15 minutes.
10	1/4 Si	1300 Ni evaporator	100 Ti evaporator	300nm dots, 20um pitch	100	56	620	100	56	10	1	80	Some arcing at first.
11	Si small sides x3 with 220nm of evp Si	1300 Ni evaporator	100 Ti evaporator	300nm dots, 20um pitch	100	56	620 - 620	100	56	10	1	80	Some arcing at first then stable. Dropped temperture to 600 with 40 minutes left.
12	1/4 Si with 200nm of evp Si	1300 Ni evaporator	100 Ti evaporator	300nm dots, 20um pitch	100	56	620 - 600	100	56	10	1	80	Some arcing at first. Dropped temperture to 600 with 40 minutes left.
13	1/4 Si	1300 Ni evaporator	100 Ti evaporator	300nm dots and 35um pitch	100	55	620	100	55	10	1.25	80	Soma arcing at first, dropping temperature didn't help to make straight fibers. So dropped C2H2 55sccm and raised 1.25A, plasma more stable.
14	1/8 wafer	1300 Ni evaporator	100 Ti evaporator	35um pitch, 300nm dot size	100	53	620	100	53	10	1.25	75	Some arcing at first, Fibers look better with lower C2H2.
15	1/8 wafer	1300 Ni evaporator	100 Ti evaporator	35um pitch, 300nm dot size	100	51	620	100	51	10	1.25	75	stable

16	1/3 Si	1300 Ni evaporator	100 Ti evaporator	35um pitch, 300nm dot size	100	49	620	100	49	10	1.25	75	Some arcing at first then stable.
17	3/4 Si Wafer	1300 Ni evaporator	100 Ti evaporator	35um pitch, 300nm dot size	100	53	620	100	53	10	1.5	70	Arced at first, then stable, images don't look good. Maybe too much time?
18	1/2 Si	2000 Ni	100 Ti	400 and 500nm dots	100	53	620	100	53	10	1.5	60	some arcing at first, then stable
19	1/4 Si	1300 Ni evaporator	50 Ti evaporator	20um pitch, 300nm dot size, 2mm x 2mm	50	100	620	100	50	10	1.25	75	Some arcing at first, stable, Added CNS after growth of fibers, heated back up to 620+, 80sccm C2H2, 100sccm of NH3, 6 torr. With H122022_1
20	1/4 Si	1300 Ni evaporator	50 Ti evaporator	20um pitch, 300nm dot size, 2mm x 2mm	100	50	620	100	50	10	1.25	80	Arcing at first
21	1/4 Si	1300 Ni evaporator	50 Ti evaporator	20um pitch, 300nm dot size, 2mm x 2mm	100	50	620	100	50	10	1.25	85	Stable
22	1/4 Si	1300 Ni evaporator	50 Ti evaporator	20um pitch, 300nm dot size, 2mm x 2mm	100	47	620	100	47	10	1.25	85	Arced at First, unstable at first, then stable, no arcing.
23	1/4 Si with 220nm Si deposited by ebeam evaporator	1300 Ni	100 Ti	20um pitch, 300nm dot size, 2mm x 2mm	100	50	620	100	50	10	1.25	80	Some arcing and not stable at first
24	1/4 Si	1500 Ni evaporator	100 Ti evaporator	35um pitch, 300nm dot size, 2mm x 2mm	100	47	620	100	47	10	1.25	85	Ran for 5 minutes for 90 minutes total, .5A, 80 sccm of C2H2, 100 sccm of NH3 to coat with carbon.

25	1/4 Si with 220wnSi deposited byebeam evaporator	1300Ni	lOOTi	20um pitch, 300om dot size, 2mmx 2mm	100	47	620	100	47	10	1.25	80	Stable, AddedCNS after growth offiben, heated back up 10620+, SOscan C2H2, lOOscanof NH3,61orr. With H120622_1
26	1/4Si	1500 i evaporator	lOOTi evaporator	35um pitch, 300om dot size, 2mmx 2mm	100	47	620	100	47	10	1.25	90	Stable
27	1/4Si	1500Ni evaporator	lOOTi evaporator	35um pitch, 300om dot size, 2mmx 2mm	100	48	620	100	*48*	10	1.25	100	Stable
28	1/4 Si with 220wnSi deposited byebeam	1300Ni	lOOTi	20um pitch, 300mn dot size, 2mml< 2mm	100	48	620	100	48	10	*1.5*	*75*	Arcing at first
29	1/4 Si with 220wnSi deposited byeheam	1300Ni	lOOTi	35um pitch, 300om dot size, 3mmx 3mm	100	48	620	100	*48*	10	*1.5*	80	Arcing at first, stable
30	1/4 Si with 220wnSi deposited byebeam	1300Ni	lOOTi	35um pitch, 300om dot *size*, 3mmx 3mm	100	46	620	100	46	10	*1.5*	75	Arcing soweat first, then stable.
31	1/4 Si v. th 220nmSi deposited byebeam	1300Ni	lOOTi	35um pitch, 300om dot size, 3mmx 3mm	100	45	620	100	45	10	*1.75*	70	Very little arcing at first. Raised current to *1.75A*. Maybe straighter fibers?
32	1/4 Si with 220wnSi deposited byebeam	1300 i	100Ti	35um pitch, 300om dot *size*, 3mmx 3mm	100	*50*	620	100	50	10	*1.75*	70	

Arcing at first then stable. Heated back			up to 640. R	anfor 5 minu	tes, 6 torr									.5A, 80 seem of C2H2, 100 seem of NH3 to coat withcaroon. 20kW,437 V	
33	l/4Si	1750Ni	lOOTi	35um pitch, 300om dot size, 3mmx 3mm	100	50	620	100	50	10	1.75	70	Sowearcing at first, stable.		

34	1/4 Si	1750 Ni	100 Ti	35um pitch, 300nm dot size, 3mm x 3mm	100	50	620	100	50	10	1.75	60	A few arcs at first, then stable.
35	1/4 Si	1750 Ni	100 Ti	35um pitch, 300nm dot size, 3mm x 3mm	100	50	620	100	50	10	1.75	55	Arcing at first, then stable.
36	1/4 Si	1750 Ni	100 Ti	35um pitch, 300nm dot size, 3mm x 3mm	100	50	620	100	50	10	1.75	50	Arcing at first then stable.
37	1/4 Si x2	1300 Ni	100 Ti	35um pitch, 300nm dot size, 3mm x 3mm	100	45	620	100	45	10	1.75	71	A few arcs at first then stable.
38	1/4 Si x2	1500 Ni	100 Ti	35um pitch, 300nm dot size, 3mm x 3mm	100	48	620	100	48	10	1.5	80	A few arcs at first then stable.
39	1/4 Si x2	1300 Ni	100 Ti	35um pitch, 300nm dot size, 3mm x 3mm	100	45	620	100	45	10	1.75	70	A few arcs at first then stable.
40	1/4 Si x2	1500 Ni	100 Ti	35um pitch, 300nm dot size, 3mm x 3mm	100	48	620	100	48	10	1.5	80	A few arcs at first then stable.
41	1/4 Si	2000 Ni	100 Ti	35um pitch, 300nm dot size, 3mm x 3mm	100	45	620	100	45	10	1.75	75	A few arcs at first then stable.
42	1/4 Si	2000 Ni	100 Ti	35um pitch, 300nm dot size, 3mm x 3mm	100	50	620	100	50	10	1.75	55	A few arcs at first then stable.

Appendix B: JoVE Paper Submission

TITLE:

Using Vertically Aligned Carbon Nanofiber Arrays on Rigid or Flexible Substrates for Delivery of Biomolecules and Dyes to Plants

AUTHORS AND AFFILIATIONS:

Jessica M. Morgan[1], Joanna Jelenska[2], Dale K. Hensley[3], Pengju Li[4], Bernadeta R. Srijanto[3], Scott T. Retterer[3,5], Robert F. Standaert[6], Jennifer L. Morrell-Falvey[5], & Jean T. Greenberg[2]

1. Biophysical Sciences, The University of Chicago, Chicago, IL
2. Molecular Genetics and Cell Biology, The University of Chicago, Chicago, IL
3. Center for Nanophase Materials Sciences, Oak Ridge National Laboratory, Oak Ridge, TN
4. Pritzker School of Molecular Engineering, The University of Chicago, Chicago, IL
5. Biosciences Division, Oak Ridge National Laboratory, Oak Ridge, TN
6. Department of Chemistry, East Tennessee State University, Johnson City, TN

Corresponding author: Jean T. Greenberg (jgreenbe@uchicago.edu)

Jessica M. Morgan: jmorgan2@uchicago.edu

Joanna Jelenska jjelenska@uchicago.edu

Dale K. Hensley: hensleydk@ornl.gov

Pengju Li: pengju@uchicago.edu

Bernadeta R. Srijanto: srijantobr@ornl.gov

Scott T. Retterer: rettererst@ornl.gov

Robert F. Standaert: standaert@mail.etsu.edu

Jennifer L. Morrell-Falvey: morrelljl1@ornl.gov

Jean T. Greenberg: jgreenbe@uchicago.edu

SUMMARY:

Methods for microfabricating vertically aligned carbon nanofibers (VACNFs), transferring VACNFs to flexible substrates, and applying VACNFs on both rigid and flexible substrates to plants for biomolecule and dye delivery are described.

ABSTRACT:

Delivery of biomolecules and impermeable dyes to intact plants is a major challenge. Nanomaterials are up-and-coming tools for delivery of DNA to plants. As exciting as these new tools are, they have yet to be widely applied. Nanomaterials fabricated on a rigid substrate (backing) are particularly difficult to successfully apply to curved plant structures. Here we describe the process for both microfabricating vertically aligned carbon nanofiber arrays and transferring them from a rigid to a flexible substrate. We detail and demonstrate how these fibers (on either rigid or flexible substrates) can be utilized for transient transformation of or dye delivery to plants. Using a modified version of a method developed by Fletcher et al.[11], we show how VACNFs can be transferred from their rigid silicon substrate to a flexible SU-8 substrate to form flexible VACNF arrays. To overcome the hydrophobic nature of SU-8, fibers in the flexible film are coated with a thin silicon oxide layer (2-3 nm). To use these fibers for dye/DNA delivery to curved plant organs, we deposit a 1 μl droplet on the fiber side of VACNF films, wait 10 min, place the films on the plant organ and employ a swab with a rolling motion to drive fibers into plant cells. With this method we have achieved dye and DNA delivery in plant organs with curved surfaces.

INTRODUCTION:

Plant transformation (both transient and stable) has yet to become widely achievable in all plant tissues and species. Traditional methods that use particle bombardment, Agrobacteria, electroporation, or polyethylene glycol treatment of protoplasts are slow or can be cumbersome. Furthermore, they are not applicable to every plant species[1-4]. The use of nanomaterials for DNA delivery is a burgeoning field that is still in its infancy[5]. Nanomaterials, specifically carbon nanofibers, have also successfully been used to deliver proteins, dextrans and dyes to plant leaves without causing a wound response[6]. The goal of this work is to provide a detailed protocol for using one type of nanomaterial, carbon nanofibers, for delivering biomolecules or dye to plants. Herein we focus on DNA as the biomolecule of choice, which permits transient transformation of cells in various plant organs.

Previously, Morgan et al.[7] demonstrated the use of carbon nanofibers affixed to a rigid silicon substrate to transiently transform leaves of lettuce, *N. benthamiana* and poplar, and both leaves and roots of Arabidopsis. Although transformations were successful on a variety of organs, fibers were more difficult to apply to plant tissues with curved surfaces, such as roots or fruits. We reasoned that a flexible backing for nanofibers might improve their efficiency of delivery by conforming better to the shape of the organ.

Herein, we detail methods utilized for fabricating and designing vertically aligned carbon nanofibers, transferring VACNFs to flexible substrates, and applying VACNFs on both rigid and flexible substrates to plants for delivery of biomolecules and dyes. Carbon nanofibers produced using a direct current catalytic plasma-enhanced chemical-vapor deposition (dc C-PECVD) with Ni catalyst. The position, diameter, and the length of Ni catalyst were controlled using a combination of electron beam lithography, metal evaporation, and lift-off processes as described by Melechko et al[8-9]. Using double layer e-beam resist, a thicker Ni catalyst can be

deposited on the substrate, to give longer fibers [10]. Fiber transfer from a rigid to a flexible substrate is based on a modification of methods described in Fletcher et al.[11], with the current methods forgoing the use of an amorphous carbon layer or a sacrificial photoresist layer. SU-8 lift-off with fiber transfer is achieved by utilizing the intrinsic tensile stress resulting from underbaking and underexposing the SU-8[12-14]. SU-8, a complex polymer, is naturally hydrophobic, which makes using it for facilitating DNA delivery difficult. To counteract the hydrophobic nature of the SU-8, we apply a thin layer of silicon oxide via atomic layer deposition[15]. Application of fibers on a rigid substrate for biomolecule/dye delivery utilizes the impact force of tweezer tapping described in Davern et al.[6] and the on-plant and on-chip methods described in Morgan et al. [7] Flexible VACNF films are applied to curved plant surfaces by first semi-drying DNA or dye droplets on the film as with the on-chip method from Morgan et al.[7] and then rolling the films on curved plant surfaces using a small makeup applicator[16-17].

PROTOCOL:

1. VACNFs Production (Figure 1)

    1. Spincoat a silicon wafer with polymethyl methacrylate (PMMA) 495 A2 resist at 4000 rpm and bake it at 180 °C for 5 min.

    NOTE: Let the wafer cool for 10 s before proceeding to the next step.

    2. Spincoat a second layer of resist (PMMA 950 A2) and bake it at 180 °C for 5 min.

    3. Use electron beam lithography to define the catalyst dots with diameters of 300 nm at a specified lateral spacing (pitch, 10 μm or 35 μm) in 3 mm x 3 mm arrays.

4. Develop the resist in 1:3 methyl-isobutyl ketone: isopropyl alcohol (IPA) for 1.5 min, followed by rinsing it with IPA and drying it with N_2.

NOTE: Check for the array of dots using a brightfield microscope (20x).

5. Clean the wafer of residual resist with a 6 s exposure in oxygen plasma (descum).

6. Use electron beam evaporation to deposit first an adhesive layer of metal (Ti or Cr, 10 nm) and then deposit a second layer, which is the Ni catalyst (130 nm or 150 nm).

7. Use sequential sonication to remove the metal (Ni) that was deposited on the underlying resist layer, leaving the Ni that was deposited directly on the silicon wafer. This process is called a lift-off. For this, prepare 3 containers with acetone and sonicate the wafer in acetone for 1 min; repeat 3 times. Rinse with IPA and dry with N_2.

NOTE: Never let acetone dry on the wafer. After the last acetone sonication immediately rinse with IPA and then dry with N_2 gas. If at any point the wafer becomes prematurely dry (prior to IPA rinse), there is the possibility that not all the excess metal and resist will be removed, and the acetone can leave a residue.

8. Check the geometry of the catalyst shape using scanning electron microscopy (SEM). The catalyst should look like a hockey puck (a compact cylinder). The height of the compact cylinder should reflect the thickness of Ni deposited on the silicon wafer.

NOTE: If the profile of the Ni dot is tall and appears to be concave at the top, resembling a volcano, then the catalyst is more likely to dewet into multiple Ni droplets resulting in branching of the carbon nanofibers[9]. This could be a result of the resist melting during metal evaporation because of long deposition times or issues with the lift-off procedure.

9. Quarter the silicon wafer and place it in the direct current plasma-enhanced chemical vapor deposition chamber (dc-PECVD) with the acetylene/ammonia mixture. Growth parameters are optimized to control the length and taper of nanofibers (tips <200 nm).

NOTE: Quarter wafers are used in the case that run parameters with the PECVD machine need to be optimized. To produce fibers with lengths greater than 40 μm and tips less than 200 nm in diameters, the following parameters are suggested: with a Ni catalyst thickness of 130 nm use a current of 1.75 A, growth time of 70 min, and an acetylene: ammonia ratio of 45 standard cubic centimeter per minute (sccm) : 100 sccm. With a Ni thickness of 150 nm use a current of 1.5 A, a growth time of 80 min, and an acetylene : ammonia ratio of 48 sccm : 100 sccm. Use the following parameters to grow VACNFs regardless of catalysts thickness: growth temperature of 620 °C, vacuum of 10 torr during plasma, and a shower head height of 20 mm.

10. Assess the geometry of the resulting fibers using SEM at a 30° tilt with an acceleration potential of 1 kV.

NOTE: Optimal fibers will be straight and non-branching. It is impossible to control the crystal orientation of the Ni catalyst with the electron beam evaporator. As a result of this, there will be some fibers that branch as a result of dewetting[9]. Also, the crystal orientation causes the VACNFs to grow to different heights so uniform heights on all VACNFs is difficult.

11. If fibers have desirable geometry, spincoat a layer of photoresist (SPR955) to the fibers at 1000 rpm for 45 s. Then dice the ¼ wafer into 3 mm x 3 mm arrays using a dicing saw. Fibers can be stored at this point for later use.

NOTE: Do not conduct step 11 if you plan to transfer fibers to a flexible substrate.

2. Transferring VACNFs to a Flexible Substrate (Figure 2)

1. After fibers have been synthesized as described above, spin coat SU-8 2015 photoresist on ¼ wafers at 4000 rpm for 45 s.

2. Softbake the wafer for 3 min at 95 °C.

3. Using a contact aligner, expose the wafer with a 3 mm x 3 mm array patterned mask that aligns with the defined pattern from electron beam lithography at 95 kJ mJ/cm^2.

NOTE: Use a proximity contact mode with an exposure gap that is at 20 μm greater than your tallest fiber. There is the possibility that fibers could be knocked over during this step in the process.

4. Perform a post-exposure bake for 6 min at 95 °C.

5. Develop wafer in SU-8 developer for 15 s, rinse it with IPA, and dry the wafer with N_2, moving from top to bottom.

NOTE: When developing the wafer, make sure that it is completely submerged.

6. Spin-coat patterned wafers with a protective layer of thin photoresist (SPR 955 CM 0.7) at 3000 rpm for 45 s and softbake for 30 s at 90 °C.

7. Deposit a thin silicon oxide layer to the wafer (2-3 nm) by placing it in an atomic layer deposition for 22 cycles at 100 °C.

8. Use a dicing saw to cut the wafer into 3 mm x 3 mm squares. Align the dicing saw to the preexisting pattern on the wafer.

9. Assess the geometry of the resulting fibers using SEM at a 30° tilt with an acceleration potential of 3 kV.

10. Stop here if storing chips for long term use (>1 week). Store chips in the dark.

11. To separate flexible substrates from rigid substrates, place individual chips in acetone for 30 min or until the SU-8 starts to curl.

12. Wash SU-8 films (either attached to or detached from rigid substrates) with IPA for 5 min and then with water for 5 min. When transporting the chips, it is best to place them on a commercial box with a sticky pad.

13. Optional: Place the fiberless side of the SU-8 film on water-soluble tape or on top of thin silicon rubber with a thin polyethylene terephthalate (PET) (12.5 μm thick) backing. Use a pair of tweezers to transfer the SU-8 film. Press on the edges of the SU-8 square to help it stick to the tape/silicon rubber-PET; this is to avoid breaking off fibers. At this point, the VACNF films are ready for immediate use.

Note: To prepare a silicon rubber/PET holder do the following: using a kit for making silicon rubber first mix 1 part of A with one part B; mix well. Next, cut out a square of PET and tape it down in a clear plastic dish. Pour a very thin layer of silicon rubber on-top of the PET and cure it at 80 °C for 1-2 h.

3. On-Plant Method, Rigid Substrate (Figure 3A)

1. Remove the photoresist with increment washes of acetone (100%, 5 min), IPA (100%, 5 min), and ddH_2O (5 min) prior to use.

2. When working with excised leaves or other tissues, place them on-top of a hard surface. When working with intact tissues, place a hard surface beneath the leaf or tissue to which you are applying the VACNFs.

3. Place a 1 µl droplet of dye or DNA onto the surface of the plant tissue.

4. Place a VACNF chip with a rigid substrate on top of the droplet with the fibers oriented such that they will come into contact with the droplet.

NOTE: The orientation of the chips can be determined by the "shininess" of the wafer. The shiny side of the chip has the fibers, and the opaque side of the chip does not.

5. Using the flat side of a pair of tweezers, tap the chip. Mark the area of the plant that the chip came into contact with using a soft-tipped marker. Remove the VACNF chips after delivery.

NOTE: The amount of force to apply when tapping will vary depending on the type of plant tissue used. It is recommended to practice tapping chips prior to conducting impalement of fibers. Avoid damage to plant tissues. Damage is apparent when one can see the outlines of the VACNF chip in the plant tissue.

6. Repeat steps 1-5 for controls (+Dye/DNA, –Fibers; –Dye/DNA, +Fibers; and –Dye/DNA, –Fibers). –Fibers is the fiberless side of a chip.

7. Store intact plants or excised plant organs in humid chambers in long day conditions (16 h light, 8 h dark) if needed. For excised organs, it may be convenient to use a plastic petri dish with wet paper towels.

4. On-Chip Method, Rigid Substrate (Figure 3B)

1. Remove the photoresist with increment washes of acetone (100%, 5 min), IPA (100%, 5 min), and ddH_2O (5 min) prior to use.

2. Drop-cast 1 µl droplet of dye or plasmid DNA (200 ng) onto the fiber side of a VACNF chip with a rigid substrate. Make sure to place the droplet in the center of the chip and covering several fibers. Let the droplet dry for 15 min.

NOTE: The orientation of the chips can be determined by the "shininess" of the wafer. The shiny side of the chip has the fibers and the opaque side the chip does not.

3. When working with leaves or other excised organs, place them on-top of a hard surface. When working with intact plants, place a hard surface beneath the organ to which you are applying the VACNFs. Remove the VACNF chip after delivery.

4. After the 15 min drying step, position the VACNF chip such that the fiber side comes in contact with the plant tissue. Tap the chip with the back end of a pair of tweezers.

NOTE: The amount of force to apply when tapping will vary depending on the type of plant tissue used. It is recommended to practice tapping chips.

6. Repeat steps 6-7 of on-plant method.

5. Applying VACNFs in SU-8 Films to Plant Tissue Using the On-Chip Method (Figure 3C)

1. Place 1 µl droplet of dye or DNA (200 ng) onto the fiber side of the SU-8 film and let it dry for 10 min. Make sure to place the droplet in the center of the chip.

NOTE: There are different drying times depending upon the substrate used.

2. Using a pair of sharp tweezers place the VACNF film onto the plant surface.

NOTE: The longer the SU-8 films are left out in the air the more brittle the films become. To limit the risk of losing the SU-8 squares, make sure to have all plants/samples and equipment near the SU-8 films.

3. Gently roll a small makeup applicator over the VACNF film. Mark the areas where the flexible substrates are placed with a soft-tipped marker. Remove the flexible substrates from the plant surface using tape.

NOTE: The amount of force to apply when rolling the makeup applicator will vary among plant tissues used. Practice applying the VACNF films prior to conducting biomolecule or dye delivery. Visible damage to plant tissues is apparent when one can see the outlines of the VACNF film in the plant tissue.

4. Repeat steps 1-4 for controls and store plants as in step 7 of on-plant method.

6. Microscopy and image analysis for all delivery methods

1. Image the samples with a confocal microscope using emission and excitation wavelengths specific for the delivered fluorescent probe/reporter.

NOTE: The time required for transient transformation varies with plant species and the marker delivered. For example, expression of fluorescent markers was detected after 48 h in Arabidopsis versus 96 h in lettuce leaves[7].

2. When imaging, try to focus on a region with detached fibers. Fibers will have different orientations. Success of delivery is not dependent on the appearance of broken-off fibers.

NOTE: Fibers will be fluorescent with the most common excitation/emission settings due to the formation silicon nitride layer resulting from fiber formation in PECVD[18].

3. Capture at least 5 images for each sample. Resulting signal will vary.

4. Fluorescence values are measured as total fluorescence (integrated density) in 20 μm x 20 μm confocal image areas[7] using ImageJ[19].

REPRESENTATIVE RESULTS:

The distinct advantage of VACNF chips on rigid or flexible substrates is the ability to deliver biomolecules or dyes to specific locations on a plant (Figure 3). Here we have used fluorescence readouts to assess delivery. Using different plants, substrates, and delivery methods (on-chip or on-plant) there can be differences in the timing of the appearance of fluorescein. To determine if VACNF chips/films work for delivery, a fast approach is to use the fibers for dye delivery (Figure 4). Images labeled with different times in Figure 4 are different fields of view from the same samples. When using the on-plant method, dye can be observed immediately after delivery using fluorescence microscopy. Additionally, if the same field of view is imaged over time after delivering fluorescein dye to a plant, the signal intensity becomes less bright over time (Figure 5). The fluorescein dye could potentially be moving from the field of view to other areas of the leaf through plasmodesmata[20-21]. Compared to the on-plant method, the on-chip method with fibers in the rigid, the dye takes more time to move throughout the impaled area (Figures 4). This could be a result of the dye detaching from fibers/rehydrating in the cells and thus taking more time to move.

Fibers in the flexible substrate were suitable for dye delivery to curved surfaces, such as strawberries and apples (Figures 6 and 7). Using a flexible substrate with strawberries, a strong fluorescein signal was observed right away (Figure 6), whereas it took 2 h to see a strong fluorescein signal in apples (Figure 7B, D). Successful delivery of plasmids encoding fluorescent

markers can be determined by using fluorescence microscopy and finding the resulting signal (Figures 7F, 8, and 9). Controls are necessary to determine if the plant of choice has autofluorescence like the fluorescent marker encoded within the plasmid being delivered by fibers. Using fibers alone is helpful to determine if the impact force applied with tweezers results in damage to the plant tissue or if the observed fluorescence within the sample is due to the VACNFs, which are inherently fluorescent because of their silicon nitride layer[18] (Figure 8C-D). Fibers impaled in plant tissue do not induce wound response, as assessed by H_2O_2 production[6]. Lastly, using the control of +DNA, –Fibers is necessary to determine if the DNA is not entering into the plant through tapping alone and confirms that the fibers are necessary for delivery into plant cells (Figure 8E-F). There should be no distinct difference when using the on-plant or on-chip methods of delivery using the VACNFs on rigid substrate, as indicated by the lack of a significant difference in fluorescence values (Figure 8I). Using the flexible VACNF films with the on-chip DNA delivery resulted in successful transient transformation of epidermal cells in store-bought apples and onions (Figures 7F and 9).

Failed experiments may have fibers broken off in the different fields of view, but there will be no resulting fluorescence signal from the attempt to deliver plasmid DNA or dye. If too much pressure is applied to the plant, there will be apparent tissue damage (Figure 10). This mechanical damage may look like small holes or transparent areas in the plant, as if a layer of cells has been removed when looking at the plant under a microscope. Sometimes imprints of the chip will be visible. An experiment in which fluorescent protein expression is not detected after DNA delivery may also be due to the use of low-quality DNA, so it may be useful to make fresh DNA preparations.

FIGURES AND FIGURE LEGENDS:

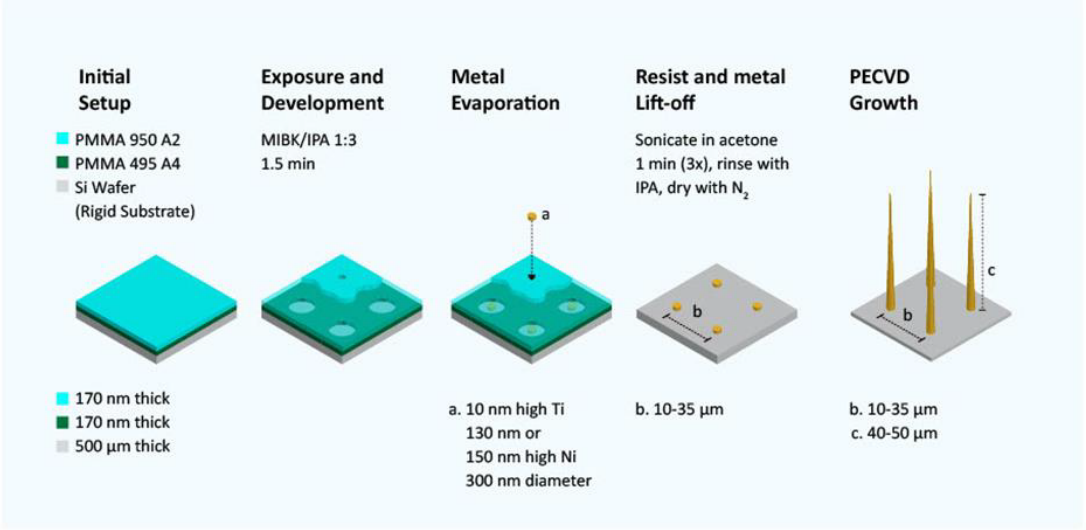

Figure 1: Workflow for making vertically aligned carbon nanofiber arrays. To produce VACNFs, a double layer of polymethyl methacrylate (PMMA 495 A4, 950 A2) is spin-coated onto a silicon wafer. Electron beam lithography is used to define an array of dots 300 nm in diameter. The resist is then developed in methyl isobutyl ketone/isopropanol (MIBK/IPA), 1:3 for 1.5 min. Using a metal evaporator, an adhesive layer of Ti (10 nm) is applied to the wafer, followed by a second layer of Ni (130 nm or 150 nm). The remaining resist is then removed via lift-off (sonication baths of acetone). The geometry of the catalyst dots is inspected via SEM. If the catalysts resemble hockey pucks and are flat, then they are placed in the plasma enhanced chemical vapor deposition (PECVD) machine and fibers are grown. Fibers are then inspected using SEM.

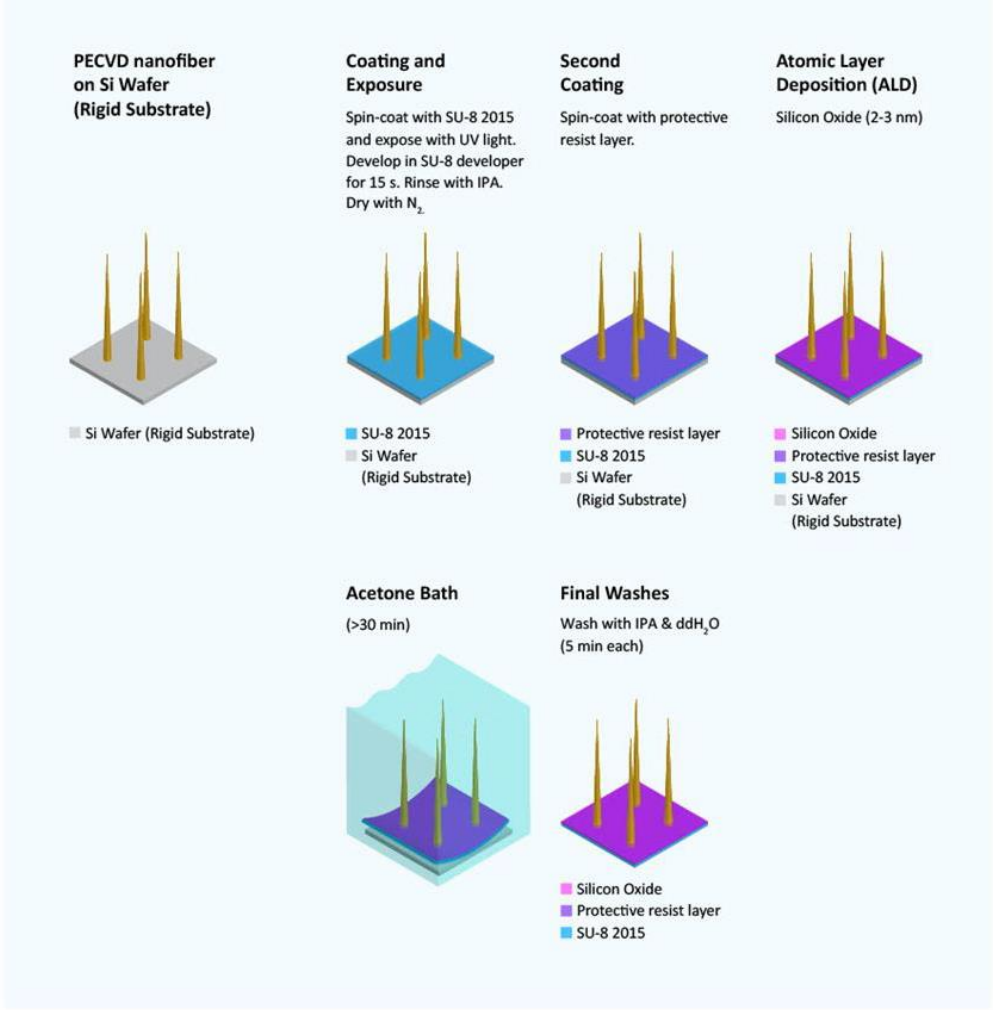

Figure 2: Workflow for transferring fibers from a rigid substrate to a flexible substrate. After nanofiber synthesis and inspection, each wafer is spun with SU-8 2015 at 4000 rpms for 45 s. The wafer is then soft baked for 3 min at 95 °C. Following this, the wafer is exposed to UV light and patterned in a mask aligner at 95 mJ/cm^2. It is then post-baked for 6 min at 95 °C. The pattern is developed in SU-8 developer for 15 s, rinsed with IPA, and dried with N_2 gas. A protective resist layer of SPR 955 CM 0.7 is spun on the wafer at 3000 rpm and softbaked at 90 °C for 30 s. A silicon oxide layer (2-3 nm) is then added to the wafer via atomic layer deposition (ALD) (22 cycles at 100 °C) to make the flexible substrate hydrophilic[15]. The wafer is then diced into 3 mm x 3 mm squares with the dicing saw. Individual chips are then placed in acetone until the SU-8 starts to curl and looks like it is concaving (>30 min). At this time the SU-8 layer on most chips can be grabbed at the edge with sharp tweezers and peeled from the underlying silicon substrate as an intact 3 mm square film. The film is then washed in IPA for 5 min and water for 5 min.

(A)

DNA/dye OnPlant

Place 1 µL droplet of DNA/dye solution on plant.

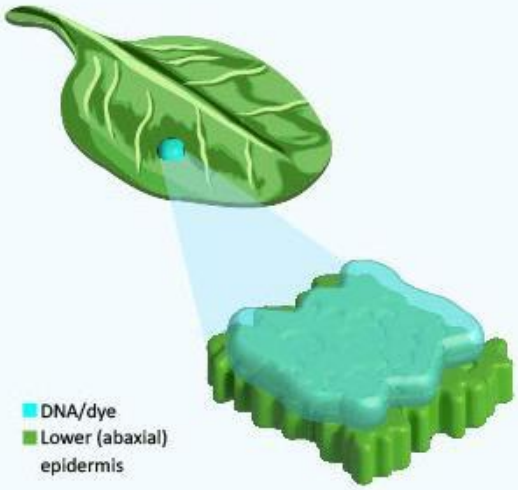

Tapping

Place chip on top of plant. Tap chip gently with tweezers to push the fibers into the leaf tissue
Tip or bottom of tweezers may be used.

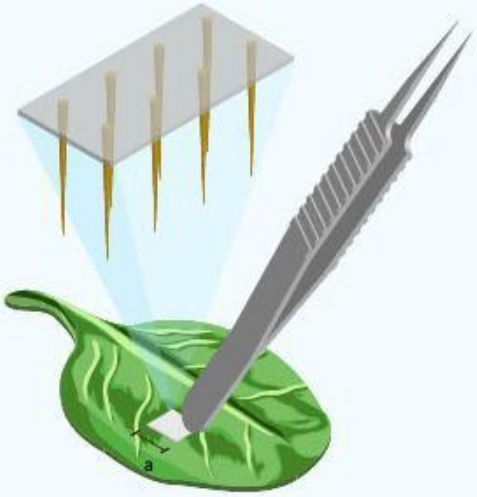

a. 3 mm x 3 mm

(B)

DNA/dye On-Chip

Place 1 µL droplet of DNA/dye solution on 3 x 3 mm chip. Dry 15 min.

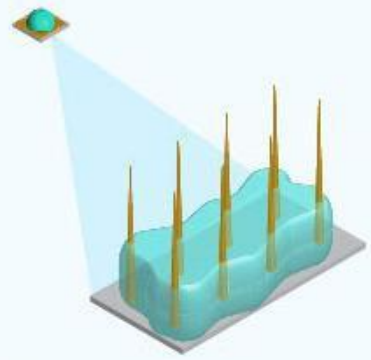

Tapping

Place chip on top of plant. Tap chip gently with tweezers to push the fibers into the leaf tissue
Tip or bottom of tweezers may be used.

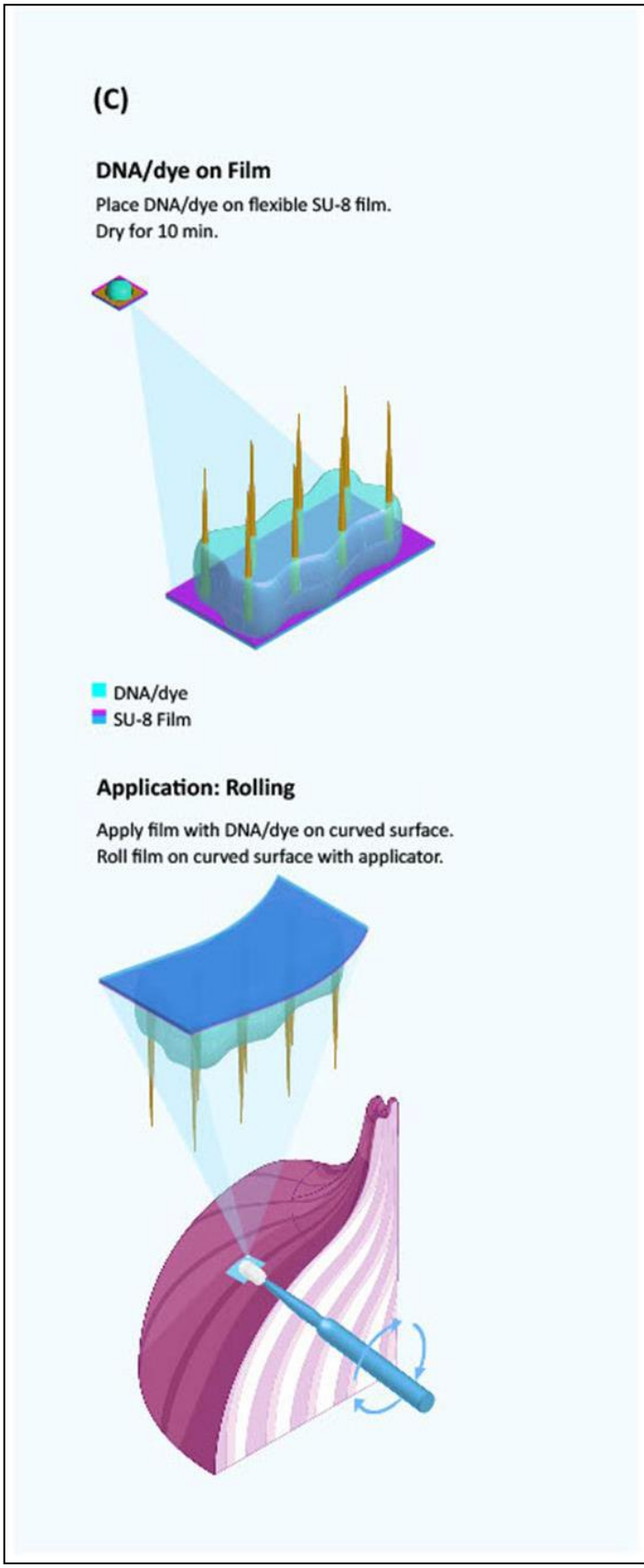

Figure 3. Schematic of dye/DNA delivery to plant tissue using fibers on rigid and flexible substrates. (A) On–plant, fiber-mediated dye/DNA delivery. A 1 µL droplet of dye/DNA solution is placed on the surface of a leaf, the VACNF chip is placed on top of the droplet. Using a pair of tweezers, the chip is gently tapped into the tissue. The rigid substrate is removed, leaving nanofibers within the tissue. (B) On-chip, fiber-mediated DNA delivery. A 1 µL droplet of dye/DNA solution is dropcast on the VACNF chip and dried for 15 min. The chip with semi-dried DNA is placed on top of the leaf surface and tapped into the tissue as in (A). (C) On-chip SU-8 film DNA delivery. Fibers are transferred from the rigid silicon substrate to flexible SU-8 substrate. A 1 µL droplet of dye/DNA solution is dropcast on the VACNF film and dried for 10 min. The VACNF film with the semi-dried dye/DNA is then rolled onto a curved plant surface using a makeup applicator.

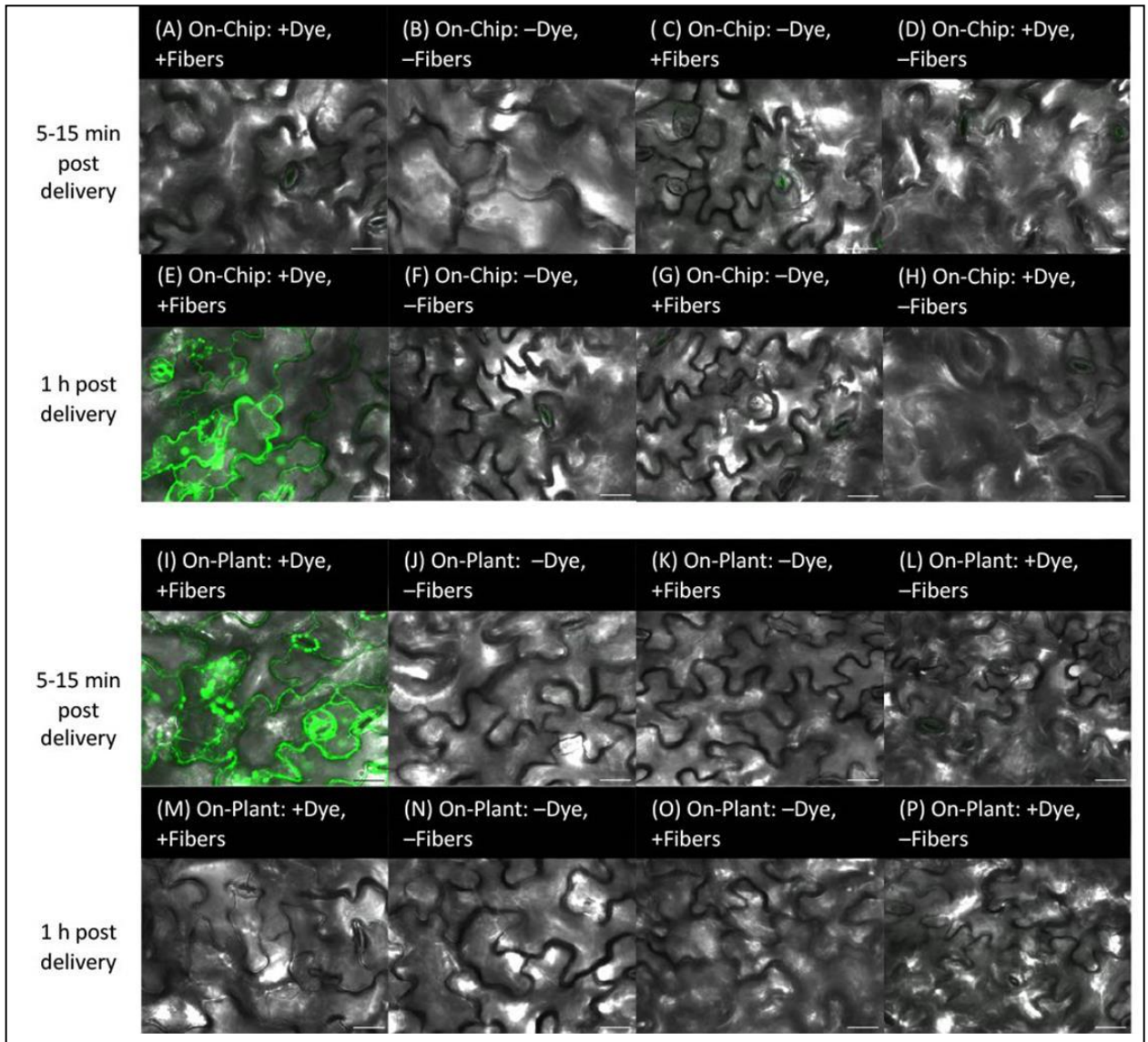

Figure 4: Dye delivery to Arabidopsis leaves using on-chip and on-plant methods with fibers on rigid substrates. Images were acquired using confocal microscopy. On-chip method (A-H): 1 µL of 10 µM fluorescein dye was dried for 15 min on VACNF chips and then the chips were tapped into the abaxial side of Arabidopsis leaves with tweezers. (A-D) Leaves imaged within 5-15 min post-delivery. (E-H) Leaves imaged 1 h after delivery. (A and E) +Dye, +Fibers. Controls: (B and F) –Dye, –Fibers; (C and G) –Dye, +Fibers; (D and H) +Dye, –Fibers. On-plant method (I-P): 1 µL of 10 µM fluorescein dye was placed on plant surface, chips were positioned such that they come into contact with the droplet, and tweezers were used to tap the chip into the abaxial side of Arabidopsis leaves. (I-L) imaged within 5-15 min post-delivery and (M-P) imaged 1 h after delivery. (I and M) +Dye, +Fibers. Controls: (J and N) –Dye, –Fibers; (K and O) –Dye, +Fibers; (L and P) +Dye, –Fibers. (A-P) are single planer images from z-stacks. Scale bars are 20 µm. Fibers have a 35 µm pitch.

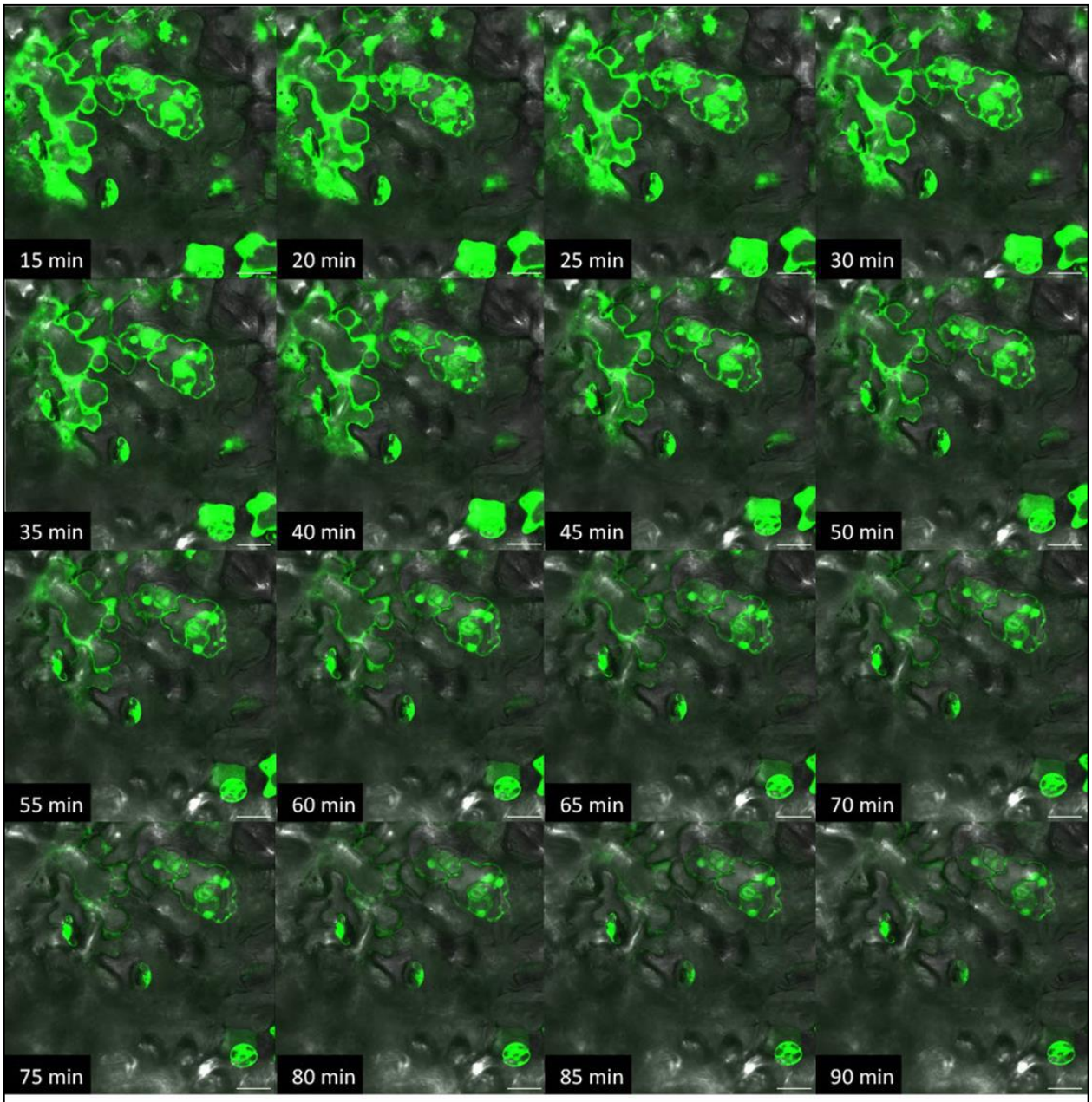

Figure 5: Time course of dye delivery in Arabidopsis via on-plant method with rigid substrate. Images were acquired using confocal microscopy. Using the on-plant method, 1 µL droplet of fluorescein dye solution (10 µM) was placed on the surface of a leaf, the VACNF chip was placed on top of the droplet. Using a pair of tweezers, the chip was gently tapped into the tissue. +Dye, +Fibers images of the same area were acquired every 5 minutes. Scale bars are 20 µm. Fibers have a 35 µm pitch. Panels are single planer images from z-stacks.

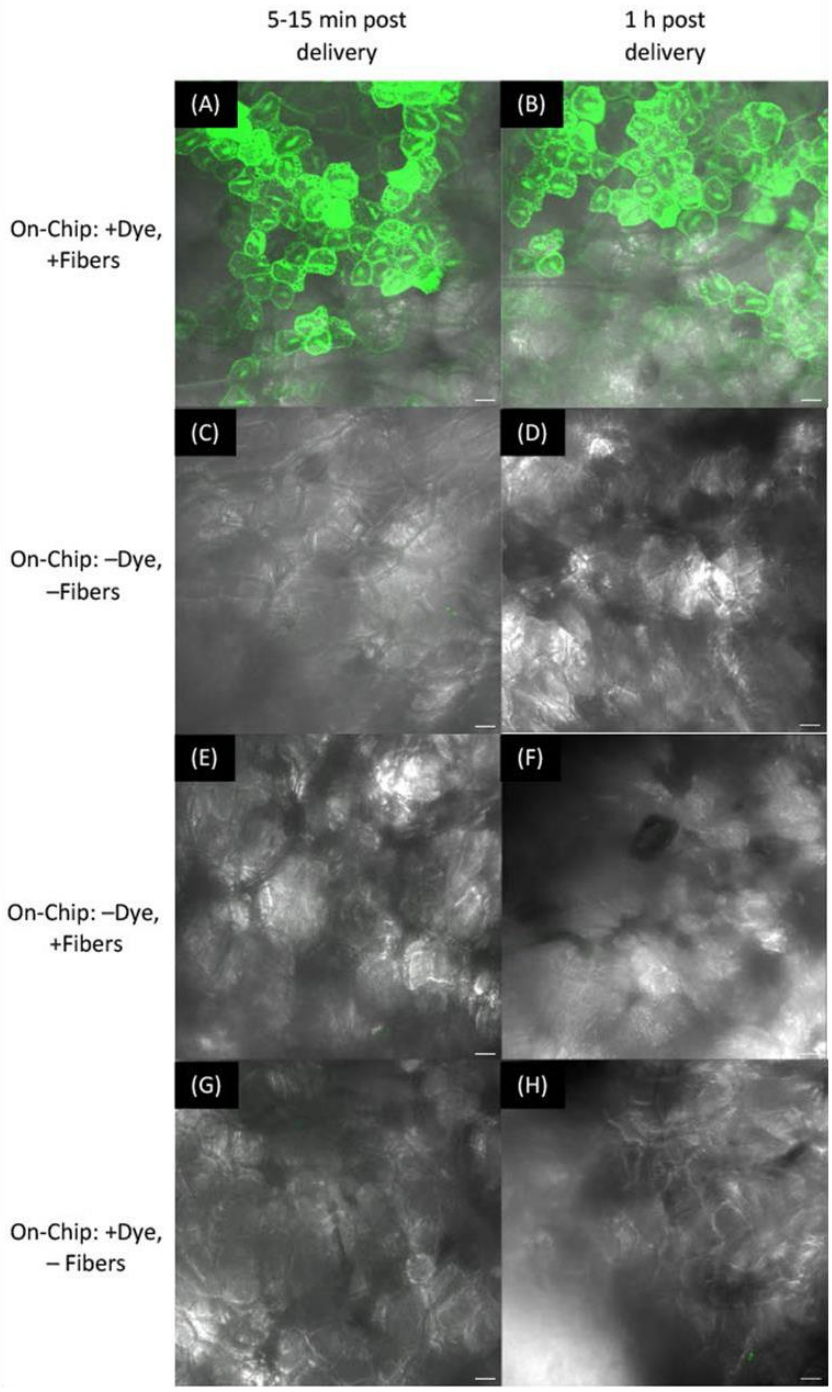

Figure 6: Dye delivery to strawberries utilizing VACNF films. Images were acquired using confocal microscopy. Using the on-chip method, dye droplets were dried on VACNF films, which were then rolled onto fruit surfaces using a makeup applicator. Fluorescein dye (10 µM) was delivered to strawberry cells and imaged after 10 min (A) and 1 h (B). Panels (C and D) show no treatment controls (–Dye, –Fibers). Panels (E and F) show –Dye, +Fibers controls after 10 min and 1 h, respectively. Panels (G and H) show +Dye, -Fibers controls after 10 min and 1 h, respectively. The scale bars are 40 µm. (A-H) are maximum projections of 188 µm z-stacks. Fibers have a 35 µm pitch.

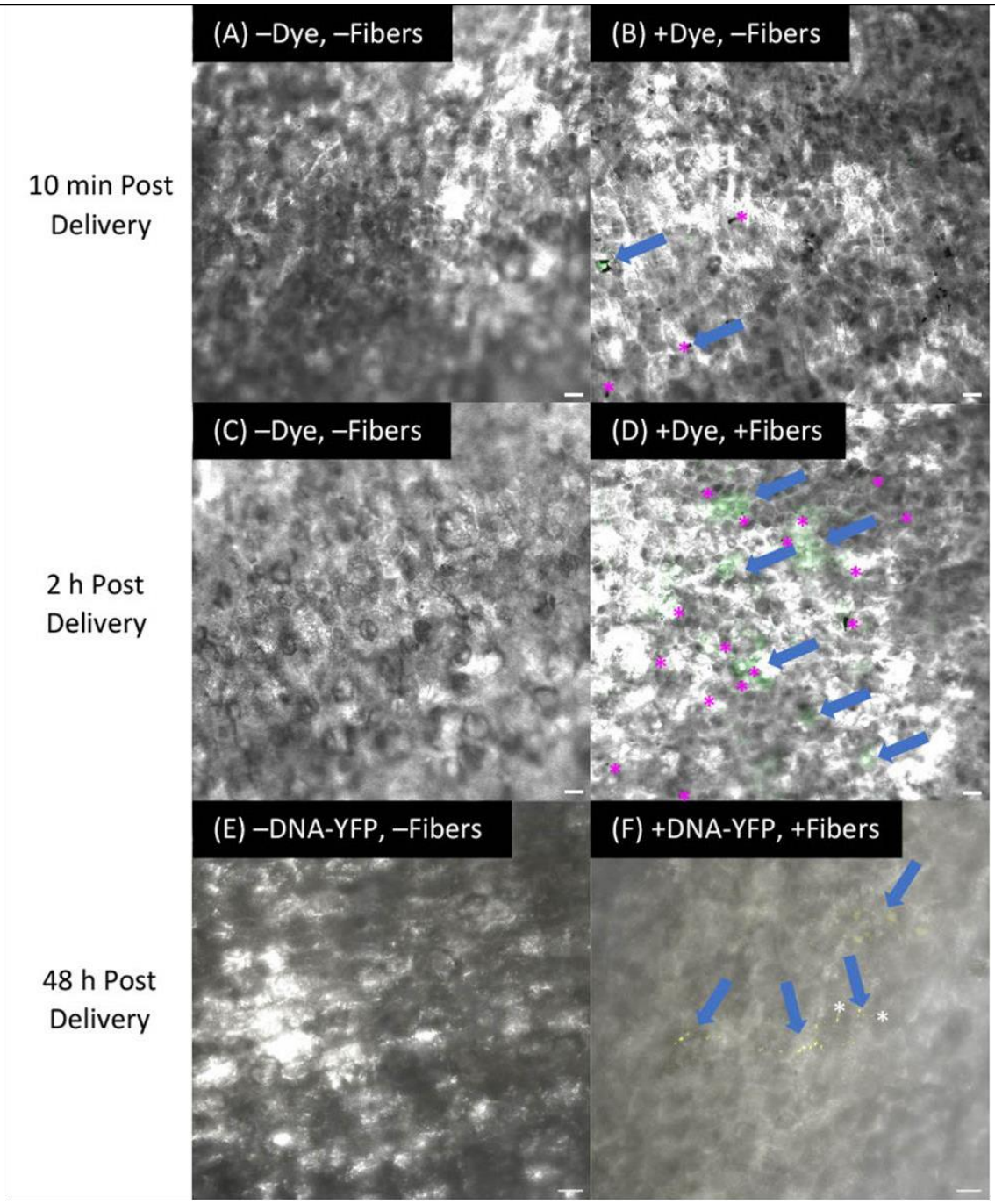

Figure 7: Dye delivery and transient transformation of apples via VACNF films. Images were generated using confocal microscopy. Using the on-chip method, 1 µL droplets of fluorescein dye (10 µM, B and D) or 1 µL of plasmid encoding $pUBQ_{10}$:YFP (DNA–YFP) (200 ng) were dried on VACNF films, which were then rolled onto fruit surfaces using a makeup applicator. Fluorescein dye was delivered to apple epidermis and imaged after 10 min (B) and 2 h (D). The dye took some time to diffuse into the cells after delivery (D). DNA-YFP delivery and expression via VACNF films after 48 h (F). Panels (A, C, and E) show no treatment controls (–Dye/DNA-YFP, –Fibers). The scale bars are 40 µm. (A-D) are single planer images from z-stacks. (E and F) are maximum projection of 53 µm z-stacks. Fiber pitch is 35 µm. Arrows denote fluorescein signal or YFP signal. * indicates a VACNF.

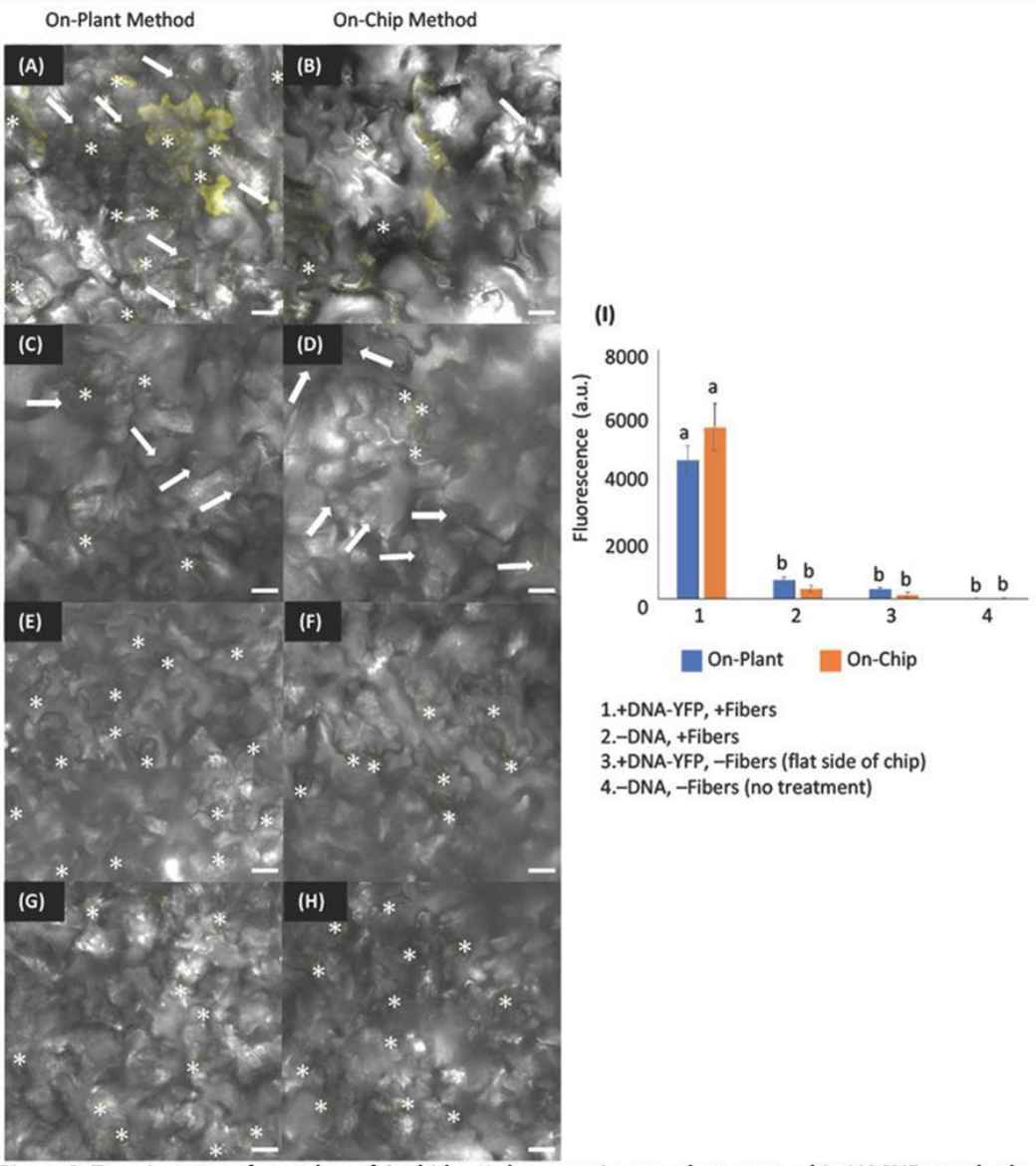

Figure 8: Transient transformation of Arabidopsis leaves using on–plant or on–chip VACNFs methods. Images were acquired using confocal microscopy 48 h after DNA delivery. On-plant method: 1 µL of plasmid encoding $pUBQ_{10}$:YFP (DNA–YFP) (200 ng) was placed on a plant surface, chips were positioned such that they came in contact with the droplet, and tweezers ware used to tap the chip into the abaxial side of Arabidopsis leaves (A, C, E, and G). On-chip method : 1 µL of DNA–YFP was dried for 15 min on VACNF chips and then the chips ware tapped into the abaxial side of Arabidopsis leaves with tweezers (B, D, F, and H). +DNA-YFP, +Fibers for on-plant (A) and on-chip (B). Controls: –DNA-YFP, + Fibers (C and D); +DNA-YFP, –Fibers (E and F); and –DNA, –Fibers (G and H). Graph representing relative average fluorescence signal intensity of 25 20 × 20 µm areas from images of 5 biological replicates combined from 2–3 experiments using fluorescence from the YFP channel (I). Regions containing stomata (*) were excluded due to autofluorescence. The average fluorescence intensity from the –DNA-YFP, –Fibers condition was subtracted from each average. 2–way ANOVA (and Tukey test) was used for significance testing, and error bars represent the standard error of the mean. Different letters show significant differences between treatments ($P < 0.0001$). All images shown are maximum projections of 40 µm z–stacks. Scale bars are 20 µm. White arrows indicate fibers in the images. Fiber pitch us 35 µm. Reprinted from reference 7, *Frontiers in Plant Science* under the terms of the Creative Commons attribution license (CC BY).

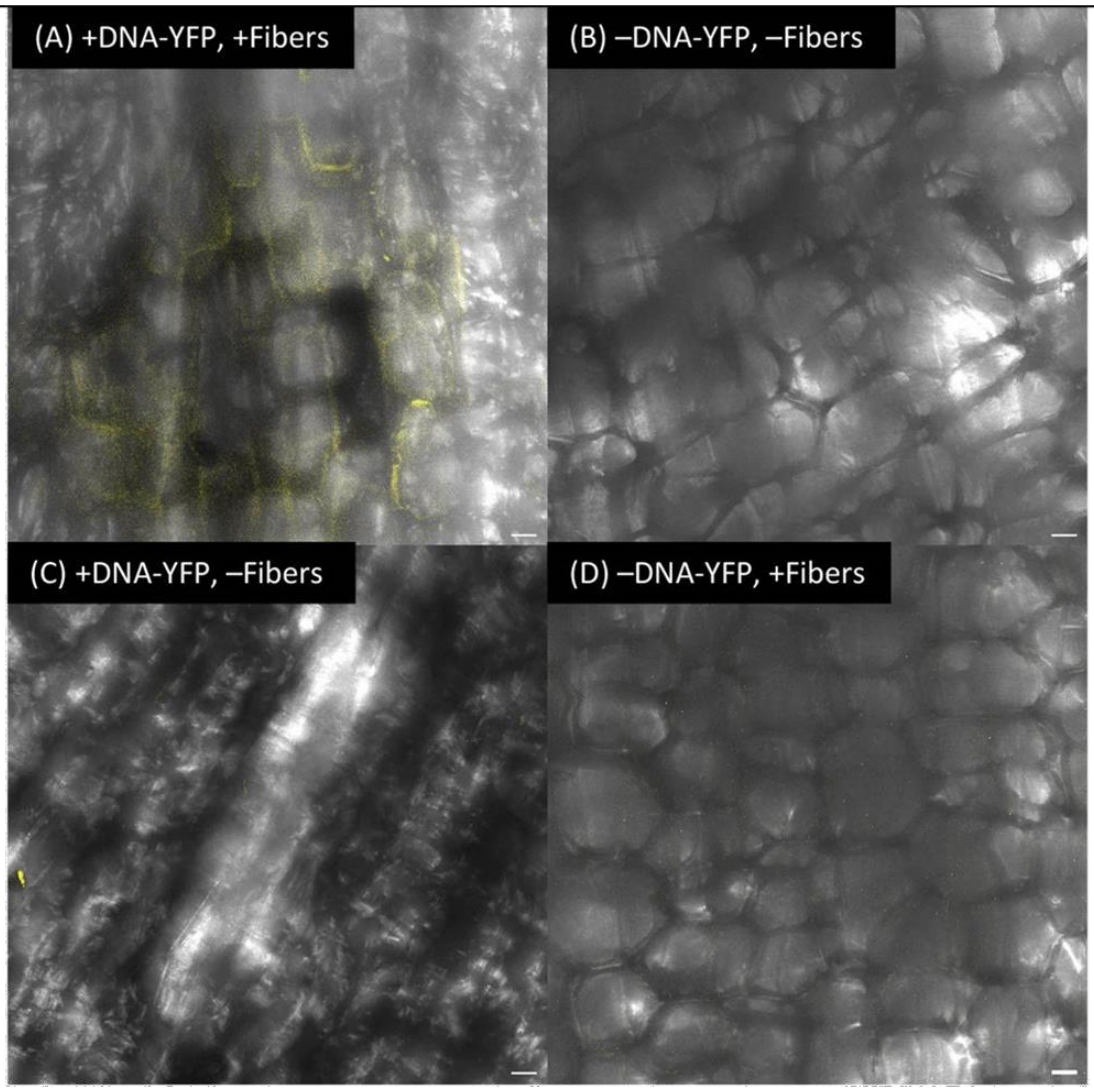

Figure 9: Transient transformation of onions using VACNF films. Images were acquired using confocal microscopy 48 h after DNA delivery. Using the on-chip method, 1 µL plasmid DNA encoding $pUBQ_{10}$:YFP (DNA-YFP) (200 ng) droplets were dried on VACNF films for 10 min, which were then rolled onto plant organ surfaces. (A) DNA-YFP was delivered to and YFP expressed in onion epidermis. Panel (B) shows no treatment control; (C) shows (–DNA-YFP, +Fibers) control and (D) shows the (–DNA-YFP, +Fibers) control. The scale bars are 40 µm. Fibers have a 35 µm pitch. Images are maximum projections of 115 µm z-stacks.

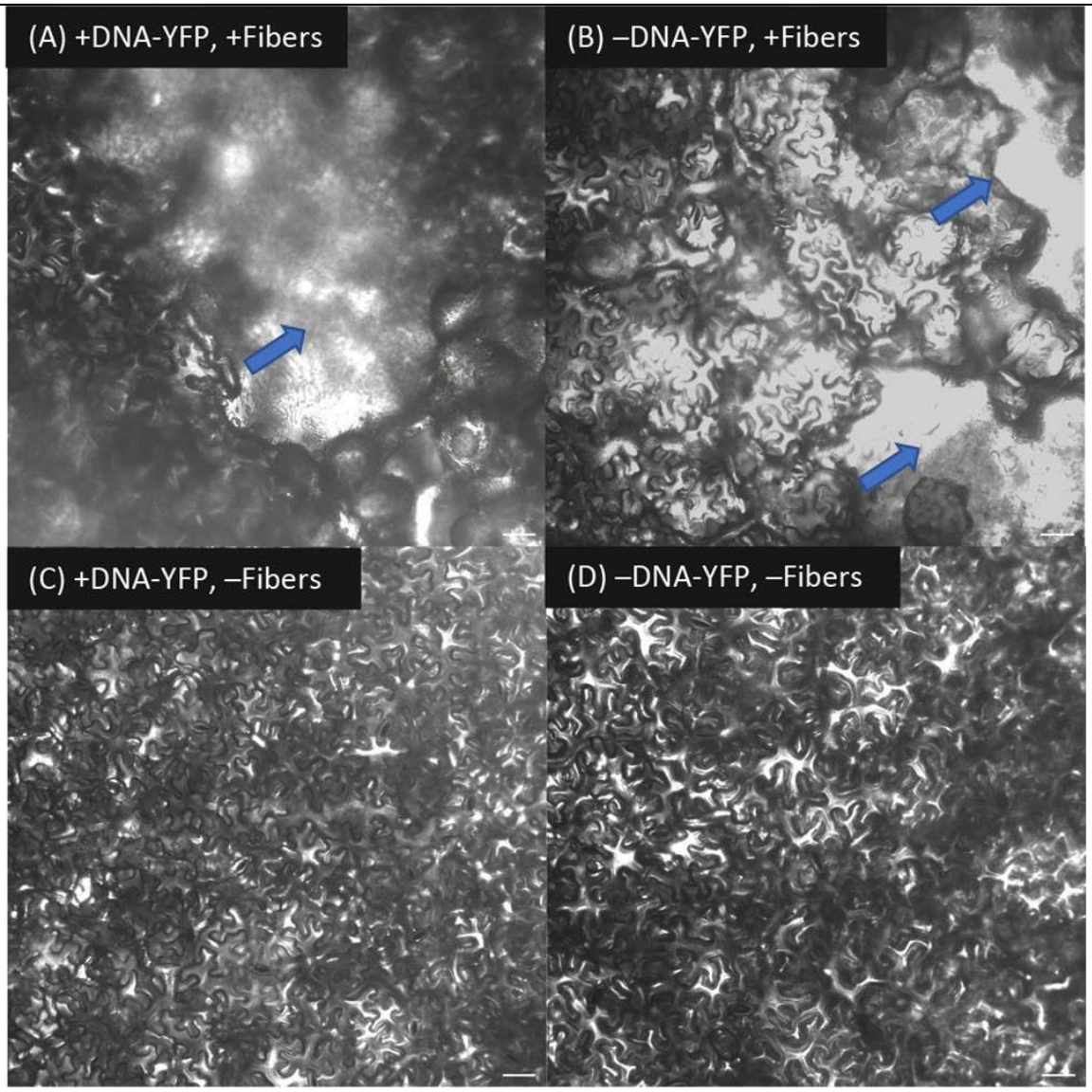

Figure 10: Tissue damage in lettuce from VACNF film application. Images were generated using confocal microscopy. On-chip method was used to deliver DNA to lettuce leaves. $pUBQ_{10}$:YFP DNA (200 ng) droplets were dried for 10 min on VACNF films, which were then rolled onto the abaxial side of detached lettuce leaves and stored in a humidity chamber for 4 d (A). (B) shows the (–DNA-YFP, +Fibers) control. (C) shows the (+DNA-YFP, –Fibers) control, and (D) is the no treatment (–DNA-YFP, –Fibers). Scale bars are 40 µm. VACNFs have a 35 µm pitch. Arrows point to plant damage resulting from rolling of the flexible substrate with too much force. Note that successful VACNF-mediated DNA delivery in lettuce was achieved in other experiments[7].

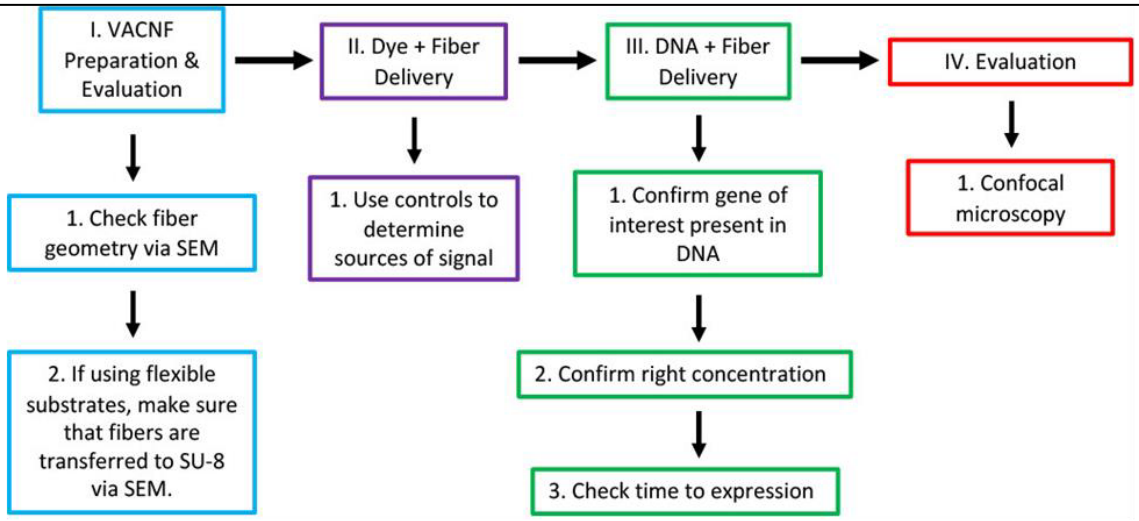

Figure 11: Workflow of VACNF-mediated delivery in plants. First, check the geometry of the fibers using SEM. For proper delivery, fibers need a tip with a diameter <200 nm. If using fibers on a flexible substrate, the next step would be to confirm that fibers are being transferred to SU-8 and to check the height of the exposed fibers via SEM. Next, test the usefulness of the fibers by trying to deliver dye into the plant/organ of choice using the rigid or flexible substrate. Use 1 µL droplet either placing it on the plant surface or briefly drying it on the chip/film. With this step and all other steps, it is imperative to use the proper controls (–Dye,–Fibers; –Dye, +Fibers; and +Dye,–Fibers), to be confident that signal comes from *bona fide* dye delivery. The third step is to confirm that the gene of interest is present in the plasmid, determine the concentration of DNA to deliver, and test the optimal amount of time after delivery to check expression. The final step is to use confocal microscopy to check expression of the delivered marker. Modified from reference 7, *Frontiers in Plant Science* under the terms of the Creative Commons attribution license (CC BY).

DISCUSSION:

In this paper we presented methods for how to construct vertically aligned carbon nanofibers, transfer these fibers to a flexible substrate, and apply fibers in either a rigid or flexible substate to plants to use for delivery of biomolecules or dyes to plants. We also described and showed results from impalefection using the on-chip or the on-plant method with fibers on a rigid substrate as well as the on-chip method using VACNF films. The application of using these fibers is simpler in practice and theory than traditional plant transformation methods (particle bombardment, protoplast transformation via PEG or electroporation) and may be used

for plants recalcitrant to Agrobacterium-mediated transformation. However, only a small number of cells are transformed.

Vertically aligned carbon nanofibers were produced at Oak Ridge National Laboratory Center for Nanophase Materials Sciences through their user program. Users can apply to use this facility. Alternatively, VACNF chips can be produced in clean rooms with direct current plasma enhanced chemical vapor deposition machines with a carbon source[22-23]. With the methods described, there are a few steps that are critical to the production of the fibers, fiber transfer, and application of the VACNF chips/films. For fiber application to work, fibers must be straight and have a tapering diameter of <200 nm at the tip for delivery in plant cells to be successful[6-7]. Additionally, the fibers need to be a certain minimum length to achieve delivery within plant cells. In theory, the carbon nanofibers can be made to have different pitches (lateral spacing) and lengths. The importance of producing fibers of different lengths is that longer fibers could be used to penetrate deeper tissue layers. Having longer fibers (greater than >40 μm in length) is important for flexible films, as the fiber transfer works by breaking the fibers from their base and requires layering SU-8 on top of the fibers. The working thickness of the SU-8 layer utilized for this protocol is 20-35 μm. The minimum height necessary to accomplish delivery within the epidermis of various plants (curved or flat) is approximately 10-15 μm[6-7]. With this knowledge in mind, fibers with lengths >40 μm are necessary for VACNF films. There are several different parameters to consider when producing carbon nanofibers: choice of catalyst material, catalyst geometry, thickness of catalyst material as well as factors when growing fibers in a PECVD chamber (gas ratio, pressure, temperature, current, showerhead height, and growth time)[8-9, 24-25]. To produce carbon nanofibers longer than 25 μm used by Morgan et al.[7] and Daven et al.[6], we increased the amount of Ni catalyst, altered the acetylene: ammonia ratio, and increased the

current and the growth time. Additionally, we paid more attention to the geometry of the catalyst material. To produce tall straight fibers, the deposited catalyst needed to have a hockey puck shape rather than a shape that resembles a volcano. Volcano structures arise from remnants of photoresist after lift-off. To prevent the formation of volcanos, a double layer of PMMA was utilized to create an undercut during electron beam lithography[26]. The undercut aids in lift-off of the deposited metal catalyst (Figure 1).

In addition to fiber height, another critical step for successful fiber transfer is the amount of time spent in the acetone bath. The VACNF films need to be left in the acetone bath long enough until their edges begin to curl; if they are left in the acetone bath for too little time, they are more difficult to lift off the chips and may break. The older the chips are, the longer they will have to remain in the acetone bath. Following the acetone bath, the films/chips are placed in isopropanol and water; the purpose of these baths is to remove access acetone as well as to remove the protective photoresist on the fibers.

Another step within the process that is of vital importance to the success of the method is ensuring that the right amount of force is applied to VACNF chips/films. The delivery mechanism is dependent upon fibers making small punctures in cell walls via the impulse force of tweezer tapping on rigid substrates[6-7] or rolling with of the mini-makeup applicator on flexible substrates. Fibers may break off and remain imbedded in plant cells[6-7]. Additionally, it is important to choose appropriate imaging time points after DNA delivery with VACNF chips/films, as time to detectable expression varies between plant species and the types of vectors being delivered[7] (Figure 11).

As broadly applicable as this method is to plants, it has a few limitations. For example, adding a thin layer of silicon oxide to the VACNF films does not always result in films being

completely hydrophilic because of the protective layer of photoresist added on top of the SU-8. To overcome this, thicker layers of silicon oxide could be applied to the VACNFs. To test if the films are hydrophobic or hydrophilic, they can be placed in water. If the films sink, they are hydrophilic and if they float, they are hydrophobic. Additionally, there can be variation between the batches of fibers produced. There are several parameters that can be altered when growing the fibers in the plasma enhanced chemical vapor deposition machine; what is described in this protocol is a set of parameters for two different amount of Ni catalyst. Additionally, the crystal orientation of the Ni catalyst cannot be controlled[27], and this will affect the potential for branching that can result in the fibers. In addition to variable chip features, there can be person to person variation in the application method, meaning that each person will apply a different amount of force when tapping rigid substrates into the plants or rolling the VACNF films onto the plants. This is typically overcome with practice and ensuring that dye delivery is achievable without apparent tissue damage.

While this method was used to demonstrate dye and DNA delivery to plant cells using both rigid and flexible substrates for this paper, it should be broadly applicable for RNAi silencing for plant systems like apples or other fruits where it would take years to produce stable transgenic lines. Moreover, these fibers could also be used to deliver genetic editing materials or for stable transformations in plants.

ACKNOWLEDGMENTS:

Nanofiber arrays were fabricated at the Center for Nanophase Material Science, which is a Department of Energy Office of Science User Facility (Proposal ID: CNMS2019-103 and CNMS2022-A-1182). Support from CNMS is awarded through a peer-reviewed proposal system

and is provided at no cost to successful applicants who intend to publish their results (http://www.cnms.ornl.gov/user/becoming_a_user.shtml). We thank Kevin Lester and the CNMS for assistance with the production of nanofiber arrays. We thank Dr. John Caughmen, Dr. Timothy McKnight, Dr. Amber Webb, Daryl Briggs, and Travis Bee for critical discussions about experimental design. We thank Leslie Carol for scientific illustrations. This work has been funded by the Bioimaging Science Program, U.S. Department of Energy, Office of Science, Biological and Environmental Research, DE-SC0019104 and the United States Department of Agriculture, 2021-67013-34835. JMM was supported by the United States Department of Agriculture: National Institute of Food and Agriculture: Agriculture and Food Research Initiative Predoctoral Fellowship 2021-67034-35167.

DISCLOSURES:

The authors have nothing to disclose.

WORKS CITED:

1. Canto, T. Transient expression systems in plants: potentialities and constraints. *Advanced Technologies for Protein Complex Production and Characterization*. 287-301 (2016).
2. Gou, Y. J., et al. Optimization of the protoplast transient expression system for gene functional studies in strawberry (Fragaria vesca). *Plant Cell, Tissue, and Organ Culture*. **141**, 41-53 (2020).
3. Baltes, N. J., Gil-Humanes, J., & Voytas, D. F. Genome engineering and agriculture: opportunities and challenges. *Progress in Molecular Biology and Translational Science*. **149,** 1-26 (2017).

4. Ren, R., et al. Highly efficient protoplast isolation and transient expression system for functional characterization of flowering related genes in Cymbidium orchids. *International Journal of Molecular Sciences.* **21** (7), 2264 (2020).
5. Kumar, S., et al. Nanovehicles for plant modifications towards pest-and disease-resistance traits. *Trends in Plant Science*. **25** (2), 198-212 (2020).
6. Davern, S. M., et al. Carbon nanofiber arrays: a novel tool for microdelivery of biomolecules to plants. *PLoS One.* **11** (4), e0153621 (2016).
7. Morgan, J.M., et al. An efficient and broadly applicable method for transient transformation of plants using vertically aligned carbon nanofiber arrays. *Frontiers in Plant Science.* **13**, 1051340 (2022).
8. Melechko, A. V., et al. Vertically aligned carbon nanofibers and related structures: Controlled synthesis and directed assembly. *Journal of Physics D: Applied Physics.* **97** (4), 3 (2005).
9. Melechko, A. V., Desikan, R., McKnight, T. E., Klein, K. L., & Rack, P. D. Synthesis of vertically aligned carbon nanofibres for interfacing with live systems. *Journal of Physics D: Applied Physics.* **42** (19), 193001 (2009).
10. Nelson-Fitzpatrick, N. *Novel Materials for the Design of Cantilever Transducers.* PhD. thesis, University of Alberta, Edmonton, Alberta (2011).
11. Fletcher, B. L. et al. Transfer of Flexible Arrays of Vertically Aligned Carbon Nanofiber Electrodes to Temperature-Sensitive Substrates. *Advanced Materials.* **18** (13), 1689-1694 (2006).
12. Keller, S., Blagoi, G., Lillemose, M., Haefliger, D., & Boisen, A. Processing of thin SU-8 films. *Journal of Micromechanics and Microengineering*. **18** (12), 125020 (2008).

13. Wouters, K., & Puers, R. Diffusing and swelling in SU-8: insight in material properties and

processing. *Journal of Micromechanics and Microengineering*. **20** (9), 095013 (2010).

14. Jamal, M., Zarafshar, A. M., & Gracias, D. H. Differentially photo-crosslinked polymers enable self-assembling microfluidics. *Nature Communications*. **2** (1), 527 (2011).

15. Williams, R., & Goodman, A. M. Wetting of thin layers of SiO_2 by water. *Applied Physics*

Letters. **25** (10), 531-532 (1974).

16. Kundu, A., Nogueira Campos, M. G., Santra, S., & Rajaraman, S. Precision vascular delivery of agrochemicals with micromilled microneedles (µMMNs). *Scientific Reports*. **9** (1), 1-8 (2019).

17. Acanda, Y., Welker, S., Orbović, V., & Levy, A. A simple and efficient agroinfiltration method for transient gene expression in Citrus. *Plant Cell Reports*. **40** (7), 1171-1179 (2021).

18. Pearce, R., et al. Synthesis and properties of SiNx coatings as stable fluorescent markers on vertically aligned carbon nanofibers. *AIMS Materials Science*. **1** (2), 87-102 (2014).

19. Schindelin, J., et al. Fiji: an open-source platform for biological-image analysis. *Nature Methods*. **9** (7), 676-682 (2012).

20. Crafts, A. S. Translocation in plants. *Plant Physiology*. **13** (4), 791 (1938).

21. Martens, H. J., Hansen, M., & Schulz, A. Caged probes: a novel tool in studying symplasmic transport in plant tissues. *Protoplasma*. **223**, 63-66 (2004).

22. Liu, J., Essner, J., & Li, J. Hybrid supercapacitor based on coaxially coated manganese

oxide on vertically aligned carbon nanofiber arrays. *Chemistry of Materials*. **22** (17), 5022-5030 (2010).

23. Saleem, A. M., et al. Low temperature and cost-effective growth of vertically aligned carbon nanofibers using spin-coated polymer-stabilized palladium nanocatalysts. *Science and Technology of Advanced Materials.* **16**, 015007 (2015).
24. Merkulov, V. I., Lowndes, D. H., Wei, Y. Y., Eres, G., & Voelkl, E. (2000). Patterned growth of individual and multiple vertically aligned carbon nanofibers. *Applied Physics Letters.* **76** (24), 3555-3557 (2000).
25. Retterer, S. T., Melechko, A., Hensley, D. K., Simpson, M. L., & Doktycz, M. J. Positional control of catalyst nanoparticles for the synthesis of high density carbon nanofiber arrays. *Carbon*, **46** (11), 1378-1383 (2008).
26. Rooks, M. J., Wind, S., McEuen, P., & Prober, D. E. Fabrication of 30-nm-scale structures for electron transport studies using a polymethylmethacrylate bilayer resist. *Journal of Vacuum Science & Technology B: Microelectronics Processing and Phenomena*. **5** (1), 318-321 (1987).
27. Fowlkes, J. D., et al. Control of catalyst particle crystallographic orientation in vertically aligned carbon nanofiber synthesis. *Carbon*. **44** (8), 1503-1510 (2006).

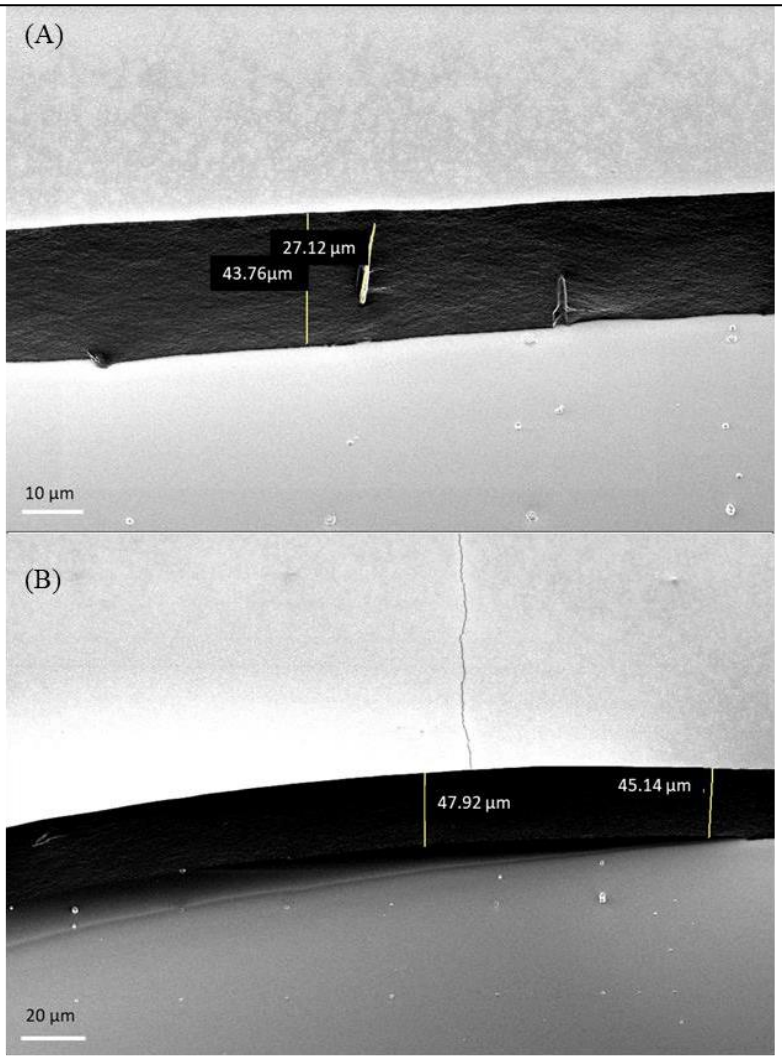

Appendix C: PDMS on top of VACNFs. VACNFs were defined with 500 nm diameter dots defined by ebeam lithography, 100 nm Ni catalyst. The fibers were grown with the following parameters in the PECVD: current of 4 A, plasma pressure of 20 torr, and a growth time of 8 minutes. The PDMS completely covered the fibers.